HAL
open science

Structural evolution of the superimposed Provençal and Subalpine fold-thrust belts (SE France)

Jocelyn Balansa, Nicolas Espurt, Jean-Claude Hippolyte, Jean Philip, Séverine Caritg

To cite this version:

Jocelyn Balansa, Nicolas Espurt, Jean-Claude Hippolyte, Jean Philip, Séverine Caritg. Structural evolution of the superimposed Provençal and Subalpine fold-thrust belts (SE France). Earth-Science Reviews, 2022, 227, pp.103972. 10.1016/j.earscirev.2022.103972 . hal-03604262

HAL Id: hal-03604262

https://hal.science/hal-03604262

Submitted on 10 Mar 2022

HAL is a multi-disciplinary open access archive for the deposit and dissemination of scientific research documents, whether they are published or not. The documents may come from teaching and research institutions in France or abroad, or from public or private research centers.

L'archive ouverte pluridisciplinaire **HAL**, est destinée au dépôt et à la diffusion de documents scientifiques de niveau recherche, publiés ou non, émanant des établissements d'enseignement et de recherche français ou étrangers, des laboratoires publics ou privés.

Structural evolution of the superimposed Provençal and Subalpine fold-thrust belts (SE France)

Jocelyn Balansa[1], Nicolas Espurt[1,2*], Jean-Claude Hippolyte[1], Jean Philip[1], Séverine Caritg[3]

[1]Aix Marseille Univ, CNRS, IRD, INRAE, Coll France, CEREGE, Aix-en-Provence, France

[2]Université Côte d'Azur, CNRS, Observatoire de la Côte d'Azur, IRD, GEOAZUR, France

[3]BRGM-French Geological Survey, Orléans, France

[*]Corresponding author at: Campus Azur CNRS, GEOAZUR, 250 rue Albert Einstein, CS 10269, 06905 Sophia Antipolis CEDEX, France.

E-mail address: espurt@geoazur.unice.fr (N. Espurt)

Abstract

Highlighting how crustal shortening is accommodated in space and time in fold-thrust belts is a major issue for understanding the long-term tectonic evolution of orogenic systems. In this study, we combine surface and subsurface data to build a 150 km-long sequentially restored balanced cross-section across two superimposed foreland fold-thrust belts in southeastern France: the upper Cretaceous-Eocene Provençal belt and Oligocene-Neogene Subalpine belt. These belts are composed of inverted Paleozoic-Mesozoic basins with Mesozoic halokinetic structures, basement thrusts, and cover thrusts-nappes detached in the Triassic evaporites. The multiphase growth of the Provençal and Subalpine belts has been constrained along the studied cross-section by syn-orogenic deposits and kinematic indicators of thrusting. The pre-orogenic palinspastic reconstruction of the cross-section to Late Santonian shows a large uplift zone in the center of the section (Durance and Valensole highs), which led to the separation of the Beausset basin (South Provence basin) to the south from the Barles-Digne basin (Vocontian basin) to the north. The Provençal shortening propagated ~NNE-ward from the Beausset basin up to folds in the Barles area during the Latest Santonian to Eocene times. Shortening value reaches 38 km and has been mainly accommodated by the inversion of the South Provence basin-Durance high. The Subalpine shortening propagated ~SW-ward from the Barles-Digne basin up to the Mediterranean coast during the Oligocene-Miocene to Quaternary times. It reaches 35 km and has been mainly consumed by the inversion of the thick Digne basin. The Provençal thrust wedge is characterized by distributed basement thrusts reworking numerous structures inherited from the Variscan belt and Permian-

Mesozoic rifts. This structural style might have favored the development of confined foreland basins, as the Arc and Rians basins. In contrast, the vertical stacking of the thick Digne Nappe and Barles basement triangle zone in the Subalpine thrust wedge might have controlled the large flexure of the Valensole foreland basin. The lack of Triassic evaporites in the Valensole high probably explains that shortening was not transferred into the cover of this domain. Consequently, the Provençal then the Subalpine shortenings might have been transferred more deeply to induce the reactivation of basement faults into the external zones. The Mesozoic halokinetic structures also strongly influenced the location of contractional deformation. This study highlights that the crustal structural inheritances influenced the structural styles and development of extensional basins and subsequent Provençal and Subalpine belts.

Keywords

Superimposed orogens; Thrust tectonics; Cross-section balancing; Sequential restoration; Structural inheritance; Provence-Alps

1. Introduction

The structural evolution of fold-thrust belts is systematically controlled by crustal heterogenities (e.g., rheology, crust-mantle coupling and crustal thickness) which are mostly inherited from previous tectonic stages of extensional, compressional, or strike-slip deformation (e.g., Lutaud, 1957; Angelier and Aubouin, 1976; Zubieta-Rossetti et al., 1993; Coward, 1996; Roure and Colletta, 1996; Beauchamp et al., 1999; Branquet et al., 2002; Kley and Monaldi, 2002; Souquet et al., 2003; Mora et al., 2006; Alvarez-Marron et al., 2006; Vergés et al., 2007; Espurt et al., 2008; Malavieille and Konstantinovskaya, 2010; Bellahsen et al. 2012; Hinsch, 2013; Mouthereau et al., 2013; Tavani et al., 2015; Lacombe and Bellahsen, 2016; Bestani et al., 2016; Butler, 2017; Calderon et al., 2017; Espurt et al., 2019a; Jourdon et al., 2019, 2020; Spitz et al., 2020; Martín-González et al., 2021; Mouthereau et al., 2021). These elements generate anisotropic behavior of the crust during contractional deformation in the Provence, where the succession of geological events generated a complex structural framework since Paleozoic (Matte, 2001; Lacombe and Jolivet, 2005; Guillot and

Menot, 2009; Schreiber et al., 2011; Advokaat et al., 2014; Tavani et al., 2018; van Hinsbergen et al., 2020; Romagny et al., 2020; Angrand and Mouthereau, 2021). In this paper we have chosen to study and discuss the anisotropic behavior of Provence crust and its role on kinematic evolution of superimposed Provençal and the Subalpine fold-thrust belts (Fig. 1; Lemoine, 1972; Siddans, 1979).

The Provençal and southwestern Subalpine foreland thrust wedges have contrasting thrust vergences and time emplacement as recorded by structural data and well preserved syn-tectonic foreland strata. Both thrust wedges are characterized by a far-field transmission of the compressional stress into the most external zones that is still poorly characterized and not yet quantified because of complex overlap of extensional and compressional deformations (e.g., Baudemont, 1985; Tempier, 1987; Delfaud et al., 1989; Guieu and Roussel, 1990; Philip, 2012; Bestani et al., 2016; Tavani et al., 2018). Thrust-fold structures related to the Provençal compression develop at more than 180 km to the north from the Provence crystalline massifs (Fig. 1). They were described in the Valensole foreland basin (Dubois and Curneille, 1978), in the Castellane arc (de Lapparent, 1935; Goguel, 1937; Kerckhove and Antoine, 1963; Roux, 1968; Roux, 1970; Campredon and Giannerini, 1982), in the Barles area (Lemoine, 1972; Haccard et al., 1989b), and in the Baronnies-Dévoluy area (Gidon et al., 1970; Lemoine, 1972; Gidon and Pairis, 1976; Fabre et al., 1985; Montenat et al., 2005). Likewise, the occurrence of deformed Neogene to Quaternary rocks in southern Provence and the seismicity data, suggest far-field reactivation of inherited structures more than 100 km to the south to the Subalpine thrust front and as far as the Ligurian continental shelf (Guieu, 1968; Angelier and Aubouin, 1976; Weydert and Nury, 1978; Dupire, 1985; Hippolyte et al., 1993; Champion et al., 2000; Baroux et al., 2001; Chardon et al., 2005; Cushing et al., 2008; Béthoux et al., 2008; Larroque et al., 2021; Fig. 1).

Low-temperature thermochronology methods which are used to constrain the chronology of thrust propagation as in many fold-thrust belts (e.g., Ege et al., 2007; Jolivet et al., 2007; Espurt et al., 2011; Parra et al., 2012; Labaume et al., 2016; Rat et al., 2019; Hernandez et al., 2020), are poorly applicable in the study area because the Provençal and Subalpine thrust wedges have experienced insufficient Cenozoic burial and the exhumation history of the inner crystalline basement of the Provençal belt has been erased by the thermal event related to the Oligocene-Miocene Ligurian-Provençal rift (Lucazeau and Mailhe, 1986; Machhour et al., 1994; Morillon, 1997; Jakni, 2000; Bestani, 2015). The study of syn-tectonic strata with growth stratal pattern deposited during contractional deformations remains thus essential for reconstructing the chronology of successive deformational events, thrust propagation, and foreland basin evolution (Vergés and Munoz, 1990). This approach can be combined with fault slip analyses to constrain deformation regimes, thrust tectonic transport directions and particularly late fault reactivation in younger and in appearance undeformed foreland strata (Angelier, 1984, 1991). Balanced cross-section method has been used to restore compressional tectonic structures to their initial stages and the geometry of the basins before their deformation (Dahlstrom, 1969; Thomas and Bayona, 2002). Integration of precise timing of thrusting provided by syn-orogenic deposits with cross-section balancing can be a powerful tool for reconstructing shortening rates and restore deformation stages (Burbank and Vergés, 1994; Zapata and Allmendinger, 1996; Meigs and Burbank, 1997; Echavarria et al., 2003; Heermance et al., 2008; Li et al., 2010).

This paper is a review and analysis of the geology and structure of the Provençal and Subalpine thrust wedges in Central Provence. To decipher the complex multistage thrusting history in space and time of these superimposed thrust wedges, we built a 150 km-long balanced and restored cross-section across the widespread dissected Provençal Beausset, Arc and Rians foreland basins, and broad Alpine Valensole foreland basin (Fig. 1) using available

surface and subsurface data. Foreland syn-tectonic deposits and fault slip data allow us to validate an accurate kinematics model of crustal shortening budget. We discuss the role of pre-existing basement-cover heterogeneities, and we confirm their dominance on long-term tectonic evolution of the orogenic belts.

2. Structural framework

From the Mediterranean coast to the south, to the Baronnies-Barles area to the north (Fig. 1), the ~E-trending folds and thrusts mainly result from the ~northward Provençal compression (so-called Pyrenean-Provençal compression; Bertrand, 1888; Zürcher, 1891; Kilian, 1892; Lutaud, 1924; Philip and Allemann, 1982; Tempier, 1987). Shortening occurred from the Latest Santonian-Campanian to the Late Eocene (~50 m.y.) in response to the N-S convergence of the Eurasian and African plates through the Sardinia-Corsica continental block (Lacombe and Jolivet, 2005; Schreiber et al., 2011; Advokaat et al., 2014; van Hinsbergen et al., 2020; Fig. 2b). During Oligocene-Miocene times, the inner Provençal thrust wedge has been affected by the E-W opening of the West-European rift then the NW-SE opening of the Ligurian-Provençal back-arc basin between Provence and Corsica-Sardinia block (Hippolyte et al, 1993; Gattacceca et al., 2007; Bache et al., 2010; Oudet et al., 2010; Nury et al., 2016; Romagny et al., 2020; van Hinsbergen et al., 2020; Fig. 2c). A SW-ward migration of the Alpine deformation front into the southern Subalpine zone and Provençal zone occurred from the Oligocene-Miocene to the present day (~30 m.y.) in response to the eastward continental subduction of Eurasia beneath Adria (Fig. 2d). It is characterized by two major arcs detached above Triassic evaporites, the Diois-Baronnies-Western Provence Arc to the west and the Digne-Castellane Arc to the east (Goguel, 1937; Siddans, 1979; Villeger and Andrieux, 1987). These arcs are separated by the poorly deformed Neogene Valensole foreland basin (Figs. 1 and 2d). The thrust systems are accommodated by NNE-trending strike-slip faults (Middle Durance fault zone, Bès fault; Hippolyte et al., 2012; Guyonnet-

Benaize et al., 2015) inherited from the Paleozoic and Mesozoic extensional fault pattern (Roure and Colletta, 1996).

Many previous local studies have described the structural architecture of the thrust systems in the Provençal zone (Kilian, 1892; Mennessier, 1959; Aubouin and Mennessier, 1962; Aubouin and Chorowicz, 1967; Morabito, 1967; Guieu, 1968; Mennessier, 1970; Tempier, 1987; Bestani et al., 2015; Guyonnet-Benaize et al., 2015; Bestani et al., 2016; Espurt et al., 2019b), in the Valensole foreland basin (Dubois and Curneille, 1978; Hippolyte and Dumont, 2000) and in the Subalpine zone of the Digne-Castellane arc (Goguel, 1937, 1939, 1944; Unalan, 1970; Lemoine, 1972; Gigot et al., 1974; Debelmas, 1974; Giannerini, 1978; Siddans, 1979; Gidon and Pairis, 1992; Laurent et al., 2000; Graham et al., 2012; Célini et al., 2020). North of the Paleozoic basement units outcropping in the Maures and Tanneron-Estérel massifs (Figs. 1 and 3), the Provençal zone consists in strongly deformed Mesozoic sediments and upper Cretaceous-Eocene foreland sedimentary units covered in places by Oligocene and Miocene-Pliocene rocks. Southward, it shows ENE-trending thrust sheets (Bandol, Sainte-Baume, Etoile-Pierresca, Aurélien Mount) associated with two large synclines (Beausset and Arc; Bestani et al., 2015). Northward, the structures are characterized by E- to ESE-trending thrusts (Sainte-Victoire Mountain, Pourrières, Pallières, Vinon, Les Maurras and Gréoux) and small synclines (e.g., Rians and Saint-Julien) interfering with NW- to NNE-trending zones of middle-upper Triassic evaporitic-carbonate (e.g., Barjols or Carcès Triassic zones; Fig. 3). These Triassic sequences show significant internal fold systems and can be associated with halokinetic synclines (Angelier and Aubouin, 1976; Baudemont, 1985; Espurt et al., 2019b). Northward, Miocene-Pliocene sediments fill the Valensole foreland basin. Its morphology corresponds to a ~55 km long and up to ~30 km plateau dissected by Quaternary rivers (Gigot et al., 1974; Dubois and Curnelle, 1978; Mercier, 1979; Fig. 3). Westward, the basin is bordered by the NNE-trending Middle Durance fault system (e.g., Roure et al, 1992). This

fault controlled extensional subsidence to the northwest of the Manosque basin during the Mesozoic and the Oligocene, and transpressional uplift during its Miocene inversion (e.g., Roure and Colletta, 1996; Guyonnet-Benaize et al., 2015). Along the northern and northeastern edges of the Valensole foreland basin, Mesozoic to Neogene strata are deformed by SW-verging anticlines (e.g., Lambruissier, Mirabeau-Mallemoisson, Aiglun, La Maurière) and overthrusted by the SW-verging Digne Nappe and Castellane arc (Goguel, 1963; Gigot et al., 1974; Dubois and Curnelle, 1978; Faucher et al., 1988, Hippolyte and Dumont, 2000; Fig. 3).

3. Stratigraphy

The basement rocks and sedimentary successions in the Provençal and Subalpine zones are summarized in Figs. 4 and 5 and described hereafter.

3.1. Variscan basement and upper Paleozoic sedimentary successions

Paleozoic rocks are exposed in the Maures and Tanneron-Estérel massifs, Cap Sicié peninsula, and punctually in the eastern Provençal zone (Carcès) and Subalpine zone of Digne-Barles (St-Geniez, Verdaches and in tectonic slices at the base of the Digne Nappe) (Baudemont, 1985; Tempier, 1987; Guiomar, 1990; Crévola and Pupin, 1994; Fig. 3). In the Maures and Tanneron massifs, the Variscan belt is formed by E-verging thrust stacking of Cambrian-Silurian foliated metasediments including phyllites, micaschists and gneisses. The upper Carboniferous stage is associated with N-S orogen-parallel transpressional shearing synchronous with the opening of intramountain basin filled by terrigenous sediments and emplacement of granitoid and dome structures (Crévola and Pupin, 1994; Onézime et al., 1999; Rolland et al., 2009; Corsini et al., 2010; Schneider et al., 2014; Simonetti et al., 2020). During the continental break-up of Pangea, the Variscan framework was unconformably overlain by a more than 800 m-thick Permian detrital and volcanoclastic sequence

accumulated in a puzzle of intracontinental basins associated with NNE- to SE-trending steeply-dipping normal faults (Bathiard and Lambert, 1968; Baudemont, 1985; Delfaud et al., 1989; Toutin-Morin et al., 1993; Durand, 1993; Cassinis et al., 2003). Well data indicate a heterogenous distribution of the upper Carboniferous-Permian depocenters under the Mesozoic-Cenozoic cover of Provençal zone and Valensole foreland basin (e.g., Morabito, 1967; Bathiard and Lambert, 1968; Dubois and Curneille, 1978; Baudemont, 1985).

3.2. Triassic to upper Santonian Tethyan, Vocontian and South Provence rift successions

Paleozoic rocks are unconformably overlain by ~30-120 m-thick lower-middle Triassic white to red fluvial conglomerates and sandstones, and red-green argillites of the Buntsandstein facies (Fig. 4). The opening of the Tethys Ocean started with the deposition of a middle-upper Triassic succession of dolomite, marls, cargneules, halite, anhydrite, and gypsum layers. The Muschelkalk facies is 100 to 600 m-thick. This unit is composed by the lower Anhydrittgruppe evaporites mainly developed in Provençal domain (Fig. 4), and upper Muschelkalk limestones (Mennessier, 1959; Caron, 1979; Brocard and Philip, 1989; Toutin-Morin et al., 1993; 1994; Espurt et al., 2019b). It is overlain by dolostones and evaporitic marls of Keuper facies, 40 to 450 m-thick in Provence and more than 1 km-thick in the Digne basin (Arnaud et al., 1976; Baudrimont and Dubois, 1977; de Graciansky et al., 1989; Fig. 4). Rhaetian rocks consist of 30 to 80 m-thick alternation of limestones and yellow-green marls. Middle-upper Triassic successions also contain ankaratrite intrusions and volcanoclastic levels (Caron, 1970).

Sedimentologic and structural studies in Provence (Philip et al., 1987; Espurt et al., 2019b) and southern Subalpine zone (Coadou et al., 1971; Rousset et al., 1983; Dardeau, 1988; Mascle et al., 1988; Lemoine and de Graciansky, 1988; Haccard et al., 1989b; Graham et al., 2012; Célini et al., 2020) suggest that the Jurassic-Santonian succession is associated with significant thickness and facies changes due to syn-rift basement faulting, thermal subsidence

and local halokinetic motions of the ductile Triassic evaporite layers. From Jurassic to Barremian, the Provençal domain consisted in dominantly marine carbonates that built huge platforms (Léonide et al., 2007; Masse et al., 2009) including shallow marine limestones, dolomites, calcareous breccias and lower Cretaceous rudist-bearing limestones with Urgonian facies (Fig. 4). The thickness of this carbonate succession varies from 300 m to 1 km. These platform sequences are superseded by pelagic facies in the Digne basin during Jurassic times. Major subsidence of the Digne basin is recorded by the deposition of up to 1.4 km-thick of lower Jurassic pelagic shales (Coadou et al., 1971; Fig. 4). During Middle Jurassic, the subsidence reaches the Barles area with the deposition of more than 1.8 km-thick upper Bathonian-lower Oxfordian black shales and turbidites (Black Shales Formation). The overlying upper Jurassic-lower Cretaceous pelagic sediments attest for persisting subsidence associated with gravitational instabilities. It consists of ~220 m-thick upper Oxfordian clayed limestones and Kimmeridgian-Tithonian limestones covered by ~350 m-thick Berriasian-Barremian clayed limestones, breccias and turbidites (Rousset et al., 1983; de Graciansky and Lemoine, 1988; Célini et al., 2020).

From Latest Barremian to the beginning of Cenomanian and probably until Late Santonian, the opening of the Bay of Biscay is associated with the Valais Ocean through the Vocontian basin and led to NNE-SSW extension between Eurasia and Sardinia-Corsica block (Advokaat et al., 2014; Tavani et al., 2018; van Hinsbergen et al., 2020; Angrand and Mouthereau, 2021; Fig. 2a). During this period, the uplift of the Durance high separates the Digne-Barles basin to the north from the Beausset basin to the south. The Beausset basin can be interpreted as the eastern prolongation of the Pyrenean Rift System (Philip et al., 1987; Hennuy, 2003; Bestani et al., 2016; Tavani et al., 2018; Floquet et al., 2021; Angrand and Mouthereau, 2021; Fig. 2a). ~350 m-thick of Aptian-Albian pelagic black shales and gravitational deposits accumulated in the southern edge of the Beausset basin (Philip et al., 1987), overlain by ~1.1

km-thick Cenomanian-Santonian marine rudist-rich carbonate including siliciclastic sediments (e.g., La Ciotat conglomerates) deposited into local troughs sourced from an emerged basement paleo-high between the Provence and the Sardinia-Corsica block (Philip, 1970; Hennuy, 2003; Floquet et al., 2005, 2006). Northward, middle Cenomanian-upper Santonian sediments progressively onlap the Durance high from the Beausset basin to the southern edge of the Arc basin (Fig. 4). The Durance high corresponds to a large E-trending dome with low relief associated with major subaerial erosion and bauxite formation from uppermost Albian to lowermost Cenomanian at least, and till Santonian (Aubouin and Chorowicz, 1967; Masse and Philip, 1976; Laville, 1981; Guyonnet-Benaize et al., 2010; Figs. 2 and 4). North of the Durance high, Aptian-Albian deposits reach ~170 m-thick in the Digne-Barles basin (Rousset et al., 1983; Friès, 1987; Haccard et al., 1989b; Breheret, 1995), and consist of marine black shales. The overlying Cenomanian-Santonian strata dominantly consist of more than 1.5 km-thick marine marls and limestones in the Digne basin (Rousset et al., 1983).

3.3. Uppermost Santonian to Eocene foreland successions in Provençal zone

Plate reconstructions suggest the onset of N-S convergence between Africa and Eurasia that led to the contraction of Corsica-Sardinia block and Provence (Advokaat et al., 2014; van Hinsbergen et al., 2020; Angrand et Mouthereau, 2021; Fig. 2b), as illustrated by the transition from marine to continental environment in Latest Santonian in the Beausset basin. The growth of Provençal belt initiates at ~84 Ma and continues until the Late Eocene toward the north (Philip, 1970; Philip et al., 1987; Tempier, 1987; Lemoine et al., 2000; Lacombe and Jolivet, 2005; Montenat et al., 2005; Espurt et al., 2012; Philip et al., 2017). The Provençal foreland succession is characterized by local continental facies dated by magnetostratigraphy (Westphal and Durand, 1990; Cojan et al., 2003) and biostratigraphy (Garcia and Vianey-Liaud, 2001; Philip et al., 2017). Upper Cretaceous-lower Eocene

foreland sequences are exposed in the Beausset, Arc, Rians, Saint-Julien and Esparron-de-Verdon basins (Fig. 4). They are described in Fig. 5a. The Valdonnian and Fuvelian facies are of Latest Santonian-Early Campanian age and correspond to lacustrine and palustrine black limestones units including lignite beds (Fabre-Taxy and Philip, 1964; Durand, 1980; Fig. 5a). The Begudian facies is of Middle Campanian age and consists in lacustrine and fluvial deposits. The Rognacian facies is of Late Campanian-Maastrichtian age. It consists in dinosaur eggshells and bones-bearing red marls, sandstones and Rousset lacustrine limestone deposits (Cojan, 1989; 1993; Garcia and Vianney-Liaud, 2001). In the Arc basin, the Cretaceous-Cenozoic boundary is located inside the Galante Formation, a 5-10 m-thick fluvial conglomerates made of well-rounded pebbles of basement quartzite sourced from the Maures massif (Durand, 1962; Cojan, 1993). The Danian corresponds to the Vitrollian facies with red silty marls including lacustrine microcodium limestones. The Selandian-Thanetian Bird Eggshells Marls Formation comprises the lacustrine limestones of Meyreuil and Saint-Marc in the Arc basin. In the Rians basin it also includes the Touars conglomerates with clasts derived from the Maures massif. The Ypresian period includes deposition of the Langesse limestone and red-grey marls with gypsum in the Arc basin, and the fluvial Bluish Sands Formation including lacustrine Bithynia bearing limestones in the Rians basin and High Var area (de Lapparent, 1938a, 1938b; Corroy, 1957; Durand and Tempier, 1962; Angelier, 1971; Philip et al., 2017; Fig. 1). Finally, the Lutetian consists in Montaiguet and Cuques lacustrine limestones cropping out in the Arc basin. The upper Cretaceous-Eocene continental sequences of the Provençal foreland basin include locally massive syn-orogenic alluvial-fan deposits with growth strata recording thrust activity (Durand and Tempier, 1962; Guieu, 1968; Angelier, 1971; Leleu et al., 2009; Espurt et al., 2012). They correspond to upper Cretaceous Begudian-Rognacian breccias and Paleocene microcodium breccias with clasts derived generally from the nearby Jurassic-Cretaceous growing reliefs (Fig. 5a).

3.4. Oligocene syn-rift and Miocene post-rift successions in Provençal zone

The Oligocene is a transitional period between the end of the Provençal compression and the initial growth of the southern Subalpine zone (Nury, 1988). In the south and east of the study area, the Provençal compressional structures were affected by the E-W opening of the West-European rift then the NW-SE opening of the Ligurian-Provençal back-arc rift between Provence and Corsica-Sardinia block (Hippolyte et al, 1993; Gattacceca et al., 2007; Advokaat et al., 2014; van Hinsbergen et al., 2014; Bestani et al., 2016; Nury et al., 2016; Romagny et al., 2020, van Hinsbergen et al., 2020; Fig. 2c). The result of these successive extensional events is the formation of large intracontinental basins like the Marseille, Aubagne, Aix-en-Provence, and Manosque basins (Fig. 3; Hippolyte et al, 1993). Smaller Oligocene basins developed in southeastern Provence. They are the NE- to E-trending Bandol, Signes-Méounes, Peypin, Saint-Zacharie and Nans basins/troughs (Popoff, 1973; Nury, 1988) (Figs. 3, 4 and 5a). In the High Var area (Fig. 1), Oligocene sediments fill N- to NNW-trending narrow basins (Touraine, 1967; Angelier, 1971; Angelier and Aubouin, 1976; Giannerini, 1978; Philip et al., 2017) like the La Combe, Bourdas and Plan d'Auron troughs (Figs. 3, 4 and 5a). In the overall, syn-rift sediments correspond to lacustrine and clastic deposits including marls and locally gypsum intercalations as in the Manosque basin (Fig. 3), but the subsidence rate was ten times larger during the Ligurian-Provençal rifting than during the West-European rifting (Hippolyte et al., 1993).

The drifting of the Ligurian-Provençal basin associated with the counterclockwise rotation of the Corsica-Sardinia block during the Miocene times led to the flooding of the inner Provençal basement thrust wedge (Guieu and Roussel, 1990; Hippolyte et al, 1993; Gattacceca et al., 2007; Oudet et al., 2010; Bestani et al., 2016; Nury et al., 2016). In the onshore domain, Miocene (Burdigalian(?) to Tortonian) continental strata with marine intercalations filled N- to NW-trending incised valleys and basins (e.g., Les Maurras, Barjols,

Nans, Signes/Méounes and Bandol). These deposits consist of basal red breccias, sandstones and marls, and upper fluvial conglomerates (Mennessier, 1959; Cornet, 1965; Angelier and Aubouin, 1976) generally originated from the erosion of nearby Jurassic reliefs (Les Maurras basin) or from the Maures massif (Nans basin) (Figs. 3 and 4; Cornet, 1961). In the west of the study area (Luberon-Nerthe; Fig. 1), shallow marine environment is associated with the formation of concomitant wave-cut platforms overlain by marine molasse including limestones and grainstones (Champion et al., 2000; Besson, 2005; Oudet et al., 2010). Basaltic clasts related to Messinian intrusions and lava flows of Evenos are found in the upper conglomerate sequences (Pliocene?) of the Bandol basin (Coulon, 1967; Baubron, 1984). Pliocene to Quaternary sediments are mainly found within paleo-valleys that were incised during the Messinian and then filled by Gilbert type deltas after the reflooding of the Mediterranean Sea at 5.46 Ma (Clauzon, 1978; 1982, Bache et al., 2012).

3.5. Cenozoic foreland successions in Subalpine zone: Barles zone and Valensole foreland basin

In the Barles zone, folded Mesozoic sequences are unconformably overlain by the poorly dated (upper Eocene-lower Oligocene?) continental Basal Breccia Formation (Lemoine, 1972; Haccard et al., 1989a,b; Fig. 5b). It is composed of breccia channels interbedded with red shales. The breccia channels are composed of clasts and olistoliths, exclusively sourced from local Jurassic and Cretaceous limestone strata, included in a red shaly matrix with microcodium (Gigot et al., 1974; Haccard et al., 1989b). The Basal Breccia Formation is interpreted as sedimentary drape sequences (with differential compaction) sealing the paleo-morphology of E-trending Eocene Provençal folds (Lemoine, 1972; Maillart et al., 1987; Haccard et al., 1989b). However, the breccia beds also exibit large sedimentary fans which could be interpreted as growth strata deformed by progressive tectonic uplift (Maillart et al., 1987). The Basal Breccia Formation might be laterally equivalent to upper Eocene

nummulitic limestones deposited immediately to the east in the Digne-Castellane basin (Haccard et al., 1989b; Fig. 4) or post-date it and of Early Oligocene age (Lichorish and Ford, 1998).

The growth of the southwestern Subalpine zone started during the Oligocene and continued throughout the Neogene. Oligocene rocks belonging to the Barles zone and northern edge of the Valensole basin consist of basal fluvial sandstone and red clay named as the Red Continental Molasse Formation and the upper brackish deposits named as the Grey Molasse Formation (Haccard et al., 1989b; Fig. 5b). This succession reaching more than 450 m-thick is interpreted as deposited as the distal foreland sediments of the inner Alps (Maillart et al., 1987; Gidon, 1997; Ford et al., 1999). Like the Basal Breccia Formation, the Red Continental Molasse Formation includes large sedimentary fans in the Barles zone and northern edge of the Valensole basin which could be interpreted as growth strata deformed by progressive limb rotation (Gidon, 1997). The Valensole foreland basin is then filled by more than 3 km-thick marine to continental Miocene-Pliocene strata with strong facies and thickness variations (Gigot et al., 1974; Gidon and Pairis, 1988; Haccard et al., 1989a,b; Clauzon et al., 1989; Cojan et al., 2013). It is connected westward to the Forcalquier and Cucuron-Pertuis basins (Fig. 3). Field studies and well data in the center part of the basin give a global insight of the Miocene-Pliocene sedimentary succession and architecture (Dubois and Curnelle 1978; Clauzon et al., 1989; Couëffe et al., 2004; Besson, 2005; Figs. 4 and 5b). The transgressive Aquitanian-Burdigalian Lower Marine Molasse Formation consists in tidal facies deposited in major subsiding environment that pass northward into siliciclastic deposits sourced from the inner Alps domain (Couëffe et al., 2004). The Langhian to Tortonian-lower Messinian succession is composed of marls, coarse-grained sandstones and limestones alternations of the Upper Marine Molasse Formation that pass laterally to prograding fluviodeltaic conglomerate sequences of the Valensole 1 Formation (Beaudouin et al., 1966, 1970; Dubois and Curnelle

1978; Mercier, 1979; Aguilar and Clauzon, 1981; Haccard et al., 1989b; Clauzon et al., 1989; Besson, 2005; Cojan et al., 2013; Fig. 5b). The Valensole 1 Formation comprises Durance conglomerates rich in siliciclastic clasts westerly sourced by the paleo-Durance river and Subalpine conglomerates rich in local Mesozoic limestone clasts easterly sourced (Haccard et al., 1989b). The Valensole 2 Formation mainly consists of marine clay and continental deposits (conglomerates, sandstones and claystones) of Pliocene to Quaternary age (Clauzon, 1979; Mercier, 1979; Clauzon et al., 1989). Locally, near Oraison (Fig. 3), a Messinian canyon was mapped by Dubar (1983, 1984). It allows the distinction between the Valensole 1 and Valensole 2 Formations, separated by a major discontinuity, the Messinian Erosional Surface (Mercier, 1978, 1979; Clauzon, 1979; Dubar, 1983, 1984; Clauzon, 1996). The Tanaron Formation is the youngest stratigraphic level in the footwall of the Digne Nappe (under the La Robine half-klippe) in the northern edge of the Valensole foreland basin (Gigot et al., 1974; Figs. 3 and 5b). The age of the Tanaron Formation is still a matter for debate. It is composed of mixed massive olistoliths (Triassic gypsum, Callovian-Oxfordian black shales, upper Jurassic-lower Cretaceous limestones, upper Eocene-Oligocene continental molasses and Miocene marine molasse) mainly sourced from the collapse of the Barles fold zone (Gigot et al., 1974). Rare olistoliths of upper Cretaceous carbonates and nummulitic limestones are interpreted to come from the erosion of the Digne Nappe (Haccard et al., 1989b). The olistoliths are included in grey-red marls and sandstones. Gigot et al. (1974), Crumeyrole et al. (1991) and Hippolyte et al. (2011) pointed out that the Tanaron Formation infills a very large scale erosional feature. At a time where the Valensole conglomerates were considered as Pliocene, Gigot et al. (1974) assigned a Late Pliocene age to the overlying Tanaron Formation. The geological map (Haccard et al., 1989a,b) ascribes a Latest Pliocene age for this formation. However, Gidon and Pairis (1988, 1992) emphasized that the Tanaron Formation is not dated biostratigraphically. The mapping of Messinian-Zanclean paleo-

valleys around Digne revealed that a Zanclean erosional surface has truncated the Tanaron Formation at La Bonnette and constrains the age of this formation as older than the Late Pliocene (Hippolyte et al., 2011). Furthermore, these authors suggested that if the erosional surface at the base of the Tanaron Formation was the Messinian Erosional Surface related to the desiccation of the Mediterranean basin at 5.6 Ma (Clauzon et al., 1996; Bache et al., 2012; Roveri et al., 2014) the age of the Tanaron Formation would be Late Miocene to Early Pliocene (Hippolyte et al. 2011).

3.6. Décollement levels

Inherited Variscan metamorphic foliation and upper Carboniferous-Permian extensional faults controlled décollement in the basement as observed in the Cap Sicié and Maures massifs and also suggested by subsurface data under the Provence cover (Tempier, 1987; Roure and Colletta, 1996; Cushing et al., 2008; Espurt et al., 2019b). The Paleozoic framework was intermittently reactivated during the Mesozoic rifting and during the Provençal and Alpine shortening episodes. The basal Muschelkalk and Keuper units are interpreted as main regional decollement levels of the sedimentary cover above the Paleozoic-Triassic (Buntsandstein) basement (Bathiard and Lambert, 1968; Caron, 1979; Gidon, 1982; Gidon and Pairis, 1992; Fig. 4). This middle-upper Triassic evaporitic-carbonate package shows major thickness variations related to local depocenters during rifting or tectonic duplication and disharmonic deformations during the compressive stages (Goguel, 1939; Bathiard and Lambert, 1968; Gigot et al., 1974; Toutin-Morin et al., 1993, 1994; Baudemont, 1985; Espurt et al., 2019b). Middle Jurassic black shales, upper Jurassic-Berriasian limestones and Oligocene-Miocene sequences (Fig. 4) promote disharmonic deformations with internal folding and shearing particularly in the Barles and Vélodrome structures (Gidon and Pairis, 1992).

4. Cross-sectional structural architecture

To illustrate the structural architecture of the Provençal and Subalpine thrust wedges, we constructed a 150 km-long crustal-scale cross-section from the Mediterranean coastal zone to the south to the Digne-Barles region to the north (Figs. 3 and 6). The cross-section trends N175°E in the coastal basement units and the Beausset basin, then N002°E across the Sainte-Baume Nappe and Aurélien Mount thrust, and finally N024°E across the northern Provençal thrusts, Valensole basin up to the Digne Nappe. This section was constructed according to thrust tectonics concepts (e.g., Dahlstrom, 1969; Hossack, 1979; Elliot, 1983; Suppe, 1985). The section is localized in a zone only weakly affected by the Oligocene rifting (Bestani et al., 2016). We used existing 1:50,000 geological maps of French Geological Survey (BRGM) and new surface structural data from several fieldworks. We also used existing cross-sectional data of Kilian (1892), Goguel (1939, 1944), Morabito (1967), Gigot et al. (1974), Debelmas, 1974; Dubois and Curnelle (1978), Combes (1984), Haccard et al., 1989b; Gidon and Pairis (1992), Hippolyte and Dumont (2000), Guyonnet-Benaize et al. (2015), Bestani et al. (2015, 2016) and Célini et al. (2020). Thrust geometries at depth and basement geometry have been constrained using exploration wells and geophysical data. We used nine major exploration wells (from south to north: Gréoux (G3, G2, G1, G4, S1, S4), Les Mées (LM1), and Mirabeau (M1, M2)) some of them (G1, S1, LM1, M2) reaching the Paleozoic substratum (Fig. 3). We interpreted two seismic reflection profiles, VL85-P and 75DV-2, that cover the central-southern part of the Valensole basin over a distance of ~28 km. These profiles have been reprocessed by Agence de l'Eau Rhône Méditerranée Corse and available for this study (Fig. 3). A time-depth conversion of seismic profiles was performed using the MOVE software and seismic velocities of sedimentary intervals provided by BRGM. Finally, fault location at depth is interpreted by some present day deep-located earthquakes (Cushing et al., 2008).

In the southern part of the Provençal zone, the cross-section trace located between the Cap Sicié and the Aurélien Mount thrust follows the section of Bestani et al. (2015) (Figs. 3 and

6). This section has been updated from previous version in terms of displacement magnitude of the thin-skinned thrust sheets and basement deformations based on new structural interpretations and new geological mapping (Laville et al., 2018). Because the section trace is located lateral to the Cap Sicié peninsula (~10 km to the east), its thrust geometry has been projected onto the section. To the north of the Aurélien Mount thrust, the cross-section has been fully constructed for this study and is presented for the first time (Fig. 3). The proposed balanced cross-section is one possible construction, but it is the most realistic solution consistent with the available surface and subsurface structural data presented in this work.

The construction, balancing and restoration of the cross-section were performed with the MOVE structural modeling software following thrust tectonic concepts and flexural-slip algorithm assuming constant bed length and thickness (Dahlstrom, 1969; Boyer and Elliott, 1982; Suppe, 1983; Suppe and Medwedeff, 1990). For the middle Jurassic black shales, and Oligocene-Miocene sequences, in zone where these ductile units promote strong internal deformations (Barles folds and Vélodrome), we assumed an area balance approach (e.g., Mitra and Namson, 1989; Mitra, 2002; Butler, 2013; Butler et al., 2020). For the ductile middle-upper Triassic evaporitic-carbonate units which may move in three dimensions (and their volumes can change as a result of dissolution, fluid migration and surface erosion during successive stages deformation and diapirism), we also achieved as much as possible an area balance approach. For deep crustal level, we also assumed an area balancing approach. The orientation of the cross-section is orthogonal to the trend of the structures of both orogenic systems (see section 6). No major strike-slip fault system is crossed except in the Huveaune zone (Fig. 3; Guillemot et al., 1973; Philip, 2018).

4.1. The Provençal zone

4.1.1. Surface structure

The surface structure of the Provençal zone is described from south to north, i.e., from the inner coastal basement units (preserved from the Ligurian-Provençal rifting) and thrust sheet domain, to outer thrust systems of High Var (Fig. 6a,b).

The Cap Sicié peninsula is formed by two imbricate thrusts. The upper N-verging Cap Sicié thrust is composed of Variscan phyllites and quartzites covered by N-dipping lower-middle Triassic strata to the north (Fig. 7a-c). The Cap Sicié thrust is folded by the lower Saint-Mandrier thrust leading to the formation of the Saint-Mandrier half-window (Zürcher, 1893; Haug, 1925; Tempier, 1987), made of lower-middle Triassic and Permian strata at the surface (Figs. 6b and 7a,c,d) and Variscan phyllittes and quartzites at depth.

North of the Cap Sicié basement imbricate, the sedimentary cover of the Provençal zone is detached northward above ductile middle-upper Triassic layers and associated Triassic highs (Gouvernet, 1963; Bathiard and Lambert, 1968; Tempier, 1987; Bestani et al., 2016; Espurt et al., 2019b). The Bandol cover thrust including the Bandol syncline is transported at the front of the Cap Sicié thrust. The Bandol thrust is emplaced above the Saint-Cyr Triassic high where lower Santonian carbonates unconformably overlain middle Triassic limestones (Philip, 1967; Philip et al., 1985, 1987; Espurt et al., 2019b; Fig. 8). Klippen of Triassic rocks of the Bandol thrust rest on upper Santonian and lower Campanian (Valdonnian-Fuvelian facies) strata of the Beausset syncline (Bertrand, 1887; Gouvernet, 1963) (Fig. 3). The Sainte-Baume Nappe transported northward the Beausset syncline (Fig. 9; Guieu, 1968; Bestani et al., 2015; Philip et al., 2018; Philip, 2019). Its hanging wall ramp consists in upper Triassic to lower Cretaceous strata dipping 10°-15° southward, deformed by out-of-sequence thrusts (Fig. 9c; Bestani et al., 2015). Its footwall is constituted by the tight Plan d'Aups syncline cored by lower Campanian strata (Fuvelian facies), Pic des Corbeaux anticline, and broad La Lare anticline mantled by upper Jurassic limestones. Small klippen of Jurassic and Barremian rocks in the Huveaune zone (Saint-Zacharie and Nans basins) indicate the northward advance

of the Sainte-Baume Nappe (Figs. 3 and 6b; Guieu, 1968). The substratum of the Huveaune zone is constituted by middle-upper Triassic rocks and relatively thin Jurassic sequences which are unconformably covered by upper Cretaceous (Valdonnian-Fuvelian and Begudian-Rognacian facies) and Oligocene strata (Fig. 3; Philip, 2018, 2019). The Aurélien Mount thrust transported northward Jurassic limestones above the Arc syncline (Figs. 6b and 10; Aubouin and Chorowicz, 1967; Guieu, 1968; Popoff, 1973). The hanging wall ramp of the Aurélien Mount thrust shows Jurassic strata dipping 12° southward. The Sainte-Baume Nappe and Aurélien Mount thrust, and southern limb of the Arc syncline are cut by NE-trending normal faults (Bestani et al., 2016). This normal faulting is contemporaneous with opening of the Aubagne, Peypin, Saint-Zacharie and Nans extensional basin framework during the Oligocene (Figs. 3 and 6b; Nury, 1988; Hippolyte et al., 1993).

The surface and well data show that the Arc basin is an asymmetrical syncline characterized by a N-thinning sedimentary wedge in first lower Santonian rudist carbonates, then upper Santonian-lower Campanian (Valdonnian-Fuvelian) to middle Campanian-Maastrichtian (Begudian-Rognacian) continental syn-orogenic facies (from ~1.1 km-thick to the south, to less than 250 m-thick to the north; Fig. 6b). The core of the syncline is constituted by ~200 m-thick flat Danian to Ypresian strata that form the Cengle plateau (Figs. 3 and 11a). Along the section, the Arc syncline is transported northward above the Pourrières thrust constituted by 12° S-dipping Jurassic-lower Cretaceous strata (Fig. 11a). The Pallières thrust system transports northward the Ollières syncline cored by upper Santonian-Campanian (Valdonnian-Fuvelian-Begudian) continental facies strata. (Fig. 6b). The Pallières thrust system is composed by two units. The upper unit corresponds to a ~5° S-dipping homocline made of upper Jurassic-lower Cretaceous limestones. The lower unit involves upper Jurassic limestones unconformably covered by Danian Microcodium breccias (Fig. 11c). The Pallières thrust system overthrusts northward the E-trending Rians syncline filled by more than 700 m-

thick Danian to Ypresian syn-orogenic package including massive alluvial fan deposits (Fig. 11c; Tempier, 1963; Mennessier, 1970; Angelier, 1971; Angelier and Aubouin, 1976; Philip et al., 2017). The Pourrières and Pallières thrusts form the eastern continuation of the bi-verging Sainte-Victoire Mountain thrust system, while to the east they branch into the Barjols Triassic zone (Figs. 3 and 11a,b). The N-verging Vinon thrust includes the Mont-Major anticline locally thrusting southward the northern flank on the Rians syncline and Triassic evaporite-cored anticline of Valavés (Figs. 3 and 6b; Mennessier, 1970). Northward, the Vinon thrust dips 12° to the south and emplaces upper Jurassic limestones on Paleocene strata of the Saint-Julien syncline (Fig. 12a). The geometry of the N-verging Les Maurras thrust is revealed by the well G2 and by intensively sheared Oxfordian marly limestones as observed in the field (Fig. 12b). The Les Maurras thrust is unconformably covered by poorly deformed red sandstones and thick breccias layers, and Pliocene conglomerates of the Valensole Formation. Eastward, the footwall of the Les Maurras thrust is constituted by the La Mourotte syncline filled by Paleocene and Ypresian strata (Fig. 3; Mennessier, 1970; Angelier and Aubouin, 1976). Finally, the N-verging Gréoux thrust emplaced lower Jurassic rocks over lower Cretaceous limestones and Paleocene strata of the Esparron-de-Verdon syncline (Fig. 12c). This thrust dips ~10° southward at surface and increases at depth at ~33° southward as revealed by the exploration wells G1 and G2 (Morabito, 1967). The thrust systems of northern Provençal zone are later cut by NW-trending normal faults (e.g., Ginasservis fault) which are associated with the development of La Combe, Bourdas, Plan d'Auron basins filled by Oligocene sediments (Fig. 3; Angelier and Aubouin, 1976; Philip et al., 2017).

The southern Provençal zone shows locally inherited Mesozoic halokinetic structures associated with normal faults previously described by Bestani et al. (2015) and Espurt et al. (2019b) as the Saint-Cyr and Huveaune Triassic highs. The northern Provençal zone connects eastward with the large Triassic depression of Barjols including halokinetic structures (Fig.

3). Along the cross-section, upper Jurassic-lower Cretaceous strata of the Pourrières thrust depict growth wedge geometry and faulting, suggesting that this thrust could be superimposed on an early SW-dipping normal fault zone with halokinetic movement of Triassic evaporites at depth (Figs. 3 and 6b). Similarly, well data show strong thickness variations in upper Jurassic carbonates into the Les Maurras thrust (Fig. 12d), suggesting early halokinesis.

4.1.2. Deep structure

Cross-section construction suggests that the Provençal zone is characterized by a heterogenous geometry of the basement-cover interface resulting from basement inheritance and basement-involved shortening. The basement of Provençal zone shows two styles of deformation along the cross-section (Fig. 6b). Southward, low-angle basement thrusts (Cap Sicié and Saint-Mandrier thrusts, and deeper thrust under the Sainte-Baume Nappe) propagate through the Variscan metamorphic foliation or inherited shear zones (Espurt et al., 2019b). The extensional geometry of the upper Carboniferous-Permian basins at depth is well preserved as imaged by E- and N-trending seismic profiles, for instance, in the Luc basin at the northwestern flank of the Maures massif (Fig. 13; Baudemont, 1985). The basins mainly correspond to half-grabens filled by more than 1 km-thick upper Carboniferous-Permian strata and associated with WNW- to NNW-dipping normal faults. These faults inherited from the rifting of Pangea can have been locally reactivated during the Mesozoic rifting events (Toutin-Morin et al., 1993, 1994; Espurt et al., 2019b). During the Provençal shortening, the extensional features were cut and transported passively above N-verging basement thrusts (Bathiard and Lambert, 1968; Baudemont, 1985; Tempier, 1987; Espurt et al., 2019b). The shortening of the basement thrusts fed the slip of cover thrusts of the southern Provençal zone (Bandol, Sainte-Baume and Aurélien Mount). In the northern Provençal domain, field and geophysical data, and cross-section constructions (Biberon, 1988; Roure and Colletta, 1996; Espurt et al., 2012, 2019) allow to infer the geometry and depth of the basement cover

interface. These data also suggest a heterogenous distribution of the upper Carboniferous-Permian to Triassic depocenters. The base of the Arc syncline is inferred at ~2.2 km bsl and the base of the Rians syncline at ~1.7 km below sea level (bsl). At the boundary between the Provençal zone and Valensole basin (footwall of the Gréoux thrust), the basement depth is located at ~1.4 km bsl. Surface data and cross-section construction suggest that the Paleozoic basement is located at a shallow depth (~800 m bsl) under the Valavès Triassic anticline. Contrary to the south, the basement structure of northern part of Provençal zone is interpreted as half-grabens delimited by major NE-dipping faults (Fig. 6b). These basement thrusts are interpreted as short-cut thrusts propagating through inherited upper Carboniferous-Permian to Triassic half-grabens (Espurt et al., 2012; 2019b). In this zone, shallow-depth earthquakes are observed (e.g., Valavés anticline; Figs. 3 and 6a). They could be tectonically connected with deeper events occurring along basement faults as suggested by cross-section construction (Cushing et al., 2008).

4.2. The Subalpine zone: Digne Nappe, Barles fold system and Valensole foreland basin

4.2.1. Surface structure

The Digne Nappe, Barles fold system and northern edge of the Valensole basin are well exposed in a N-S section along the Bès valley (Figs. 3 and 14). The stratigraphy and the main tectonic structures along this valley have been described for a long time by geologists (e.g., Goguel, 1939, 1944; Debelmas et al., 1970, 1974; Lemoine, 1972; Gigot et al., 1974; Gidon, 1982, 1989; Debelmas et al., 1983; Gidon and Pairis, 1986, 1988, 1992; Haccard et al., 1989b). This area around the Barles village became famous for fieldworks with students coming from national and international universities. More recent studies discussed the timing of deformation (Fournier et al., 2008; Hippolyte et al., 2011) and tried to decipher Jurassic salt tectonics through an overprint of Cenozoic contractional tectonics (Graham et al., 2012;

Célini et al., 2020). The surface structure of the Subalpine zone is described from north to south, i.e., from the inner Digne-Barles units to Valensole foreland basin.

The Digne Nappe involves a thick (up to 4.5 km) Jurassic-Cretaceous pelagic succession initially deposited in the Digne basin, and covered by Eocene-Oligocene strata northeastward (Fig. 4; Goguel, 1944; Rousset et al., 1983). The paleo-temperature (~100 °C) recorded by Oligocene-Miocene rocks in the footwall of the Digne Nappe indicates that the thickness of the Digne Nappe was about 2.9 km above the Barles tectonic half-window (Schwartz et al., 2017a,b; Figs 6c and 14). The Digne Nappe involves locally basement tectonic slices (Fig. 15) and internal folding (Guiomar, 1990). It is regionally detached SW-ward above a thick Triassic evaporitic-carbonate layer and overthrusts the Barles fold system and the northeastern edge of the Valensole foreland basin (Figs. 6c and 14). North of Digne, its frontal part is constituted by the syncline-shaped La Robine half-klippe which overlies the upper Miocene-lower Pliocene sequences of the Thoard syncline. Northward, the hanging-wall of the Digne Nappe displays a large antiform, leading to the formation of the erosional Barles half-window (Figs. 6c and 14). Along the cross-section, the Digne Nappe roots north of the Verdaches anticline in thin layer of middle-upper Triassic strata. The E-trending asymmetric Verdaches anticline is underlined by middle Triassic limestones and basal Triassic sandstones which unconformably overlain upper Carboniferous coal and sandstone beds (Figs. 6c and 15; Haccard et al., 1989b; Guiomar, 1990). The northern backlimb dips 10° northward while the southern forelimb dips 25° southward. The structure of the Barles antiform corresponds to very tight anticlines (La Petite Cloche, La Grande Cloche and La Maurière anticlines along the cross-section) mantled by upper Jurassic-lower Cretaceous limestones and cored by Callovian-Oxfordian black shales (Fig. 14). The anticlines are bounded by synclines cored by uppermost Eocene-Oligocene strata that unconformably overlain Mesozoic sequences (Fig. 16; Lemoine, 1972; Gidon, 1982; Haccard et al., 1989a).

Cross-section construction suggests that the Barles fold system is detached southward above middle-upper Triassic strata (Fig. 6c). The La Petite Cloche thrust transports southward the Les Sauvans syncline filled by thick Callovian-Oxfordian black shales (Fig. 6c). Its vertical to overturned northern limb is the Barre de Chine armed by ~200 m-thick lower Jurassic limestones overlain by a huge volume of Triassic shales, cargneules and gypsum of the Barles diapir (Arnaud et al., 1976; Haccard et al., 1989a; Gidon and Pairis, 1992; Graham et al., 2012). Although the Barles fold zone and Digne Nappe recorded strong contractional deformation, field data show structural evidence of pre-existing halokinetic structures and normal faulting (Gidon, 1982). For instance, the minibasin structures in La Robine half-klippe and of the Les Sauvans syncline-Barre de Chine flap are interpreted as resulting from halokinetic motion of Triassic evaporites during the Jurassic-Early Cretaceous times (Graham et al., 2012; Célini et al., 2020).

South of the Barles anticlines, the three-dimensional Vélodrome syncline develops, involving mainly Miocene rocks (Marine Molasse and Valensole 1 Formations) unconformably covered by the olistolithic Tanaron Formation (Fig. 14). This complex structure exibits important contractional growth strata along syncline limbs with fold-accommodation faults including out-of-syncline thrusts and disharmonic folding (Goguel, 1939; Gigot et al., 1974; Pairis and Gidon, 1987; Gidon, 1989; Gidon and Pairis, 1992). Recently, it has been speculated that the three-dimensional structure of the Vélodrome may correspond to a Miocene minibasin that sank into a hypothetical Oligocene salt layer (Célini et al., 2020; Célini, 2020). The Vélodrome structure corresponds to the northern limb of the Thoard syncline. The thickness of the Miocene-Pliocene syn-tectonic deposits increases southward, from 1 km in the Vélodrome to more than 3.3 km in the core of the Thoard syncline (Figs. 6c and 17). This syncline is transported southward onto the Aiglun and Mirabeau-Mallemoisson S-verging fault-propagation folds armed by Miocene conglomerate

beds and probably detached in Triassic strata. The northern Aiglun anticline displays a backlimb dipping 35-40° northward and a forelimb dipping 70° southward (Fig. 18a). The southern Mirabeau-Mallemoisson anticline has a 40° N-dipping backlimb and a vertical forelimb (Fig. 18b). Well data indicate that this later is associated with a thrust dipping 38° northward. Well data also reveal that a sub-thrust develops in the footwall block. South of the Bléone river (Fig. 3), Miocene strata are deformed by the Quaternary Lambruissier fold-propagation fault (Hippolyte and Dumont, 2000) probably detached in the upper Triassic strata. It is characterized by a 10-15° N-dipping backlimb and a 80° S-dipping forelimb. The displacement on Lambruissier thrust decreases rapidly westward, explaining why it is not visible in map view as well as in subsurface data near Les Mées borehole (Figs. 3 and 19). Southward, the Valensole foreland basin is filled by upper Miocene conglomerates of the Valensole 1 Formation topped by the Valensole 2 Pliocene Formation whose surface forms the slightly S-dipping Puimichel plateau (Fig. 18c). In the southern edge of the Valensole basin, upper Miocene-Pliocene rocks lie unconformably on lower Cretaceous strata.

4.2.2. Deep structure

In the southern part of the Valensole basin, reprocessed seismic reflection profiles and well data have been used to interpret the geometry of hidden thrust systems under the Miocene-Pliocene sedimentary infill (Fig. 19). The seismic profile 75DV-2 confirms that the Miocene strata are unconformably deposited on top of a deep basement high, the Les Mées high, underlined by folded Mesozoic strata with a thin (less than 30 m-thick) Triassic succession (Dubois et Curnelle, 1978). The uplift of the Les Mées high is controlled by a N-dipping basement ramp proved by subsurface data (Dubois and Curnelle, 1978). The basement ramp branches upward into the Triassic strata then splits into two S-verging branches deforming Miocene-Pliocene deposits under the Asse river as observed on the seismic profile VL85-P. These hidden compressional structures are interpreted as Provençal folds and thrusts (Dubois

and Curnelle, 1978), slightly reactivated during the Alpine compression (Hippolyte and Dumont, 2000; Godard et al., 2020).

Like the Provençal zone, cross-section construction and subsurface data illustrates that the Subalpine zone (including the Valensole foreland basin) is characterized by a heterogenous geometry of the basement-cover interface resulting mainly from basement-involved shortening. Northward, the Carboniferous and lower Triassic teguments of the Verdaches anticline were uplifted, as a result of reverse motions on a reactivated upper Carboniferous normal fault (Fig. 15). However, the structural culmination of the Verdaches anticline is associated with a deeper basement thrust wedge propagating under the Valensole foreland basin in the Triassic evaporites as initially proposed by Goguel (1944) and Gigot et al. (1974). Southward, cross-section construction suggests that the depth of basement is located at ~4.2 km bsl under the axis of the Thoard syncline (Fig. 6c) which is consistent with previous cross-section constructions in this zone (Combes, 1984; Graham et al., 2012). Its depth decreases progressively toward the south, at ~2.2 km bsl under the Mirabeau-Mallemoisson anticline and at ~1 km bsl in the Les Mées basement thrust. Southward, the depth of basement-cover interface goes down at ~2.5 km bsl, then decreases gradually toward the south (Figs. 6c and 19).

5. Restoration of the Mesozoic extensional basin framework

The balanced cross-section has been restored just before the Provençal compression considering the top of upper Santonian marine strata as a regional flat template from the South Provence basin domain (preserved from the Beausset syncline to the southern edge of Arc syncline) to the Vocontian domain to the north (Digne Nappe). This template connects with the subaerial erosional flat surface of the Durance high, which was used to unfold the Mesozoic-Jurassic sedimentary cover in the northern Provençal belt, the Valensole high and the Barles zone (Figs. 4 and 20a).

The pre-shortening restoration illustrates the initial extensional framework with a large uplift zone (Durance high and Valensole high) in the center of the section, which led to the separation of the Beausset basin (as part of the South Provence basin) to the south and the Digne basin (as part of the Vocontian basin) to the north (Fig. 20a). The southern Beausset rift-related structures and the southern edge of the Durance high have preferentially accommodated the Provençal shortening along the Bandol thrust, Sainte-Baume Nappe and Aurélien Mount thrust whereas the northern Digne rift-related structures have preferentially accommodated the Alpine shortening of the Digne Nappe. Restoration of the Beausset basin geometry is well determined by rift sequences preserved from erosion in the hanging-wall and footwall of the Sainte-Baume Nappe (Fig. 20a). In contrast, cross-section restoration suggests that a large part of the frontal Digne Nappe has been eroded (Fig. 20a). This eroded part might correspond to the adjacent halokinetic Turriers basin located to the west and transported ahead of the Digne Nappe along the studied cross-section (Gidon, 1982; Célini et al., 2020, 2021). The restoration suggests that the Digne basin was initially located at ~8 km to the north from the Barre de Chine and Barles diapir (Fig. 20a; Gigot et al., 1974).

In agreement with the structural data of Baudemont et al. (1985) and Espurt et al. (2019b), cross-section restoration suggests that the basement incorporates a set of ~E- to ENE-trending ~N-dipping normal faults associated with Permian half-graben systems (Fig. 20a). These basement faults are reactivated intermittently during the Tethyan, Vocontian and South Provence extensional episodes (Espurt et al., 2019b). They played a first order control on the subsidence of the Beausset and Digne basins and thick syn-rift Jurassic-middle Cretaceous sedimentary infilling (~2.4 km-thick in the Beausset basin and ~4.5 km-thick in the Digne basin). This strong sediment load in the Beausset and Digne depocenters could have induced the evacuation of the ductile Triassic evaporitic-carbonate layers from under the subsiding zones toward local halokinetic features. This early halokinesis drives early folding of the

sedimentary pile including large subsiding synclines to narrow minibasins structures characterized with growth wedges, normal faulting, and gravitational instabilities together with local salt domes and diapirs initiated from basement faults (e.g., Saint-Cyr, Huveaune, High Var and Barles halokinetic areas; Graham et al., 2012; Bestani et al., 2015; Espurt et al., 2019b; Célini et al., 2020; Fig. 20a).

The southern edge of the Beausset basin show major E-W thickness and facies changes in the Jurassic-middle-upper Cretaceous succession that depict depocenters and structural highs with minor normal faulting (Philip, 1967, 1970; Philip et al., 1987; Espurt et al., 2019b). For instance, the western Saint-Cyr Triassic high located in the footwall of the Bandol thrust, was probably controlled by a N-dipping basement fault together with Triassic salt movement at depth. Similar geometry has been used to restore the structures located in the footwall blocks of the future Sainte-Baume Nappe and Aurélien Mount thrust (e.g., Huveaune Triassic high; Guillemot et al., 1973; Bestani et al., 2015; Philip, 2019). In the Durance high, the halokinetic activity during Late Jurassic-Early Cretaceous is more discrete with small sediment trapping and normal faulting (e.g., future Pourrières and Les Maurras thrusts). Its result is the formation of Triassic domes and long-wavelength syncline depocenters where the Jurassic-Cretaceous platform shows successions with thickness changes (Fig. 20a; Espurt et al., 2019b).

The pre-shortening restoration also suggests that fold structures observed in the footwall (Barles diapir and Barre de Chine flap, Les Sauvans minibasin and Barles folds) and hanging-wall (La Robine) of the Digne Nappe have been initiated by early halokinetic deformations through the Jurassic and maybe until the Early Cretaceous (Fig. 20a; Graham et al., 2012; Célini et al., 2020, 2021).

6. Tracking superimposed compressions using syn-orogenic sedimentation and fault slip data

Deciphering the timing of deformations and shortening directions in the superimposed Provençal and Subalpine thrust wedges are fundamental for produce a robust sequential restoration model. The low-temperature thermochronology data available in the study area are in the Oligocene-Miocene footwall rocks of the Digne Nappe, upper Cretaceous Arc basin and Paleozoic basement of Maures and Tanneron-Estérel massifs (Jakni, 2000; Bestani, 2015; Schwartz et al., 2017a). In the Maures massif, Oligocene-Miocene cooling ages are mainly related to a reheating of the Paleozoic basement during the back-arc rifting of the Ligurian-Provençal basin associated with Miocene volcanism (Jakni, 2000; Bestani, 2015). The cooling ages in sedimentary cover are interpreted as detrital or partially reset ages by small reburial below the Mesozoic-Cenozoic sedimentary cover or tectonic covering. In the Subalpine zone thermal modeling of low-temperature thermochronological data suggested a cooling of the Barles half-window at ~6 Ma (Schwartz et al., 2017a).

To constrain the timing of the thrusting, we used syn-orogenic basin infill and growth strata (Suppe et al., 1992). The syn-orogenic deposits are either related to the Provençal or Subalpine compression. They are described by previous studies (e.g., Gigot et al., 1974; Dubois and Curnelle, 1978; Maillart et al., 1987; Haccard et al., 1989a; Espurt et al., 2012) or highlighted in this work. The analysis of the temporal and spatial distribution of these deposits was used to determine the growth and/or reactivation of contractional structures along our section and the progressive advance of the thrust wedges toward the forelands (Fig. 21). In Provençal zone, there is no evidence of growth strata in Neogene deposits. However, numerous examples of deformed Oligocene and Miocene-Pliocene strata testify to the presence of Alpine contractional reactivation of pre-existing Provençal thrusts and Ligurian-Provençal extensional structures (e.g., Hippolyte et al., 1993).

Fault slip data were used to determine regional stress regimes and the thrust transport directions (Angelier, 1984, 1991). Variations in stress regimes through geological times can be stratigraphically dated by reconstructing paleo-stresses at different stratigraphic levels (Hippolyte et al., 1993). Furthermore, the fault slip analysis in growth strata deposits can provide a direct dating of paleo-stresses (Hippolyte et al., 1992). Paleo-stress studies have already been done in the Provençal zone in the Oligocene basins, the Arc syncline and the Sainte-Victoire Mountain by Combes (1984), Gaviglio (1985), Lacombe et al. (1992), Hippolyte et al. (1993), Guignard et al. (2005), and Espurt et al. (2012), and in the Subalpine zone of Digne-Barles by Combes (1984), Fournier et al. (2008) and Hippolyte et al. (2012). In this study, fault slip data were collected in zone with single deformation phase and far from oblique structures or ramps producing local rotations and stress deviations (Lacombe, 2012) as observed locally in the Sainte Victoire Mountain (Espurt et al., 2012). We measured striated fault surfaces along the cross-section at twenty three new sites and computed paleo-stresses using the Angelier method (INVD method, Angelier, 1990). We added to our data five previously published fault sites along our cross-section that were analyzed with the same method in the southern flank of Sainte-Victoire Mountain (Espurt et al., 2012), in the Valensole basin (Hippolyte and Dumont, 2000), and in the Digne area (Hippolyte et al., 2012). The trends of the computed shortening directions (maximum horizontal stress axes σ_1) are presented in Fig. 21 and all computed data and diagrams in Table 1 and Fig. 22.

6.1. Record of the Provençal shortening

The map of Fig. 21a shows the Provençal compressional structures and associated upper Cretaceous to Eocene syn-orogenic basins. In the southernmost part of the Provençal zone, the transition from marine to continental deposits in the Latest Santonian of the Beausset syncline could be related to basement stacking in the inner part of the orogen (Philip, 1970; Philip et al., 1987; Tempier, 1987). The growth of the Sainte-Baume Nappe is recorded by

somewhat later Maastrichtian breccias (Rognacian facies) preserved in the folded footwall block (Fig. 9b; Aubouin and Chorowicz, 1967; Corroy and Philip, 1964; Guieu, 1968; Philip et al., 2018). Northward, Rognacian facies strata lie unconformably on middle-upper Triassic rocks and record the uplift of the Huveaune antiform during the Late Cretaceous (Bestani et al., 2015; Philip, 2018, 2019). Syn-tectonic deposits are not preserved along the Aurélien Mount thrust. Because it overthrusts Maastrichtian (Rognacian facies) strata of the Arc syncline (Fig. 10a), we can infer that this thrusting might have occurred during the Latest Cretaceous like the neighboring Sainte-Baume and Etoile Nappes and then later during the Paleocene (Fig. 3; Aubouin and Chorowicz, 1967; Guieu, 1968; Popoff, 1973). The initial growth of the Pourrières thrust is attested by a major pinch out of the continental upper Cretaceous sequences with intercalated breccia beds in middle Campanian strata (Begudian facies) (Durand and Mennessier, 1964; Popoff, 1973). A later activity can be also inferred for the Pourrières thrust as this thrust connects laterally to the S-verging Sainte-Victoire Mountain thrust with Paleocene growth strata (Espurt et al., 2012; Fig. 11a,b). The Paleocene growth of the Pallières, Vinon, Les Maurras and Gréoux thrust systems is clearly recorded by alluvial fan systems of microcodium breccias with local growth strata infilling the Rians, Saint-Julien, La Mourotte and Esparron-de-Verdon synclines (Figs. 4, 11c and 12; Angelier, 1971; Philip et al., 2017). These thrusts and basins have recorded ongoing deformation maybe until the Early Eocene (Angelier and Aubouin, 1976; Philip et al., 2017).

In the Valensole basin, subsurface data indicate that the Les Mées and Mirabeau-Mallemoisson structures overprint Provençal thrusts which have been eroded and sealed by basal Miocene strata (Fig. 19; Dubois and Curnelle, 1978; Gigot et al., 1981a). We can speculate a similar pre-structuration of the neighboring Lambruissier and Aiglun structures. Farther to the north evidence of Provençal deformation is also found in the Barles area (Fig. 3). In the Barles tectonic half-window, all E-trending compressional folds have been eroded

and unconformably covered by the Basal Breccia Formation with growth stratal architectures (Lemoine, 1972; Maillart et al., 1987; Haccard et al., 1989a,b). For instance, onlaps and fan shaped-geometry of the breccia beds can be observed in the northern limb of the Feissal syncline west of Barles (Fig. 16b). Although the age of these deposits remains poorly constrained (Latest Eocene-Early Oligocene) this occurrence of growth stratal wedging with reverse faulting provides evidence for compressional syn-tectonic sedimentation in the northernmost parts of the Provençal belt in Late Eocene times (Priabonian?). Interestingly, well dated evidence for late Provençal shortening is found farther west in the E-trending Eygalayes syncline of the Baronnies area (Fig. 3). Here, Montenat et al. (2005) described Lutetian to Bartonian lacustrine and conglomerate deposits with growth stratal geometries which recorded the initial folding of Eygalayes syncline during Middle-Late Eocene before its reactivation during the Alpine compression.

To determine the trend of the compressional stress in the Provençal thrust wedge, we measured fault-slip data at eleven sites into syn-tectonic conglomerates or growth strata described above, and in Jurassic-Cretaceous units of clearly define Provençal thrusts (Fig. 21a). Our paleo-stress computation shows evidence for a regional ~NNE-trending compression as previously shown by Gaviglio (1985), Lacombe et al. (1992) and Espurt et al. (2012) in the Sainte-Victoire Mountain-Arc syncline area. Syn-depositional tilting and faulting of the Danian growth strata in the Sainte-Victoire Mountain as well as in the Rians basin (Figs. 11b, 21a and 22) show that this ~NNE-trending compression occurred at least during the Danian (Espurt et al., 2012). In the Barles area, paleo-stress studies by Fournier et al. (2008) and Hippolyte et al. (2012) show a complex polyphase history with structures with different axial trends and ages interfering. Syn-depositional faulting in the Basal Breccia Formation growth strata in the slightly deformed ~E-trending Feissal syncline indicates a ~N-trending shortening (Fig. 16b). This trend is consistent with of the compression characterized

by Fournier et al. (2008) in the folded Mesozoic limestones of the Barles canyon. Thus, we can infer that the ~NNE-trending Provençal compression propagated northward to the outermost part of the belt in Late Eocene times (Fig. 21a) as previously suggested by Montenat et al. (2005) for the Baronnies area.

6.2. Record of the Alpine shortening

The map of Fig. 21b shows the Alpine compressional structures and associated syn-orogenic basins. In the Barles area, folding was recorded immediately after the Provençal compression by growth stratal geometries in the Oligocene continental Red Molasse Formation, then in the Grey Molasse Formation south of La Maurière anticline (Maillart et al., 1987). This Oligocene deformation is consistent with growth stratal geometries in the Esparron syncline as described by Gidon (1997) and Célini et al. (2021) more to the north (Fig. 3). The growth of the La Maurière anticline (and probably also other inner folds) was then recorded by Aquitanian-Burdigalian Lower Marine Molasse Formation, then Langhian, Serravallian and Tortonian-lower Messinian conglomerates with growth stratal architecture in the Vélodrome structure (Fig. 14; Gigot et al., 1974; Pairis and Gidon, 1987; Gidon, 1989; Gidon and Pairis, 1992). West of La Robine half-klippe along the Duyes valley, growth strata in upper Miocene subalpine conglomerates are identified in second order fold of the Thoard syncline (Figs. 3 and 17; Haccard et al., 1989b). The upper Miocene-lower Pliocene olistolithic Tanaron Formation which unconformably lies above folded Oligocene-upper Miocene rocks, recorded the final growth of the Barles fold system before the emplacement of the Digne Nappe (Gigot et al., 1974; Pairis and Gidon, 1987; Hippolyte et al., 2011; Fig. 14).

Based on thermal modeling of low-temperature thermochronological data from lower Miocene rocks of the Vélodrome structure, Schwartz et al. (2017a) proposed that the thrusting of the Digne Nappe started before the cooling of its footwall at ~6 Ma. They proposed that the modeled upper Miocene cooling and exhumation was controlled by regional basement

tectonic thickening under the Valensole foreland basin. However, almost all of samples of the Barles half-window have Late Pliocene or younger minimum apatite (U-Th)/He cooling ages (Schwartz et al., 2017b) which is consistent with the proposed Late Miocene-Early Pliocene age of the Tanaron Formation in the footwall of the Digne Nappe (Hippolyte et al., 2011). Southward, the Aiglun, Mirabeau-Mallemoisson, Lambruissier, Les Mées and Asse structures deform upper Miocene conglomerates of the Valensole 1 Formation (Fig. 18; Haccard et al., 1989a). No growth strata that could support a syn-sedimentary shortening of these folds, was found on the field and subsurface. This suggest that the growth of these folds occurred after Late Miocene times (Hippolyte and Dumont, 2000; Godard et al., 2020).

Although Provençal and Oligocene structures are often unconformably covered and sealed by Miocene-Pliocene sequences in the Provençal zone, numerous evidence of contractional deformations are observed. South of the Valensole foreland basin, the Gréoux, Les Maurras and Vinon thrusts are unconformably covered by Miocene-Pliocene conglomerates of the Valensole 1-2 Formations. Along the fault traces, these conglomerates show striated and sheared pebbles (Figs. 21b, 22 and 23a), suggesting small reverse-reactivation of the inherited thrusts. The eastern edge of the Vinon thrust, the Rians syncline and Pallières thrust are also unconformably overlain by Oligocene conglomerate beds of the La Combe half-graben (Fig. 3; Angelier and Aubouin, 1976). The conglomerate beds are also tilted and cut by reverse faults (Fig. 23b). This evidence of Alpine shortening is consistent with perched Miocene strata on the Mont-Major and Pallières thrusts; similar strata are located ~100 m lower on the Valavés anticline to the north (Fig. 3; Angelier and Aubouin, 1976). South of the Aurélien Mount thrust, Miocene conglomerates, sandstones and shales are folded and faulted, and unconformably overlie Campanian shales (Begudian facies; Fig. 23c) or middle Triassic Muschelkalk limestones (Espurt et al., 2019b). To the south, in the Signes and Méounes grabens, that belong in the Sainte-Baume Nappe, Oligocene-Miocene strata are locally

exposed (Nury and Rousset, 1986). At the northern edge of Signes graben, vertical to overturned Oligocene-Miocene conglomerates unconformably overlie Campanian-Maastrichtian continental strata (Begudian-Rognacian facies; Répelin, 1922) (Fig. 24a). These field data reveal Alpine contractional deformation in this zone. Evidence of Alpine shortening are also observed in the Oligocene basins of Saint-Zacharie, Peypin, Destrousse, Aubagne and Marseille (Fig. 3). The Oligocene strata infilling these basins are generally affected by normal faults (Hippolyte et al., 1991), but they are also later folded (Guieu, 1968; Weydert and Nury, 1978; Dupire, 1985) and faulted by strike-slip and reverse faults (Hippolyte et al., 1993). For example, the surface cross-section of Fig. 24b shows that the Peypin basin is an Oligocene half-graben bounded to the southwest by the Mauvais Vallon normal fault. This Oligocene basin develops on the eastern edge of the Etoile-Pierresca nappe system (Fig. 3), which propagated northward above the Arc syncline during the Provençal compression (Aubouin and Chorowicz, 1967; Guieu, 1968). The present day syncline shape of the Peypin basin associated with disharmonic folds and strike-slip faults in the Oligocene strata results from Alpine shortening. Similar deformed Oligocene (Miocene?) strata are also described westward in the Etoile Nappe near the Les Maurins trough (Figs. 3 and 23d; Nury and Raynaud, 1986; Hippolyte et al., 1993; Villeneuve et al., 2018). Alpine shortening is also found at the southern edges of the Marseille and Aubagne basins (Figs. 3 and 23e). In these areas, lower Cretaceous limestones of the Carpiagne anticline are interpreted as overthrust on northward tilted to overturned and faulted Oligocene limestone and conglomerate beds (Guieu, 1968; Weydert and Nury, 1978; Dupire, 1985; Villeneuve et al., 2018). A last example of Alpine shortening is recognized in the southernmost Bandol basin along the Mediterranean coast where Oligocene-Miocene conglomerates (Gouvernet, 1963) dip 20° toward the south and are cut by numerous small-scale reverse faults (Fig. 23f).

To reconstruct the orientation of the Alpine compression along our cross-section in the Subalpine zone and Provençal zone, we measured striated faults in seventeen sites in Oligocene, Miocene and Pliocene strata (Fig. 21b). Paleo-stress computation reveals a widespread ~NE-trending compression from the northern edge of the Valensole foreland basin to the Aubagne and Marseille basins to the south, and up to the Bandol basin along the Mediterranean coast. This ~NE-trending compression is contemporaneous with the deposition of upper Miocene growth strata in the Thoard syncline (Fig. 17) and observed up to Pliocene strata of the Digne area (Hippolyte et al., 2012). Generally, shortening direction may differ from stress orientation depending for example on the amount of displacement on strike-slip faults. It was demonstrated that a SSW transport direction of the Digne Nappe was related to an about NE-SW trend of compression at thrust front (Hippolyte et al., 2012). The post-Oligocene NE-SW trend identified in Provence is thus similar to the contemporaneous trend of compression in the Alps. That locally the Miocene-Pliocene trend of compression was similar to the upper Cretaceous-Eocene one may result from stress reorientation along Provençal structures. The distinction between the two stress fields was possible only because we worked in sites where the deformation can be dated. According to other works around the study area, this ~NE-trending Alpine compression which propagated southwestward into the Subalpine zone then, in the whole Provençal zone (Fig. 21b), probably prevailed since the Middle Miocene (Combes, 1984; Gaviglio, 1985; Villeger and Andrieux, 1987; Ritz, 1992; Champion et al., 2000; Clauzon et al., 2011).

6.3. Modern compressional stress

Beyond the predominant Miocene-Pliocene NE-trending compression presented above, modern NE- and NNW-trending compressional stresses have been identified by previous studies. Active shortening in the study area is revealed by earthquakes (Mw < 3.5) distributed in the sedimentary cover and Paleozoic basement (Nicolas et al., 1990; Ritz, 1992; Baroux et

al., 2001; Cushing et al., 2008). The modern state of stress revealed by earthquake focal mechanisms in the Digne-northern Valensole foreland basin area is consistent with NE-trending shortening (Baroux et al., 2001; Cushing et al., 2008). It would be responsible for the Quaternary deformation in the Digne Nappe east of the Bès fault, as well as at the Lambruissier and Les Mées anticlines of the Puimichel plateau (Collina-Girard and Griboulard, 1990; Hippolyte and Dumont, 2000; Hippolyte et al., 2012; Godard et al., 2020; Fig. 18c). The Provençal zone is also characterized by a modern NNW-trending strike-slip regime along the Middle Durance left lateral strike-slip fault (Ritz, 1992; Baroux et al., 2001; Cushing et al., 2008; Mazzotti et al., 2020). This NNW-trending stress regime is consistent with fault slip data collected in Pliocene rocks along the Middle Durance fault zone (Guignard et al., 2005) or very locally in Oligocene rocks of the Marseille basin (Hippolyte et al., 1993). The origin of the modern shortening in Subalpine and Provençal areas is still debated. Some authors proposed that they could be controlled by the buoyancy forces in the core of the Alps, driving compression in the foreland (Le Pichon et al., 2010; Walpersdorf et al., 2018) with local deviations along pre-existing faults (e.g., Guignard et al., 2005), or related to the modern Africa/Europe convergence (Ritz, 1992; Baroux et al., 2001; Mazzotti et al., 2020).

7. Structural evolutionary model of the superimposed Provençal and Subalpine foreland thrust wedges

Based on the above mentioned structural data together with the review of deformation in space and time, we built a sequentially balanced cross-section illustrating the long-term thrust kinematic and shortening budget of superimposed Provençal and Subalpine thrust wedges from Latest Santonian to present day (Fig. 20). The structural evolutionary model presented here allows to discuss the role of crustal-scale rift-related anisotropies on vertical partitioning of the shortening, foreland flexure and syn-orogenic sedimentation. The amounts of

calculated shortening/extension are minimum because the footwall and hanging wall cut-offs of some structures are not clearly determined.

7.1. Cross-section trace and thrust transport directions in the frame of the Provençal and Subalpine compressions

Drawing cross-sections approximately parallel to the slip direction, i.e., parallel to the thrust transport direction is a prerequisite for cross-section balancing and restorations, and quantifying shortening (Dahlstrom, 1969; Elliot and Johnson, 1980). However, it appears relatively difficult to study superimposed orogenic deformations with a single and continuous section. In this study, we proposed to show and evaluate the role of pre-existing structures on subsequent deformations on a continuous cross-section with three segments of different trends (Fig. 3) that respect the structural grain of the main structures and the shortening directions. Thus, the cross-sectional trace chosen for this study integrates with tolerable obliquity the different shortening directions of the two mountain ranges: the mean direction of compression trends NNE in the Provençal thrust wedge while it trends NE in the Subalpine thrust wedge (Fig. 21). Small variations in the direction of compressional are related to strike-slip structures (e.g., Bès fault, site 14 in Fig. 21b; Hippolyte et al., 2011). The magnetic fabric geometry also suggests SW-directed tectonic transport in all the Subalpine chains (Aubourg et al., 1999). These trends are consistent with the trace of the balanced cross-section in the zone where maximum horizontal shortening is recorded (Fig. 21 and see below). Therefore, our balanced cross-section that trend ~N to NNE can be sequentially restored to illustrate the structural evolution of Provençal and Subalpine superimposed foreland thrust wedges. To the south, the cross-section is somewhat oblique to the Alpine shortening direction, which implies that the amount of Alpine shortening is probably underestimated in this zone.

7.2. Kinematic restoration of the Provençal thrust wedge

The distribution of the upper Cretaceous foreland deposits permits to restore the first episode of thrust propagation in the inner part of the Provençal foreland between Latest Santonian and Maastrichtian (Fig. 20b). The transition from marine to continental deposits described in the uppermost Santonian strata of the Beausset syncline could be related to inner basement thrust stacking of the Provençal wedge related to the inversion South Provence basin and basement thrusting. The emplacement of the Cap Sicié basement thrust fed at least the slip of the Bandol cover thrust (other inner cover thrusts may have been eroded) above the Saint-Cyr Triassic high. The activity of these thrusts probably occurred during the Campanian-Maastrichtian because lower Campanian rocks (Fuvelian facies) are the youngest strata in the footwall of the Bandol thrust. The initial growth of the Sainte-Baume Nappe and deformation of Plan d'Aups and Pic des Corbeaux folds are recorded by upper Campanian-Maastrichtian (Begudian-Rognacian facies) syn-tectonic conglomerates. It is fed by the deep Saint-Mandrier thrust. The uplift of the Huveaune Triassic high is recorded by strata of Fuvelian or Rognacian facies unconformably resting on the Triassic basement, although these strata could have been transported onto the incipient Huveaune Triassic high during the overthrusting of the Etoile Nappe (Fabre et al., 1975; Philip, 2019). The restoration shows that the displacement of the deep basement Sainte-Baume thrust sheet was first accommodated by the Arc syncline and then by the Pourrières frontal ramp in the Middle Campanian-Maastrichtian. This frontal early growth might also result from the reactivation of basement faults to the north, similarly to this proposed for the early reactivation of the Sainte-Victoire Mountain deep basement thrusts (Espurt et al., 2012). Northward, the eroded area of the Valensole high could be interpreted as a forebulge during the Latest Cretaceous (Fig. 20b).

The Paleocene-Eocene period (Fig. 20c) corresponds to the complete emplacement of the southern basement thrusts and complete tectonic covering of the Sainte-Baume Nappe and Aurélien Mount thrust. Shortening propagates northward in the cover units (Pourrières,

Pallières, Vinon and Gréoux thrusts) as recorded by Paleocene syn-tectonic conglomerates and subsiding thrust-top basins (i.e., Arc, Rians, Saint-Julien, La Mourotte, Esparron-de-Verdon synclines; Fig. 3). Although a huge volume of Triassic evaporites is suspected under the Pallières, Vinon and Gréoux units, the restoration suggests that Provençal thrusting also propagated northward at depth level into the basement of the Valensole high. The shortening recorded in cover of the outer part of the Provençal wedge was partly fed from the south (e.g., Pourrières and Pallières thrusts) but was also controlled by the inversion of basement inherited fault system along S-verging thrusts with inferred shortcut trajectories. Although we have no growth strata in subsurface data because of the erosion at the base of the Miocene strata (Fig. 19), the initial growth of the Asse-Les Mées basement thrust system may have occurred with a similar structural style (S-verging basement wedge) during this stage. The growth of the Lambruissier, Mirabeau-Mallemoisson and Aiglun thrusts might also have started as small domes during this stage (Dubois and Curneille, 1978). According to field data, the restoration also shows the propagation of the deformation front up to the northern edge of Valensole high as shown by the reactivation of the halokinetic folds of the Barles area during the Late Eocene (Fig. 20c; Lemoine, 1972). Interestingly, the late Provençal shortening has been recorded west of Barles area by Lutetian-Bartonian growth strata in the small Eygalayes syncline (Montenat et al., 2005; Fig. 3). In addition, structural and stratigraphic data in onshore Languedoc region confirm that Provençal shortening was active up to Priabonian time (Séranne et al., 2021). An alternative interpretation is that the growth of the Barles fold system comes from to the north from the early Alpine belt (Ford et al., 1999). However, the N-trending compression reconstructed from growth strata (Fig. 16b), and the E-W trend of the folds in this zone are rather consistent with the Provençal compression, the Alpine compression being oriented more to the NE (Fig. 21). This outer Provençal shortening

in the northern portion of the Valensole high up to and beyond the Barles zone implies that shortening was transmitted at depth through the basement under the Valensole high.

The Provençal thrust wedge accommodated a minimum of 38 km (i.e., 17%) of total shortening (Fig. 20c). The main part of this shortening, i.e., 32 km, is accommodated by the inversion of the South Provence basin to the south in the Provençal zone, the remaining 6 km is accommodated in the Valensole high (Les Mées thrust) and Barles area. The sequential restoration (Fig. 20a,b,c) allow to calculate a shortening amount of 8.9 km between Latest Santonian and Maastrichtian (i.e., ~0.5 km Ma^{-1}), and of 29.1 km between Danian and Late Eocene (i.e., ~0.9 km Ma^{-1}).

7.3. Oligocene breakup of the Provençal zone

South of the Valensole high, most of the structural development in the Oligocene is related to the breakup of the Provençal thrust wedge by N-S, NNW-SSE and NE-SW extensional fault systems (Fig. 20d; Angelier and Aubouin, 1976; Giannerini, 1978; Nury, 1988; Hippolyte et al., 1993). The amount of extension remains small (~1.6 km) in the continental Provençal margin and focused south of the cross-section in the Provençal zone (Bestani et al., 2016). Most of the normal faults are reactivated thrust ramps, strike-slip faults (Roure et al., 1992) or diapiric features (Angelier and Aubouin, 1976; Philip, 2018, 2019), which accommodate the E-W opening of the West-European rift, then the NNW-SSE stretching of the southern Provence crust due to the Ligurian-Provençal back-arc rifting between Provence and Corsica-Sardinia block (Hippolyte et al., 1990, 1991, 1993; Bestani et al., 2016).

7.4. Kinematic restoration of the Subalpine thrust wedge

Following the Provençal shortening, the early orogenic building of the internal Alpine wedge during Late Eocene-Oligocene times has been probably associated with major flexural subsidence north of the Barles area (Fig. 20d; Ford et al., 2006; Graham et al., 2012).

According to field data, the cross-section suggests small reactivation (less than 500 m of shortening) of the pre-existing halokinetic folds of the Barles area (Maillart et al., 1987; Gidon, 1997; Célini et al., 2021). This Oligocene deformation might be interpreted as distal shortening in the Oligocene Alpine foreland.

The Late Miocene restored stage (Fig. 20e) shows the southward shift of subsidence into the Valensole high that became a large foreland basin. The syn-orogenic Miocene sedimentary package of the Valensole foreland basin exhibits a wedge-shaped geometry, with a more than 3 km-thick sequence in the depocenter zone and a few hundred meters in the south of basin. Southward, the Provençal zone was uplifted without fault reactivation. There, thin marine to continental sequences fill paleo-valleys overprinting the paleo-morphology of the Provençal thrusts, or cover marine abrasion surfaces (Mennessier, 1959; Cornet, 1965; Angelier and Aubouin, 1976; Besson, 2005; Oudet et al., 2010). The Provençal zone may represent a flexural forebulge, accompanying the subsidence of the Valensole foredeep depozone. This uplift is likely to have also been controlled by the Ligurian-Provençal passive margin setting to the south. The initial subsidence of the Valensole basin was first recorded by the transgressive Aquitanian-Burdigalian Lower Marine Molasse Formation on Mesozoic rocks previously folded and faulted during the Provençal compression. Subsidence continues through the Langhian to Tortonian (early Messinian?) with the deposition of the Upper Marine Molasse Formation that passes laterally and vertically to prograding fluvio-deltaic conglomerates of the Valensole 1 Formation. Synchronous syn-folding sedimentation is localized in the northern edge of the Valensole basin where growth strata in clastic sediments of the Vélodrome structure record the activity of the La Maurière anticline and other inner folds through the Miocene (Pairis and Gidon, 1987). Such deformation and uplift of the Barles fold system require the existence of basement thrust wedge under the Barles area. Although the ductile behavior of the Triassic detachment undeniably participated to the

growth of the folds in cover, we propose that shortening was mainly controlled by the inversion of the deep Verdaches half-graben (named here the Verdaches horse) and the formation of an inferred frontal basement thrust (named the Barles horse) that propagated southward in the Triassic evaporites under the Thoard syncline. To the south of the Valensole basin, no growth strata are found within the upper Miocene conglomerate sequences, suggesting no contractional reactivation of the pre-existing Provençal structures.

The comparison between the Late Miocene and present day stages (Fig. 20e,f) allows to evaluate the upper Miocene-Pliocene thrusting of the Digne Nappe above the Valensole and the southward transfer of the shortening into the Valensole foreland basin and Provençal zone. The olistolithic Tanaron Formation in the stratigraphically highest part of the Thoard syncline indicates strong erosion of the La Maurière anticline (Pairis and Gidon, 1987). The Digne Nappe moved above the Valensole basin mainly after the deposition of the upper Miocene-lower Pliocene Tanaron Formation. The present antiformal shape of the Digne Nappe is related to renewed basement thrusting under the Barles area, leading to the development of the present erosional Barles half-window. In this way, the Digne Nappe was folded later probably during the Pliocene by the underlying basement thrust wedge (Schwartz et al., 2017a,b). During the Pliocene-Quaternary, shortening of the basement thrust wedge was transferred southward through a Triassic décollement in the Valensole basin, leading to the complete development of the Aiglun, Mirabeau-Mallemoisson and Lambruissier anticlines. This period is also marked by the contractional reactivation of Provençal thrusts in the Valensole basin and Provençal zone, and inversion of Oligocene-Miocene basins as far as Aubagne, Marseille and Bandol basins along the Mediterranean coast. This outer Alpine shortening through the Provençal zone implies that part of the shortening was transmitted at depth through the continental crust.

Globally, the kinematic restoration shows that the Subalpine thrust wedge is characterized by a first order shortening transfer from hinterland to foreland zones (Fig. 20d,e,f). However, the structural evolution of the Subalpine Thoard syncline and Digne Nappe show interaction between thrusting and syn-tectonic sedimentation and erosion disturbing here temporally this forward thrusting sequence as observed in many natural examples and analog and numerical models (e.g., Baby et al., 1995; Bonnet et al., 2008; Uba et al., 2009; Fillon et al., 2013; Erdős et al., 2015; Butler, 2020; Wu et al., 2021). The structural inversion in the southern margin of the Digne basin can be interpreted as a triangle zone model (McMechan, 1985; Price, 1986; Jamison, 1993). The large accumulation (up to 3.3 km-thick) of Miocene syn-tectonic sediments at the front of Barles basement triangle zone may have influenced the frictional properties (increase of the vertical stress) of the potential Triassic décollement under the Thoard syncline (Fig. 14b). We suggest that from Oligocene to Late Miocene this behavior may have prevented forward thrust propagation, localizing in a first step the deformation front at the northern edge of the Valensole basin in the Thoard-Vélodrome zone (Wu et al., 2021). When stresses were too strong and the Barles triangle zone could no longer accommodate the shortening by folding in the Thoard-Vélodrome zone, the broad Digne Nappe activated and cuts the pre-structured folds of the Barles area (Gidon and Pairis, 1992; Fig. 20e,f), characterizing an out-of-sequence kinematics as suggested by Vann et al. (1986). After the emplacement of the Digne Nappe, the development of the basement thrust wedge continued (folding of the Digne Nappe) and its shortening was transferred southward in the Aiglun, Mirabeau-Mallemoisson and Lambruissier cover structures.

The Subalpine thrust wedge accommodated a minimum of ~35 km (i.e., 19%) of total shortening between Oligocene and present day (Fig. 20f). The main part of this shortening, i.e., 22 km, is accommodated by the Digne Nappe, 10 km in the Barles fold system and northern Valensole foreland basin, the rest, i.e., 3 km, is accommodated southward by

reactivated Provençal basement thrusts (south of the Lambruissier anticline). The sequential restoration (Fig. 20d,e,f) allows to calculate a shortening amount of 13.8 km between Aquitanian and Late Miocene (i.e., ~0.6 km Ma^{-1} for the Aquitanian-Late Miocene period), and of 21.2 km between the Late Miocene and present day (i.e., ~2.1 km Ma^{-1}). The calculated upper Miocene to present day shortening rate is three times larger than the post-Zanclean slip (0.7 km Ma^{-1}) along the Bès fault deduced from the 2.3 km displacement of a dissected post 3.4 Ma infilled drainage network (Hippolyte at al., 2012).

7.5. Foreland basin development

The propagation of the Provençal and Subalpine thrust wedges led to tectonic loading and foreland basin flexure (DeCelles and Giles, 2001). Both thrust wedges exhibit similar flexure angle toward hinterland zones of ~7° (Fig. 20c,f). However, the Provençal and Subalpine thrust wedges are characterized by foreland basins with contrasted developments and geometries. The Provençal thrust wedge is characterized by distributed basement thrusts along the cross-section reworking numerous structures inherited from the Variscan belt and Permian-Mesozoic rifts. As previously suggested by Roure and Colletta (1996), the inversion of this complex structural framework might have favored the development of several upper Cretaceous to Eocene foreland depocenters (Beausset, Arc, Rians, Saint-Julien, La Mourotte, Esparron-de-Verdon basins; Fig. 3), incorporated into the thrust wedge (Fig. 20c). In contrast, the Subalpine thrust wedge is characterized by the stacking of the thick Digne Nappe and Barles basement triangle zone. This duplex induced strong tectonic loading which might have controlled the large flexure of the Valensole basin, partly incorporated into the thrust wedge (Fig. 20f).

8. Discussion

8.1. Basement inheritance and Triassic décollement level

Inherited or neo-formed décollement levels have strong influence on the vertical partitioning of the shortening in fold-thrust belts (e.g., Torres Carbonell et al., 2017). Inherited discontinuities in the Paleozoic basement (inherited faults, shear zones, or metamorphic foliations) act as decoupling levels that connect at depth with lower crustal level (e.g., Espurt et al., 2008; Lacombe and Bellahsen, 2016; Bellahsen et al., 2016). Salt and ductile shale levels are also recognized as major decollement levels in the sedimentary cover. The tectonic style of both Provençal and Subalpine foreland thrust wedges consists in mixed thick- and thin tectonic styles: deep basement thrust wedges kinematically linked with shallow thrust wedges detached in middle-upper Triassic evaporites. The basal Muschelkalk and Keuper units constitute major decollement levels in the sedimentary cover (Caron, 1979; Gidon, 1982; Baudemont, 1985; Tempier, 1987; Gidon and Pairis, 1992; Gidon, 1997). The structural data and cross-section restorations reveal that the shortening propagated through heterogenous basement frameworks involving the reactivation of pre-existing structures related to Permian and Mesozoic rift events (Bathiard and Lambert, 1968). The thinner crust of the former Mesozoic rift basins (i.e., the Beausset and Digne basins) associated with ductile lower crust might have favored the inversion of basement normal faults and the formation of inner thick-skinned thrust wedges during convergence. This style of shortening is most likely to occur in a young lithosphere like Europe (Mouthereau et al., 2013; Mouthereau et al., 2021). Our kinematic model shows that the Valensole high, separating the Beausset and Digne basins, remained a basement block poorly deformed by successive Provençal and Alpine orogens (Fig. 20a). If we analyze the distribution of the Triassic evaporites in the study area, we observed that these latter have controlled the transfer of the thin-skin tectonic displacement into the cover and the geometry of Provençal and Subalpine thin-skinned thrust wedges. The Provençal and Subalpine external compressional structures developed along the pinchouts of the Triassic evaporites located onto the flanks of the

Valensole high. The near absence of potential Triassic layer overlying the basement of Valensole high (Les Mées area) and the relatively thin Mesozoic cover (less than 1 km-thick; Figs. 19 and 20) seem to have prevented the propagation of the decollements at shallow level into the cover. The restoration suggests that both Provençal and Alpine compressional stresses have consequently been transmitted under the basement of the Valensole high (Fig. 20c,f) perhaps onto a deep crustal (lower crust?) detachment level (e.g., Lacombe and Mouthereau, 2002; Mouthereau et al., 2013, 2014; Lacombe and Bellahsen, 2016; Laborde et al., 2019; Mouthereau et al., 2021). During the Oligocene-Miocene Ligurian-Provençal back-arc extension, the southern Provence crust (Maures massif) was reheated, thinned, and weakened (Guieu and Roussel, 1990; Jakni, 2000; Bestani et al., 2016). This may explain the involvement of the basement in the shortening related to the Alpine compression as far as the Marseille-Bandol zone to the south. Such outer thick-skin deformation related to thermal event was already suggested by Jourdon et al. (2014) in the external Castellane area (Fig. 1). In the same way, the Provençal shortening has been transmitted under the Valensole high up to the weakened zone of the Vocontian rift during the Late Eocene times.

On a larger scale (Fig. 1), the cross-section presented in this study and previously published cross-sections constructed across the southwestern Subalpine thrust front (Lickorish and Ford, 1998; Laurent et al., 2000; Jourdon et al., 2014; Guyonnet-Benaize et al., 2015; Bestani et al., 2016) show that the irregular basement architecture inherited from Paleozoic and Mesozoic tectonic stages and the distribution of the Jurassic-Cretaceous basins underlain by Triassic evaporites controlled the along-strike geometry of the Subalpine thrust front (Roure and Colletta, 1996; Macedo and Marshak, 1999). The Diois-Baronnies-Western Provence Arc (Villeger and Andrieux, 1987) and Digne-Castellane Arc (Goguel, 1937) coincide with Jurassic-Cretaceous depocenters (more than 5600 m-thick in the western Provence, and 1300-2200 m-thick in the Castellane Arc; Ménard, 1979; Laurent et al., 2000;

Guyonnet-Benaize et al., 2015; Bestani et al., 2016) whereas the Valensole high is overlain by a thin succession (150-1000 m-thick). We suggest that the shape of the Diois-Baronnies-Western Provence Arc (Villeger and Andrieux, 1987) and the Digne-Castellane Arc (Goguel, 1937) has been preferentially controlled by these paired Jurassic-Cretaceous basins underlain by huge volumes of Triassic evaporites. It was well established that the southern units of these arcs accommodated Alpine shortening in Miocene. In the Western Provence Arc, the Luberon, Costes and Trévaresse thrusts recorded shortening in Middle-Late Miocene as revealed by growth strata deposits and uplifted staircase wave-cut platforms (Anglada and Colomb, 1967; Champion et al., 2000; Besson, 2005; Clauzon et al., 2011). In the southern units of the Castellane Arc, growth strata in the upper Miocene-Pliocene conglomerates of the southeastern edge of the Valensole basin, and Eoulx-Brenon, Roque-Esclapon and Aubarède synclines more to the east have also recorded the Alpine shortening (Gigot et al., 1976; Giannerini et al., 1977; Giannerini, 1978; Dardeau et al., 2010; Fig. 1). In map view, the Valensole high can be interpreted as a reentrant between the Diois-Baronnies-Western Provence Arc and the Digne-Castellane Arc. The thinning of the Triassic evaporites onto the northeastern flank of the Valensole high prevented the large SW-ward propagation of the thin-skinned shortening, which was accommodated into the Aiglun, Mirabeau-Mallemoisson and Lambruissier anticline, probably recently and partly during the Quaternary for the Lambruissier anticline (Hippolyte and Dumont, 2000). The along-strike structural variations in the kinematic of the Subalpine thrust systems were accommodated by the development of NNE-trending strike-slip systems and oblique structures on lateral ramps on both sides of the Valensole foreland basin (e.g., Middle Durance fault zone and Bès fault; Laurent et al., 2000; Hippolyte et al., 2012; Guyonnet-Benaize et al., 2015; Fig. 1). Along the study area, the transfer of shortening into the basement of Provence induced the small reactivation of

inherited basement faults under the central-southern Valensole basin and Provençal zone, causing their uplift during the Pliocene-Quaternary.

Although the shape of the Eocene Provençal frontal thrusts has been strongly modified by the Alpine deformation, we also show that the along-strike configuration of the Mesozoic basins has controlled the ~NNE-ward propagation of the thin-skinned Provençal thrust front (Fig. 1). In the Western Provence Arc, balanced cross-sections of Bestani et al. (2016) illustrating the geometry of the Provençal fold-thrust belt at the end of Eocene show that the combination of thick sedimentary cover and Triassic evaporitic detachment layers favored the propagation of the thin-skinned thrust front up to the Baronnies area north of the Ventoux-Lure thrust system (Montenat et al., 2005). Similarly, restored balanced cross-sections of Laurent et al. (2000) and Jourdon et al. (2014) suggest that the Provençal cover detached easily northward up to the Vocontian basin thank to the Triassic decollements. During this period, the NNE-trending Middle Durance fault zone and probably the Barjols Triassic zone (Figs. 1 and 3) accommodated the along-strike kinematic of the Provençal thrust systems (Bestani et al., 2016).

8.2. Accommodation of the shortening by halokinetic structures

During shortening, the pre-existing halokinetic structures were generally reactivated, localizing preferentially the shortening in the cover. The initial geometry of these pre-existing halokinetic structures can be strongly modified during the contractional deformations as documented, for instance, in the Pyrenees (Saura et al., 2016; Labaume and Teixell, 2020; Burrel and Teixell, 2021), in Provence (Angelier and Aubouin, 1976; Espurt et al., 2019b), in the Alps (Dardeau et al., 1990; Granado et al., 2018; Célini et al., 2020, 2021), in the Zagros (Callot et al., 2007, 2012), and in the eastern Carpathians (Tămaș et al., 2021). Shortening induces the lateral and vertical evacuation of the mobile evaporitic material. Inherited salt dome structures constitute weak zones, which can evolve in diapirs with upturning flanks

leading to thrust welding. Minibasins related to sedimentary loading evolve in tight synclines. As revealed by the palinspastic restoration of Fig. 20a and previous works in the study area, the Provençal and Subalpine thrust wedges incorporate numerous pre-existing halokinetic structures that initially developed during Mesozoic rifting stages (e.g., Graham et al., 2012; Bestani et al., 2015, 2016; Espurt et al., 2019b; Célini et al., 2020, 2021; Wicker and Ford, 2021) and locally also during the Oligocene (Angelier and Aubouin, 1976). The Mesozoic halokinetic structures associated with variable thickness of Triassic evaporites and sedimentary cover undeniably generated anisotropic behavior in deformation during shortening. In the following, we discuss the role and evolution of some of these pre-existing halokinetic features in the Provençal and Subalpine thrust wedges.

Halokinesis and its relationship with basement faulting has been previously analyzed and quantified by Espurt et al. (2019b) in eastern Provençal zone where a succession of early halokinetic folds have been later deformed by the Provençal and Alpine compressions. This work has provided new ideas leading to the reinterpretation of some structures located further west along the cross-section studied in this paper. For instance, the emplacement of the Bandol thrust was controlled by the Saint-Cyr Triassic high developed earlier at least up to the Early Santonian (Philip, 1967; Philip et al., 1987). The initial geometry of the dome has been squeezed and probably decapitated by the Bandol thrust. Shortening may have also driven salt migration and the northward expulsion of the Saint-Cyr Triassic evaporites onto the floor of the Beausset syncline (Fig. 8). The dip of the northern limb of the dome, made of lower Santonian limestone beds, has been enhanced during Provençal shortening and sheared by low-angle reverse faulting. Although we have no direct evidence of early halokinetic motion in the footwall block of the Sainte-Baume Nappe, we inferred that its emplacement might have been initiated on an early halokinetic structures above a N-dipping basement normal fault. However, we interpret the present day tight geometry of the Plan d'Aups

syncline as mostly resulting from the emplacement of the far-travelled Sainte-Baume Nappe and contractional shear into its footwall block (e.g., Bertagne tectonic slice; Fig. 9b). A tectonic model implying an early growth (Jurassic?) of diapiric structures can be proposed for the Huveaune Triassic high (Bestani et al., 2015; Philip, 2018; 2019). This high is interpreted as an early dome controlled by a huge volume of Triassic evaporites overlying a basement fault (Guillemot et al., 1973). The restoration suggests that the dome has been strongly squeezed by Provençal shortening. As suggested by analog models in Callot et al. (2007), the initial shape of the dome controlled the propagation of the hanging-wall flat of the Aurélien Mount thrust through southern limb of the former dome. Surface exposure of the halokinetic structures after the Provençal compression might explain why some of them (e.g., the Huveaune or Barjols Triassic zones; Fig. 3), constituted by ductile material, have been easily reactivated during the Oligocene extension and Alpine compression (Angelier and Aubouin, 1976; Philip, 2018, 2019; Espurt et al., 2019b).

North of the Arc syncline, field data and cross-section restoration suggest that thrust systems are superimposed on Jurassic-lower Cretaceous salt domes and large synclines with local normal faults (Fig. 20a,b,c). Folding of the Rians syncline may have initiated during the Jurassic. However, its present tight geometry could rather result from the combined effects of halokinetic processes and thrusting (Cojan, 1993). We suggest that syn-tectonic sedimentary loading of the Paleocene-Eocene Rians syncline has favored its sinking into the thick ductile Triassic evaporitic-carbonate layer (Fig. 20c) as previously shown in the Sivas basin in Turkey by Kergaravat et al. (2016).

In the Subalpine zone, cross-section restoration and field data also confirm that halokinetic features located in the hanging-wall and footwall of the Digne Nappe have localized and accommodated Alpine shortening. As suggested by the restored stage (Fig. 20a), the Digne Nappe involves frontal halokinetic structures (lateral continuation of the Turriers unit (now

eroded) and La Robine; Célini et al., 2020). These structures are not only passively transported within the nappe but recorded major internal contractional deformation. The Barles diapiric structure is interpreted as a major halokinetic structure that localized the leading edge of the Digne Nappe (Fig. 20a; Graham et al., 2012). Beneath this thrust, and in contrast to the cross-sections of Graham et al. (2012) and Célini et al. (2020), the Barles fold system is not interpreted as an allochthonous unit transported above inferred deep cover sub-thrust. Although we have no subsurface data at Barles to highlight the thrust system geometry at depth, our construction favors a simple detachment fold interpretation as previously proposed by Goguel (1944) (Fig. 14b). The La Grande Cloche and La Maurière anticlines are detached from the underlying basement along Triassic evaporites. We agree that in places, folding has been initiated during Mesozoic rifting as a result of motion of the Triassic evaporites together with normal faulting as observed immediately north of the La Grande Cloche anticline in the Les Sauvans minibasin and Barles diapir. These pre-existing folds naturally localized contractional deformation during shortening. The present squeezed geometry of the detachment folds at Barles and complete overturning of the Barre de Chine flap were likely favored by ductile behavior of Triassic evaporites, but also by compaction of the ductile Callovian-Oxfordian shales in fold cores (Fig. 14c). Thus, the present day squeezed geometry of the Barles folds has been likely enhanced by shortening and the emplacement of the overlying Digne Nappe. Recently, Célini et al. (2020) interpreted the Neogene Vélodrome syncline as a mini-basin structure and the contact between the La Maurière anticline and the Vélodrome as a salt weld. These interpretations require a salt or allochtonous salt sheet Oligocene in age but the Oligocene strata exposed near Esclangon are fluvial deposits without any evidence of salt level.

To sum up, Mesozoic halokinetic structures belonging in the South Provence and Vocontian extensional basins were rejuvenated and squeezed by Provençal and Alpine

compressions. These structures localize preferentially the shortening and a significant amount of shortening might have been also accommodated by internal deformation within evaporitic layers. It appears therefore important to perform microstructural analysis into the evaporitic layers of salt-core structures to better constrain the amount of internal deformation accommodated within these structures during subsequent shortening (Malavieille and Ritz, 1989; Rowan et al., 2019; Tămaș et al., 2021).

9. Conclusion

In this study, available surface and subsurface data together with the construction of a 150 km-long sequentially restored balanced cross-section were combined to provide a regional overview of geology, structural evolution and quantification of crustal shortening budget of the superimposed Provençal and Subalpine fold-thrust belts in Central Provence region. Along the studied cross-section, the multistage growth of the fold-thrust belt systems has been remarkably recorded by well-preserved syn-orogenic deposits, growth strata and kinematic indicators of thrusting in the foreland basins. The major points arising from this study case are as follow:

- The Provençal and Subalpine thrust wedges are characterized by a mixed thick- and thin-skinned tectonic style including basement thrusts propagating through inherited basement discontinuities (Variscan structures and normal faults delimiting upper Carboniferous-Permian basins, Mesozoic Tethyan, Vocontian and South Provence basins, and Oligocene basins) and cover thrusts detached in the middle-upper Triassic evaporites. The palinspastic restoration of the thrust wedges to Late Santonian shows a large uplift zone in the center of the study area (Durance high and Valensole high), which led to the separation of the Beausset basin (as part of the South Provence basin) to the south and the Digne basin (as part of the Vocontian basin) to the north. These extensional basins reactivated ~N-dipping normal faults related to upper Carboniferous-Permian basins.

- The Provençal shortening propagated NNE-ward from the inverted Beausset basin up to the Barles area during Latest Santonian-Campanian to Late Eocene (i.e., ~50 m.y.). The Subalpine shortening propagated SW-ward from the inverted Digne basin up to the Mediterranean coast during Oligocene-Aquitanian to present (i.e., ~30 m.y.). In Provence, the Provençal and Alpine episodes of shortening are clearly separated by the Oligocene rifting events including the West-European rift followed by the back-arc rift of the Ligurian-Provençal basin destroying the inner Provence crystalline thrust wedge. In the studied area, NNW-SSE extension was mainly accommodated by crustal thinning and upper crustal ENE-trending normal faults together with major phases of erosion and sedimentation. In contrast, the recognition of upper Eocene, Oligocene and Miocene growth strata in the Subalpine zone of Barles might suggest a continuum of contractional deformation.

- The amount of horizontal crustal shortening, derived from sequential restoration, is relatively similar in both thrust wedges: 38 km (17%) in the Provençal thrust wedge and 35 km (19%) in the Subalpine thrust wedge.

- By distributing the deformation though numerous inherited Permian-Mesozoic basement structures, the Provençal thrust wedge might have favored the development of confined foreland basins, as the Arc and Rians basins. In contrast, the vertical stacking of the thick Digne Nappe and Barles basement triangle zone in the Subalpine thrust wedge might have controlled the large flexure of the Valensole foreland basin.

- The sequential restoration suggests that the shortening has been mainly controlled by the inversion of the South Provence basin-Durance high (Provençal shortening) to the south, by the inversion of the Vocontian basin (Alpine shortening) to the north, and by other factors as the pinch out of the Triassic décollement level onto the Valensole high and early halokinetic structures. At the scale of our cross-section, we show that syn-tectonic sedimentation has small and localized impact on thrusts kinematics (i.e., Digne Nappe).

- This study highlights that the development of pre-shortening extensional basins and long-term structural evolution of the Provençal and Subalpine fold-thrust belts have been controlled by inherited crustal structures. These crustal heterogeneities have greatly influenced the propagation of the contractional deformation and foreland basin development in space and time.

Acknowledgments

Financial support for fieldworks in the frame of the Phd thesis of Jocelyn Balansa came from the BRGM-RGF (French Geological Survey-Référentiel Géologique de la France) Alpes et bassins périphériques program. We thank the Agence de l'Eau Rhône Méditerranée Corse for providing seismic profiles in the Valensole basin. This paper is also part of the Karst-Huveaune project (2018-2022) funded by Agence de l'Eau Rhône Méditerranée Corse, Région Sud-Provence Alpes Côte d'Azur, Conseil Départemental des Bouches-du-Rhône, Aix-Marseille Provence Métropole, BRGM, Aix-Marseille Université. We thank Stéphane Marc, Eglantine Husson and Marie Genevier from BRGM for seismic profile interpretation, and Myette Guiomar from the Réserve naturelle géologique de Haute-Provence for field assistance. We also thank Pierre Henry, Michel Corsini, Gérard Giannerini and David Baudemont for useful discussions. The MOVE Software Suite was donated by Petroleum Experts Limited. Finally, we acknowledge Eldert Advokaat and an anonymous reviewer for the constructive comments and suggestions which greatly helped to improve the original manuscript.

Data Availability

Datasets related to this article can be consulted by contacting J. Balansa (balansa@cerege.fr)

References

Advokaat, E. L., van Hinsbergen, D. J., Maffione, M., Langereis, C. G., Vissers, R. L., Cherchi, A., Schroeder, R., Columbu, S., 2014. Eocene rotation of Sardinia, and the paleogeography of the western Mediterranean region. Earth and Planetary Science Letters, 401, 183-195, https://doi.org/10.1016/j.epsl.2014.06.012.

Aguilar, J.-P., Clauzon, G., 1981. Découverte de trois nouveaux gisements à Rongeurs d'âge miocène en Provence nord-orientale. Implications géodynamiques et paléogéographiques. C. R. Acad. Sci. Paris, 292, II, 909-912.

Alvarez-Marron, J., Rodriguez-Fernandez, R., Heredia, N., Busquets, P., Colombo, F., Brown, D., 2006. Neogene structures overprinting Palaeozoic thrust systems in the Andean Precordillera at 30o S latitude. Journal of the Geological Society, London, 163, pp. 949-964, doi:10.1144/0016-76492005-142.

Angelier, J, 1971. La partie septentrionale de la bande triasique de Barjols (Var). Paris, PhD thesis.

Angelier, J., 1984. Tectonic analysis of fault slip data sets**.** Journal of Geophysical Research, Vol. 89, No. B7, 5835-5848.

Angelier, J., 1990. Inversion of field data in fault tectonics to obtain the regional stress. III-a new rapid direct inversion method by analytical means. Geophysical Journal International, 103, 363-376.

Angelier, J., 1991. Inversion directe et recherche 4-D : comparaison physique et mathématique de deux modes de détermination des tenseurs des paléocontraintes en tectonique de failles. C. R. Acad. Sci. Paris, 312, II, 1213-1218.

Angelier, J., Aubouin, J., 1976. Contribution à l'étude géologique des bandes triasiques provençales : de Barjols (Var) au bas Verdon. Bull. B.R.G.M., 2, 1, no. 3, 187-217.

Anglada, R., Colomb, E., 1967. Precisions tectoniques sur le flanc sud de l'anticlinal du Grand-Luberon (Vaucluse). Bulletin de la Société Géologique de France; S7-IX (4): 596–599, doi-org.insu.bib.cnrs.fr/10.2113/gssgfbull.S7-IX.4.596.

Angrand, P., Mouthereau, F., 2021. Evolution of the Alpine orogenic belts in the Western Mediterranean region as resolved by the kinematics of the Europe-Africa diffuse plate boundary. Bulletin de la Société Géologique de France - Earth Sci Bulletin. https://doi.org/10.1051/bsgf/2021031.

Arlhac, P., Catzigras, F., Colomb, E., Gervais, J., Gouvernet, C., Gueirard, S., Lambert, C., Mercier, H., Nury, D., Rousset, C., Tempier, C., Viencent, H., Weydert, P., 1970. Carte géol. France (1/50000), feuille PERTUIS (995). Orléans: Bureau de recherches géologiques et minières.

Arnaud, H., Debelmas, J., Flandrin, J., Gidon, M., Kerckhove, C., 1976. Remarques et réflexions à propos de l'attribution au Néogène d'une partie des cargneules et des gypses alpins. Bull. Soc. géol. Fr., 7, XVIII, No. 4, 973-979, doi:10.2113/gssgfbull.S7-XVIII.4.973.

Aubouin, J., Mennessier, G., 1962. Essai sur la structure de la Provence. In Durand-Delga M. (Coord.) : Livre à la Mémoire du Professeur Paul Fallot, Mémoire hors-série de la Société géologique de France, II, p. 45-98, pl. I.

Aubouin, J., Chorowicz, J., 1967. Le chevauchement sud-provençal : de l'Etoile à la Sainte-Baume. Bull. Soc. géol. Fr., 9, 600-608.

Aubourg, C., Rochette, P., Stéphan, J.-F., Popoff, M., Chabert-Pelline, C., 1999. The magnetic fabric of weakly deformed Late Jurassic shales from the southern subalpines chains (French Alps): evidence for SW-directed tectonic transport direction. Tectonophysics, 307, 15-31

Baby, P., Colletta, B., Zubieta, D., 1995. Etude géométrique et expérimentale d'un bassin transporté : exemple du synclinorium de l'Alto Beni (Andes centrales). Bull. Soc. géol. Fr., t. 166, no 6, pp. 797-811.

Bache, F., Olivet, J. L., Gorini, C., Aslanian, D., Labails, C., Rabineau, M., 2010. Evolution of rifted continental margins: the case of the Gulf of Lions (Western Mediterranean Basin). Earth and Planetary Science Letters, 292(3-4), 345-356.

Bache, F., Popescu, S.-M., Rabineau, M., Gorini, C., Suc, J.-P., Clauzon, G., Olivet, J.-L., Rubino, J.-L., Melinte-Dobrinescu, M.C., Estrada, F., Londeix, L., Armijo, R., Meyer, B., Jolivet, L., Jouannic, G., Leroux, E., Aslanian, D., Dos Reis, A.T., Mocochain, L., Dumurdžanov, N., Zagorchev, I., Lesić, V., Tomić, D., Çağatay, M.N., Brun, J.-P., Sokoutis, D., Csato, I., Ucarkus, G., Çakir, Z., 2012. A two-step process for the reflooding of the Mediterranean after the Messinian Salinity Crisis. Basin Research, 24,125–153.

Baroux, E., Béthoux, N., Bellier, O., 2001. Analyses of the stress field in southeastern France from earthquake focal mechanisms. Geophys. J. Int., 145, 336–348.

Bathiard, M., Lambert, C., 1968. Rapports entre la tectonique de socle et la tectonique de couverture sur la bordure ouest des Maures. Bull. Soc. géol. Fr., 7, X, 428-435.

Baubron, J.C., 1984. Volcanisme du Sud-Est de la France. In Synthèse géologique du Sud-Est de la France, Mém. BRGM, n° 125, p. 514-517.

Baudemont, D., 1985. Relations socle-couverture en Provence orientale. Evolution tectonosédimentaire permienne du bassin du Luc (Var). Université Louis Pasteur, Strasbourg, PhD thesis.

Baudrimont, F., Dubois, P., 1977. Un bassin mésogéen du domaine péri-alpin : le sud-est de la France. Bull. Centres Rech. Explor. Elf-Aquitaine, 1, 261–308.

Beauchamp, W., Allmendinger, R.W., Barazangi, M., Demnati, A., El Alji, M., Dahmani, M., 1999. Inversion tectonics and the evolution of the High Atlas Mountains, Morocco, based on a geological-geophysical transect. Tectonics 18, 2, 163-184.

Beaudouin, B., Cavelier, C., Haccard, D., Lanteaume, M., Perrin, M., 1966. A propos de l'âge des molasses de Tanaron (Basses-Alpes) ; la redécouverte du gisement de Cérithes et ses conséquences structurales. Bull. Soc. géol. Fr., 7, VIII, 458-460.

Beaudouin, B., Gigot, P., Haccard, D., 1970. Flysch et molasse, approche sédimentologique. Bull. Soc. géol. Fr., 7, XII, No. 4, 664-672.

Bellahsen, N., Sebrier, M., Siame, L., 2016. Crustal shortening at the Sierra Pie de Palo (Sierras Pampeanas, Argentina): near-surface basement folding and thrusting. Geol. Mag., 153, (5/6), 992-1012, doi:10.1017/S0016756816000467.

Bellahsen, N., Jolivet, L., Lacombe, O., Bellanger, M., Boutoux, A., Garcia, S., Mouthereau, F., Pourhiet, L.L., Gumiaux, C., 2012. Mechanisms of margin inversion in the external Western Alps: Implications for crustal rheology. Tectonophysics 560, 62-83. https://doi.org/10.1016/j.tecto.2012.06.022.

Bergerat, F., 1987. Stress fields in the European platform at the time of Africa-Eurasia collision. Tectonics 6, 99-132, doi:10.1029/TC006i002p00099.

Bertrand, M., 1887. Ilot triasique du Beausset (Var). Analogie avec le bassin houiller franco-belge et avec les Alpes de Glaris. Bull. Soc. géol. Fr., 3, XV, 667-702.

Bertrand, M., 1888. Nouvelles études sur la chaîne de la Sainte-Baume. Allure sinueuse des plis de la Provence. Bull. Soc. géol. Fr., 3, XVI, 748-778.

Besson, D., 2005. Architecture du bassin rhodano-provençal miocène (Alpes, SE France). Relations entre déformation, physiographie et sédimentation dans un bassin molassique d'avant-pays. Mines ParisTech, Paris, France, PhD thesis.

Bestani, L., 2015. Géométrie et cinématique de l'avant-pays provençal : modélisation par coupes équilibrées dans une zone à tectonique polyphasée. Aix-Marseille Université, PhD thesis, https://agse-geologues.fr/documents/docs_sciences/theses/2014_L.Bestani-CoupesEqu.Prov.18-12-2014.pdf.

Bestani, L., Espurt, N., Lamarche, J., Floquet, M., Philip, J., Bellier, O., Hollender, F., 2015. Structural style and evolution of the Pyrenean-Provence thrust belt, SE France. Bull. Soc. géol. Fr., 2015, 186, 3-19, doi:10.2113/gssgfbull.186.4-5.223.

Bestani, L., Espurt, N., Lamarche, J., Bellier, O., Hollender, F., 2016. Reconstruction of the Provence Chain evolution, southeastern France. Tectonics, 35, doi:10.1002/2016TC004115.

Béthoux, N., Tric, E., Chery, J., Beslier, M.-O., 2008. Why is the Ligurian Basin (Mediterranean Sea) seismogenic? Thermomechanical modeling of a reactivated passive margin. Tectonics, vol. 27, TC5011, doi:10.1029/2007TC002232.

Biberon, B., 1988. Mécanismes et évolution des chevauchements à vergences opposées. Exemple des structures de la Sainte-Victoire (Provence). Université Joseph Fourier, Grenoble, France, PhD thesis.

Blanc, J.-J., Caron, J.-P., Choquet, C., Gouvernet, C., Guieu, G., Mennessier, G., Nahon, D., Philip, J., Rouire, J., Tempier, C., 1974. Carte g´eol. France (1/50000), feuille CUERS (1045). Orléans: Bureau de recherches géologiques et minières.

Blanc, J.-J., Gouvernet, C., Philip, J., Tempier, C., Froget, C., Muschotti, E., 1977. Carte géol. France (1/50000), feuille LA CIOTAT (1063). Orléans: Bureau de recherche géologiques et minières.

Blanc, J.-J., Weydert, P., Masse, J.-P., Roux, M., de Peyronnet, P., 1973. Carte géol. France (1/50000), feuille SAULT-DE-VAUCLUSE (942). Orléans: Bureau de recherches g´eologiques et minières.

Bonnet, C., Malavieille, J., Mosar, J., 2008. Surface processes versus kinematics of thrust belts: impact on rates of erosion, sedimentation, and exhumation – Insights. In: analogue models. Bull. Soc. géol. Fr., 179(3), 297-314, doi:10.2113/gssgfbull.179.3.297.

Bordet, P., Chamley, H., Blanc, J.-J., Jeudy de Grissac, A., 1976. Carte géol. France (1/50000), feuille HYERES-PORQUEROLLES (1065). Orléans: Bureau de recherches géologiques et minières.

Boyer, S.E., Elliott, E., 1982. Thrust Systems. The American Association of Petroleum Geologists Bulletin, 66, No. 9, 1196-1230.

Branquet, Y., Cheilletz, A., Cobbold, P.R., Baby, P., Laumonier, B., Giuliani, G., 2002. Andean deformation and rift inversion, eastern edge of Cordillera Oriental (Guateque-Medina area), Colombia. J. South Am. Earth Sci., 15, 391–407, doi:10.1016/S0895-9811(02)00063-9.

Bréhéret, J.-G., 1995. L'Aptien et l'Albien de la fosse Vocontienne (des bordures au bassin) : évolution de la sédimentation et enseignements sur les évènements anoxiques. PhD thesis. Université François Rabelais-Tours, tel-00805488.

Brocard, C., Philip, J., 1989. Précisions stratigraphiques sur le Trias de la Provence orientale : conséquences structurales et paléogéographiques. Géologie de la France, 3, 27-32.

Burbank, D.W., Vergés, J., 1994. Reconstruction of topography and related depositional systems during active thrusting. Journal of Geophysical Research, 99, No. B10, 20,281-20,297.

Burrel, L., Teixell, A., 2021. Contractional salt tectonics and role of pre-existing diapiric structures in the Southern Pyrenean foreland fold–thrust belt (Montsec and Serres Marginals). Journal of the Geological Society, 178, doi:10.1144/jgs2020-085.

Butler, R.W.H., 2013. Area balancing as a test of models for the deep structure of mountain belts, with specific reference to the Alps. J. Struct. Geol., 52, 2-16.

Butler, R.W.H., 2017. Basement-cover tectonics, structural inheritance, and deformation migration in the outer parts of orogenic belts: A view from the western Alps. *in* Law, R.D., Thigpen, J.R., Merschat, A.J., and Stowell, H.H. (Eds.), Linkages and Feedbacks in Orogenic Systems: Geological Society of America Memoir 213, p. 55-74, doi:10.1130/2017.1213(03).

Butler, R.W.H., 2020. Syn-kinematic strata influence the structural evolution of emergent fold–thrust belts. In : Hammerstein, J.A., Di cuia, R., Cottam, M.A., Zamora, G., Butler, R.W. H. (Eds), Fold and Thrust Belts: Structural Style, Evolution and Exploration. Geological Society, London, Special Publications, 490, 57-78.

Butler, R.W.H., Bond, C.E., Cooper, M.A., Watkins, H., 2020. Fold-thrust structures – where have all the buckles gone? in: Bond, Lebit, H.D. (Eds), Folding and Fracturing of Rocks: 50 Years of Research since the Seminal Text Book of J. G. Ramsay. Geological Society, London, Special Publications, 487, 21-44, doi:10.1144/SP487.7.

Calderon, Y., Baby, P., Hurtado, C., Brusset, S., 2017. Thrust tectonics in the Andean retro-foreland basin of northern Peru: Permian inheritances and petroleum implications. Marine and Petroleum Geology, 82, 238-250, doi:10.1016/j.marpetgeo.2017.02.009.

Callot, J.-P., Jahani, S., Letouzey, J., 2007. The role of pre-existing diapirs in fold and thrust belt development. In Lacombe, O., Lavé, J., Roure, F., Vergés J. (Eds.), Thrust belts and foreland basins. Berlin Heidelberg: Springer-Verlag, 309-325.

Callot, J.-P., Trocmé, V., Letouzey, J., Albouy, E., Jahani, S., Sherkati, S., 2012. Pre-existing salt structures and the folding of the Zagros Mountains. Geological Society, London, Special Publications, 363(1), 545–561. https://doi.org/10.1144/SP363.27.

Campredon, R., Giannerini, G., 1982. Le synclinal de Saint-Antonin (arc de Castellane, chaînes subalpines méridionales) Un exemple de bassin soumis à une déformation compressive permanente depuis l'Eocène supérieur. Géologie Alpine, t. 58, 15-20.

Cassinis, G., Durand, M., Ronchi, A., 2003. Permian-Triassic continental sequences of northwest Sardinia and south Provence: stratigraphic correlations and palaeogeographical implications. Bolletino della Società Geologica Italiana, Volume speciale, 2, 119-129.

Catzigras, F., Colomb, E., Durand, J.-P., Guieu, G., Rousset, C., Tempier, C., 1969. Carte géol. France (1/50000), feuille AIX-EN-PROVENCE (1021). Orléans: Bureau de recherches g´eologiques et minières.

Caron, J.P., 1970. Episodes volcaniques et volcano-détritiques dans le Trias moyen de la partie méridionale de l'arc de Barjols (Var). In: Comptes rendus de l'Académie des Sciences, Paris. vol. 270. pp. 12231226 D.

Caron, J.-P., 1979. Trias au sud de l'Argens (Var). In: Rouire et al., Notice géologique de la feuille Brignoles à 1/50.000, 6‑7.

Célini, N., 2020. Le rôle des évaporites dans l'évolution tectonique du front alpin : cas de la Nappe de Digne. Université de Pau et des Pays de l'Adour, Pau, France, PhD thesis.

Célini, N., Callot, J.-P., Ringenbach, J.-C., Graham, R., 2020. Jurassic Salt Tectonics in the SW Sub-Alpine Fold-and-Thrust Belt. Tectonics, 39, e2020TC006107, doi:10.1029/2020TC006107.

Célini, N., Callot, J.-P., Ringenbach, J.-C., Graham, R., 2021. Anatomy and evolution of the Astoin diapiric complex, sub-Alpine fold-and-thrust belt (France). BSGF - Earth Sciences Bulletin, Vol: 200052, doi:10.1051/bsgf/2021018.

Champion, C., Choukroune, P., Clauzon, G., 2000. La déformation post-Miocène en Provence occidentale. Geodinamica Acta, 13, 67-85.

Chardon, D., Hermitte, D., Nguyen, F., Bellier, O., 2005. First paleoseismological constraints on the strongest earthquake in France (Provence) in the twentieth century. Geology, v. 33, no. 11, 901-904, doi:10.1130/G21713.1.

Clauzon, G., 1978. The Messinian Var canyon (Provence, southern France): Paleogeographic implication. *In*: Cita, M.B., Ryan, B.F. (Eds), Messinian erosional surfaces in the Mediterranean marine geology. Mar. Geol., 27, (3/4), 203-222.

Clauzon, G., 1979. Le canyon messinien de la Durance (Provence, France): une preuve paléogéographique de bassin profond de dessiccation. Palaeogeography, Palaeoclimatology, Palaeoecology, 29, 15-40.

Clauzon, G., 1996. Limites de séquence et évolution géodynamique. Géomorphologie : relief, processus, environnement, 1, 3-22.

Clauzon, G., 1982. Le canyon messinien du Rhône: une preuve décisive du « dessicated deep-basin model » [Hsü, Cita et Ryan, 1973]. Bull. Soc. géol. Fr., 7, XXIV, 597-610.

Clauzon, G., Aguilar, J.-P., Michaux, J., 1989. Relation temps-sédimentation dans le Néogène méditerranéen français. Bull. Soc. géol. France, 8, V, No. 2, 361-372.

Coadou, A., Beaudoin, B., Mouterde, R., 1971. Variations lithologiques et corrélations stratigraphiques dans le Lias moyen et supérieur de Barles et du Plateau de Chine (Alpes de Haute-Provence). Bull. Soc. géol. Fr., 7, 5–12.

Clauzon, G., Fleury, T. J., Bellier, O., Molliex, S., Mocochain, L., Aguilar, J. P., 2011. Morphostructural evolution of the Luberon since the Miocene (SE France), Bull. Soc. géol. Fr., 182, 95–110, doi:10.2113/gssgfbull.182.2.95.

Cojan, I., 1989. Discontinuités majeures en milieu continental. Proposition de corrélation avec des événements globaux (Bassin de Provence, S. France, Passage Crétacé/Tertiaire). C. R. Acad. Sci. Paris, 309, II, 1013-1018.

Cojan, I., 1993. Alternating fluvial and lacustrine sedimentation: tectonic and climatic controls (Provence Basin, S., France, Upper Cretaceous/Palaeocene). Spec. Publs Int. Ass. Sediment., 17, 425-438.

Cojan, I., Renard, M., Emmanuel, L., 2003. Palaeoenvironmental reconstruction of dinosaur nesting sites based on a geochemical approach of eggshells and associated palaeosols (Maastrichtian, Provence basin, France). – Palaeogeogr., Palaeoclimatol., Palaeoecol., 191, 111-138.

Cojan, I., Bialkowski, A., Gillot, T., Renard, M., 2013. Paleoenvironnement and paleoclimate reconstruction for the early to middle Miocene from stable isotopes in pedogenic carbonates (Digne-Valensole basin, southeastern France). Bull. Soc. géol. France, 184, No. 6, 583-599.

Collina-Girard, J., Griboulard, R., 1990. The deep-structure of the Valensole Plateau (French Alps). Contribution of network valley and topographic analysis. Géologie méditerranéenne, 17, 153–171.

Combes, P., 1984. La tectonique récente de la Provence occidentale microtectonique, caractéristiques dynamiques et cinématiques : méthodologie de zonation tectonique et relations avec la séismicité. Université Louis Pasteur, Strasbourg, France, PhD thesis.

Cornet, C., 1961. Le delta vindobonien du bas-pays de Saint-Maximin et de Ginasservis (Var). Bull. Soc. géol. Fr., 7, III, 424-431, doi:10.2113/gssgfbull.S7-III.5.424.

Cornet, C., 1965. Evolution tectonique et morphologique de la Provence depuis l'Oligocène. Mém. Soc. Géol. France, nouv. sér., XLIV, No. 103, Paris, PhD thesis.

Corroy, G., 1957. La Montagne Sainte-Victoire. Bulletin du Service de la Carte géologique de la France, LV, 251, 1-46.

Corroy, G., Philip, J., 1964. Le brachyanticlinal des pics des Corbeaux dans le massif de la Sainte-Baume (Var). Bull. Soc. géol. Fr., 7, VI, 560-563.

Corsini, M., Bosse, V., Féraud, G., Demoux, A., Crevola, G., 2010. Exhumation processes during post-collisional stage in the Variscan belt revealed by detailed 40Ar/39Ar study (Tanneron Massif, SE France). Int J Earth Sci (Geol Rundsch) (2010) 99:327–341, doi:10.1007/s00531-008-0397-x

Couëffé, R., Tessier, B., Gigot, P., Beaudouin, B., 2004. Tidal rhythmites as possible indicators of very rapid subsidence in a foreland basin: an example from the Miocene marine molasse formation of the Digne foreland basin, SE France. Journal of sedimentary research, 74, No. 6, 746–759, doi:10.1306/040904740746.

Coulon, C., 1967. Le volcanisme tertiaire de la région toulonnaise (Var). Bull. Soc. Géol. France 7, 691-700.

Coward, M.P., 1996. Balancing sections through inverted basins, in: Buchanan, E.G., Nieuwland, D.A. (Eds), Modem Developments in Structural Interpretation, Validation and Modelling. Geological Society Special Publication No. 99, pp. 51-77.

Crévola, G., Pupin, J.-P., 1994. Crystalline Provence: structure and Variscan evolution, in: Keppie J.D. (ed.), Pre-Mesozoic Geology in France and Related Areas, Springer Verlag, Berlin, 426-441. C. R. Geoscience, 341, 214-223.

Crumeyrolle, P., Rubino, J.-L., Clauzon, G., 1991. Miocene depositional sequences within a tectonically controlled transgressive-regressive cycle. Spec. Publs. Int. Ass. Sediment., 12, 373-390.

Cushing, E.M., Bellier, O., Nechtschein, S., Sébrier, M., Lomax., Volant, P., Dervin, P., Guignard, P., Bove, L., 2008. A multidisciplinary study of a slow-slipping fault for seismic

hazard assessment: the example of the Middle Durance Fault (SE France). Geophys. J. Int., doi:10.1111/j.1365-246X.2007.03683.x.

Dahlstrom, C.D.A., 1969. Balanced cross-sections. Can. J. Earth Sci., 6(4), 743-757.

Dardeau, G., 1988. Tethyan evolution and Alpine reactivation of Jurassic extensional structures in the French “Alpes maritimes”. Bull. Soc. géol. Fr., 4, 651-657.

Dardeau, G., de Graciansky, P.-C., 1990. Halocinèse et rifting téthysien dans les Alpes-Maritimes (France). Bulletin des Centres de Recherches Exploration-Production Elf-Aquitaine, 14(2), 443–464.

Dardeau, G., Dubar, M., Toutin-Morin, N., Courme, M.-D., Crévola, G., Mangan, Ch., 2010. Notice explicative, Carte géol. France (1/50 000), feuille Grasse-Cannes (999). Orléans, BRGM, 194 p. Carte géologique par Dardeau G., Dubar M., Toutin-Morin N., Courme M.-D., Crévola G., Mangan Ch.

Debelmas J., 1974. Les chaines plissées du cycle alpin et leur avant-pays. Géologie de la France, volume II, doin éditeurs, Paris. 2, 293 p.

Debelmas J., Arnaud, H., Caron, C., Gidon, M., Kerckhove, Cl., Lemoine, M., Vialon, P., 1970. Guides géologiques régionaux: Alpes (Savoie et Dauphiné). France, Masson (Ed), 214 p.

Debelmas J., Arnaud, H., Gidon, M., Kerckhove, Cl., Giraud, P., Lemoine, M., Menot, J.P., Monjuvent, G., Vialon, P., 1983. Guides géologiques régionaux: Alpes du Dauphiné. France, Masson (Ed), 198 p.

DeCelles, P.G., Giles, P.C., 2001. Rates of shortening, propagation, underthrusting, and flexural wave migration in continental orogenic systems. Geology. 29, 135–138.

Delfaud, J., Toutin-Morin, N., Morin, R., 1989. Un cône alluvial en bordure d’un bassin intramontagneux : La formation permienne du Rocher de Roquebrune (Bassin du Bas-Argens, Provence orientale). C. R. Acad. Sci. Paris, II, 309, 1811-1817.

Dorkel, A., Grégoire, J.-Y., Belleville, J.-M., Pachoud, A., Savornin, J., Destombes, J.-P., Roch, E., de Peyronnet, P., Demarcq, G., 1966. Carte géol. France (1/50000), feuille REILLANE (968). Orléans: Bureau de recherches g´eologiques et minières.

Dubar, M., 1983. Reconnaissance de la discontinuité de ravinement messinienne dans le bassin de Riez-Valensole ; implications stratigraphiques. C. R. Acad. Sci. Paris, II, 885-887.

Dubar, M., 1984. Chronologie et signification des dépôts continentaux de Néogène supérieur du bassin de Riez-Valensole (Alpes-de-Haute-Provence, France). Bull. Soc. géol. Fr., 7, XXVI, No. 5, 971-978.

Dubois, P., Curnelle, R., 1978. Résultats apportés par le forage Les Mées no 1 sur le plateau de Valensole (Alpes de Haute-Provence). C. R. somm. Soc. géol. Fr., 4, 181-184.

Dupire, S., 1985. Étude cartographique au 1/25 000 de la zone sud du bassin de Marseille. Les Travertins de Marseille : aperçu géomorphologique et néotectonique. Université de Provence, PhD thesis.

Durand, J.-P., 1962. Sur le poudingue de la Galante (région d’Aix-en-Provence). C.R. Soc. géol. Fr., 4, 109-111.

Durand, J.-P., 1980. Les sédiments fuvéliens du synclinal de l’Arc (Provence). Industrie Minérale, « Le gisement de charbon du bassin de l’Arc », 62, 13-25.

Durand, J.-P., Mennessier, G., 1964. Sur l'existence d'une discordance entre le Bégudo-Rognacien et le Fuvélien à l'extrémité orientale du synclinal de l'Arc en Basse-Provence occidentale. C. R. Somm. Soc. géol. Fr., 253-254.

Durand, J.-P., Tempier, C., 1962. Etude tectonique de la zone des brèches du massif de Sainte-Victoire dans la région du Tholonet (Bouches-du-Rhône). Bull. Soc. géol. Fr., 7, IV, 97-101.

Durand, M., 1993. Un exemple de sédimentation continentale permienne dominée par l'activité de chenaux méandriformes : la Formation de Saint-Mandrier (Bassin de Toulon, Var). Géologie de la France (2), 43-55.

Echavarria, L., Hernandez, R., Allmendinger, R., Reynols, J., 2003. Subandean thrust and fold belt of northwestern Argentina: Geometry and timing of the Andean evolution. AAPG Bulletin, 87, No. 6, 965-985.

Ege, H., Sobel, E.R., Scheuber, E., Jacobshagen, V., 2007. Exhumation history of the southern Altiplano plateau (southern Bolivia) constrained by apatite fission track thermochronology. Tectonics, 26, TC1004, doi:10.1029/2005TC001869.

Elliott, D., 1983. The construction of balanced cross-sections. J. Struct. Geol., 5, No. 2, 101.

Elliott, D., Johnson, M.R.W., 1980. The structural evolution of the northern part of the Moine thrust zone. Royal Soc. Edinburgh Trans. Earth Sci., 71, 69-96.

Erdős, Z., Huismans, R.S., van der Beek, P., 2015. First-order control of syntectonic sedimentation on crustal-scale structure of mountain belts. J. Geophys. Res. Solid Earth, 120, 5362–5377, doi:10.1002/ 2014JB011785.

Espurt, N., Brusset, S., Baby, P., Hermoza, W., Bolaños, R., Uyen, D., Déramond, J., 2008. Paleozoic structural controls on shortening transfer in the Subandean foreland thrust system, Ene and southern Ucayali basins, Peru. Tectonics, vol. 27, TC3009, doi:10.1029/2007TC002238.

Espurt, N., Barbarand, J., Roddaz, M., Brusset, S., Baby, P., Saillard, M., Hermoza, W., 2011. A scenario for late Neogene Andean shortening transfer in the Camisea Subandean zone (Peru, 12o S): Implications for growth of the northern Andean Plateau. Geological Society of America Bulletin, 123, pp. 2050-2068, doi:10.1130/B30165.1.

Espurt, N., Hippolyte, J.-C., Saillard, M., Bellier, O., 2012. Geometry and kinematic evolution of a long-living foreland structure inferred from field data and cross section balancing, the Sainte-Victoire System, Provence, France. Tectonics, vol. 31, TC4021, doi:10.1029/2011TC002988.

Espurt, N., Angrand, P., Teixell, A., Labaume, P., Ford, M., de Saint Blanquat, M., Chevrot, S., 2019a. Crustal-scale balanced cross-section and restorations of the Central Pyrenean belt (Nestes-Cinca transect): Highlighting the structural control of Variscan belt and Permian-Mesozoic rift systems on mountain building. Tectonophysics, 764, 25-45, doi:10.1016/j.tecto.2019.04.026.

Espurt, N., Wattelier, F., Philip, J., Hippolyte, J.-C., Bellier, O., Bestani, L., 2019b. Mesozoic halokinesis and basement inheritance in the eastern Provence fold-thrust belt, SE France. Tectonophysics, 766, pp. 60-80, doi:10.1016/j.tecto.2019.04.027.

Fabre, J., Guieu, G., Philip, J., Tronchetti, G., 1975. Mise en évidence d'une écaille crétacée superposée au Trias de l'Huveaune, près de Roquevaire (Bouches-du-Rhône). Conséquences structurales. C. R. Acad. Sci., Paris, (D), 281, 11-114.

Fabre, P., Lami, A., Pairis, J.L., Gidon, M., 1985. Déformations synsédimentaires paléogènes, du Pelvoux au Dévoluy (Alpes externes). Terra cognita, vol.5, no 2-3, 243.

Fabre-Taxy, S., Philip, J., 1964. La zone du Plan d'Aups dans sa région type, la Sainte-Baume (Var). Bull. Soc. géol. Fr., 7, VI, 554-559.

Faucher, T., Gidon, M., Pairis, J.L., Mascle, G., 1988. Directions de transport au front de la nappe de Digne (chaînes subalpines méridionales). C. R. Acad. Sci. Paris, 306, II, 227-230.

Fillon, C., Huismans, R.S., van der Beek, P., 2013. Syntectonic sedimentation effects on the growth of fold-and-thrust belts. Geology, 41, 83–86, doi:10.1130/G33531.1.

Flandrin, J., Gottis, M., Viallix, J., Golenko, N., Riche, P., Parant, J., Rebelly, G., Bejanin, J., Issenmann, O., Teisserenc, P., Mollier, M., Cochet, E., 1964. Carte géol. France (1/50000), feuille SEDERON (916). Orléans: Bureau de recherches géologiques et minières.

Floquet, M., Gari, J., Hennuy, J., Léonide, P., Philip, J., 2005. Sédimentations gravitaires carbonatées et silicoclastiques dans un bassin en transtension, séries d'âge cénomanien à coniacien moyen du Bassin sud-provençal. Livret guide d'excursion géologique, 10e Congrès français de Sédimentologie, 14-15 octobre 2005, Publication ASF, Paris, 52.

Floquet, M., Philip, J., Léonide, P., Gari, J., 2006. Sédimentation et géodynamique du Bassin Sud-Provençal au Crétacé supérieur. Livret-guide d'excursion géologique, Université de Provence, Centre Saint-Charles, Marseille, Ouvrage en dépôt à la SGF Paris.

Floquet, M., Leleu, S., Tortosa, T., 2021. Du bassin marin au bassins continentaux sud-provençaux durant la Crétacé supérieur et au Paléogène, de -100 à -43 Ma. In: La Géologie des Bouches-du-Rhône - Roches et paysages remarquables – éditions du BRGM. 447p., chap. 2.5., 69-116.

Ford, M., Lickorish, W.H., Kusznir, N.J., 1999. Tertiary foreland sedimentation in the Southern Subalpine Chains, SE France: a geodynamic appraisal. Basin Research, 11, 315-336. doi:10.1046/j.1365-2117.1999.00103.x.

Ford, M., Duchêne, S., Gasquet, D., Vanderhaeghe, O., 2006. Two-phase orogenic convergence in the external and internal SW Alps. Journal of the Geological Society, London, 163, 815-826.

Fournier, M., Agard, P., Petit, C., 2008. Micro-tectonic constraints on the evolution of the Barles half-window (Digne nappe, southern Alps). Implications for the timing of folding in the Valensole foreland basin. Bull. Soc. géol. Fr., 179, No. 6, 551-568.

Friès, G., 1987. Dynamique du bassin subalpin méridional de l'Aptien au Cénomanien. Université Paris VI, Paris, France, 1986, Mém. Sci. Terre ENS Mines Paris 4, PhD thesis.

Garcia, G., Vianey-Liaud, M., 2001. Nouvelles données sur les coquilles d'oeufs de dinosaures Megaloolithidae du Sud de la France : systématique et variabilité intraspécifique. C. R. Acad. Sci. Paris, Sciences de la Terre et des planètes / Earth and Planetary Sciences, 332, 185-191, doi:10.1016/S1251-8050(00)91401-0.

Gattacceca, J., Deino, A., Rizzo, R., Jones, D. S., Henry, B., Beaudoin, B., Vadeboin, F., 2007. Miocene rotation of Sardinia: New paleomagnetic and geochronological constraints and geodynamic implications. Earth Planet. Sci. Lett., 258, 359–377, doi:10.1016/j.epsl.2007.02.003.

Gaviglio, P., 1985. A fault and stress field analysis in a coal mine (Gardanne, Bouches du Rhône, France. Tectonophysics, 113, 349-366.

Giannerini, G., Gigot, P., Campredon, R., 1977. Le Tertiaire de La Roque-Esclapon (front sud de l'arc de Castellane) : la superposition de deux déformations synsédimentaires oligocène et miocène et des bassins sédimentaires associés. Bull. BRGM, Fr., (2), Section 1, n°3, 179-188.

Giannerini, G., 1978. Contribution à l'étude géologique de la bordure méridionale de l'arc de Castellane entre Mons et Bargème (Var) : relations entre les déformations tectoniques et la sédimentation au cours du Tertiaire. PhD thesis. Université Nice Sophia Antipolis.

Gidon, M., 1982. La reprise de failles anciennes par une tectonique compressive : sa mise en évidence et son rôle dans les chaînes subalpines des Alpes occidentales. Géologie Alpine, 58, 53-68.

Gidon, M., 1989. La rupture des charnières anticlinales par cisaillement dans les flancs longs des plis : un mode méconnu de formation des chevauchements, observable dans les chaînes subalpines des Alpes occidentales françaises. Géologie alpine, t.65, 65-74.

Gidon, M., 1997. Les chaînons subalpins au nord-est de Sisteron et l'histoire tectonique de la nappe de Digne. Géologie Alpine, 73, 23-57.

Gidon, M., Arnaud, H., Pairis, J.L., Aprahamian, J., Uselle, J.P., 1970. Les déformations tectoniques superposées du Dévoluy méridional (Hautes-Alpes). Géologie Alpine, t. 46, 87-110.

Gidon, M., Pairis, J.L., 1976. Le rôle de mouvements tectoniques éocènes dans la genèse des structures de l'extrémité NE du Dévoluy et dans celle du chevauchement de Digne. Géologie alpine, t. 52, 73-83.

Gidon, M., Pairis, J.L., 1986. La nappe de Digne (Chaînes subalpines méridionales): origine, déplacement et signification régionale. C.R. Acad. Sc. Paris, t.303, Série II, n°10, 981-984

Gidon, M., Pairis, J.L., 1988. La structure des environs de Digne (Chaînes subalpines méridionales, Alpes-de-Haute-Provence) : un exemple d'interférence entre l'avancée d'une nappe de charriage épiglyptique et la sédimentation sur son front. C.R. Acad. Sci. Paris, 307, II, 1283-1288.

Gidon, M., Pairis, J.L., 1992. Relations entre le charriage de la Nappe de Digne et la structure de son autochtone dans la vallée du Bès (Alpes de Haute-Provence, France). Eclogae geol. Helv., Vol.85/2, 327-359.

Gidon, M., Pairis, J.L., Arnaud, H., Aprahamian, J., Uselle, J.P., 1970. Les déformations tectoniques superposées du Dévoluy méridional (Hautes-Alpes). Travaux du Laboratoire de Géologie de l'Université de Grenoble, t.46 (1970), 87-110.

Gigot, P., Cotillon, P., Haccard, D., Montjuvent, G., Dardeau, G., 2013. Carte géol. France (1/50000), feuille SISTERON (917). Orléans: Bureau de recherches géologiques et minières.

Gigot, P., Grandjacquet, C., Haccard, D., 1974. Evolution tectono-sédimentaire de la bordure septentrionale du bassin tertiaire de Digne depuis l'Eocène. Bull. Soc. géol. Fr., 7, XVI, no. 2, 128-139.

Gigot, P., Mein, P., Truc, G., 1976. La série continentale du pont d'Aiguines près de Moustiers-Sainte-Marie : un équivalent latéral du Miocène marin du bassin de Digne (Alpes-de-Haute-Provence). Géobios, 9, 795-799.

Gigot, P., Thomel, G., Colomb, E., Dubar, M., Durozoy, G., Damiani, L., 1981a. Notice explicative, Carte géol. France (1/50000), feuille FORCALQUIER (943). Orléans : Bureau de recherches géologiques et minières.

Gigot, P., Thomel, G., Colomb, E., Dubar, M., Durozoy, G., Damiani, L., 1981b. Carte géol. France (1/50000), feuille FORCALQUIER (943). Orléans : Bureau de recherches géologiques et minières.

Godard, V., Hippolyte, J.-C., Cushing, E., Espurt, N., Fleury, J., Bellier, O., Ollivier, V., the ASTER team, 2020. Hillslope denudation and morphologic response across a rock uplift gradient. Earth Surf. Dynam., 8, 221-243, doi:10.5194/esurf-8-221-2020.

Goguel, J., Vuillermoz, M., Lanteaume, M., Lemoine, M., 1964. Carte géol. France (1/50000), feuille DIGNE (944). Orléans: Bureau de recherches géologiques et minières.

Goguel, J, 1963. L'interprétation de l'arc des Alpes occidentales. Bulletin de la Société Géologique de France, 7, V.

Goguel, J., 1944. La tectonique de fond dans la zone externe des Alpes. Bulletin de la Société Géologique de France, 5, 14, 201-218, doi:10.2113/gssgfbull.S5-XIV.4-6.201.

Goguel, J., 1939. Tectonique des chaînes subalpines entre la Bléone et la Durance-Alpes. Bulletin des services de la carte géologique de France, 202(XLI), 1-48.

Goguel, J., 1937. Description tectonique de la bordure des Alpes de la Bléone au Var. Université de Paris, PhD thesis.

Gouvernet, C., Blanc, J.-J., Philip, J., Caron, J.-P., Coulon, C., Gueirard, S., 1969. Carte géol. France (1/50000), feuille TOULON (1064). Orléans: Bureau de recherches géologiques et minières.

Gouvernet, C., 1963. Structure de la région toulonnaise. Mémoire de la Carte géologique détaillée de la France, 244 p.

Graciansky, P.-C. de, Dardeau, G., Lemoine, M., Tricart, P., 1989. The inverted margin of the French Alps and foreland basin inversion. Geol. Soc. London, Spec. Publ., 44, 87–104, doi:10.1144/GSL.SP.1989.044.01.06.

Graciansky, P.-C. de, Lemoine, M., 1988. Early Cretaceous extensional tectonics in the southwestern French Alps : A consequence of North-Atlantic rifting during Tethyan spreading. Bull. Soc. géol. Fr., 8, IV, No. 5, 733-737, doi:10.2113/gssgfbull.IV.5.733.

Granado, P., Roca, E., Strauss, P., Pelz, K., Muñoz, J.A., 2018. Structural styles in fold-and-thrust belts involving early salt structures: The Northern Calcareous Alps (Austria). Geology, 47, 51-54, doi:10.1130/G45281.1.

Guieu, G., 1968. Etude tectonique de la région de Marseille. Université d'Aix-Marseille, France, PhD thesis, 604 p.

Guieu, G., Roussel, J., 1990. Arguments for the pre-rift uplift and rift propagation in the Ligurian-Provençal basin (Northwestern Mediterranean) in the light of Pyrenean Provençal orogeny. Tectonics, 9, No. 5, 1113-1142.

Graham, R., Jackson, M., Pilcher, R., Kilsdonk, B., 2012. Allochthonous salt in the sub-Alpine fold-thrust belt of Haute Provence, France. Geological Society, London, Special Publications 2012, 363, 595-615, doi:10.1144/SP363.30.

Guignard, P., Bellier, O., Chardon, O., 2005. Géométrie et cinématique post-oligocène des failles d'Aix et de la moyenne Durance (Provence, France). C. R. Geoscience, 337, 375-384, doi:10.1016/j.crte.2004.10.009.

Guillemot, J., Guy M., Lobjoit, M., 1973. Un système cohérent d'alignements structuraux commun aux Alpes et aux Pyrénées mis en évidence par le satellite ERTS 1. C. R. Acad. Sci., Paris, 277, 481-484.

Guillot, S., Menot, R.-P., 2009. Paleozoic evolution of the External Crystalline Massifs of the Western Alps. C. R. Geosci., 341, 253–265.

Guiomar, M., 1990. Le Carbonifère des chaînes subalpines de Haute-Provence (France) dans son cadre structural. Université de Provence, Marseille, France, PhD thesis.

Guyonnet-Benaize, C., Lamarche, J., Hollender, F., Visuer, S., Münch, P., Borgomano, J., 2015. Three-dimensional structural modeling of an active fault zone based on complex outcrop and subsurface data: The Middle Durance Fault Zone inherited from polyphase Meso-Cenozoic tectonics (southeastern France). Tectonics, 34, 265–289, doi:10.1002/2014TC003749.

Guyonnet-Benaize, C., Lamarche, Masse, J.-P., Villeneuve, M., Viseur, S., 2010. 3D structural modelling of small-deformations in poly-phase faults pattern. Application to the Mid-Cretaceous Durance uplift, Provence (SE France). Journal of Geodynamics, 50, 81–93, doi:10.1016/j.jog.2010.03.003.

Haccard, D., Beaudoin, B., Gigot, P., Jorda, M., et al., 1989a. Carte géol. Fr. (1/50 000), Feuille LA JAVIE (918). Orléans : Bureau de recherches géologiques et minières.

Haccard, D., Beaudoin, B., Gigot, P., Jorda, M., 1989b. Notice explicative, Carte géol. Fr. (1/50 000), feuille LA JAVIE (918). Orléans : Bureau de recherches géologiques et minières.

Haug, E., 1925. Les nappes de charriage de la Basse-Provence. Première partie. La région toulonnaise. Mémoire du Service de la Carte géologique détaillée de la France, 304 p.

Hennuy, J., 2003. Sédimentation carbonate et silicoclastique sous contrôle tectonique, le bassin sud-provençal et sa plate-forme carbonatée du Turonien moyen au Coniacien moyen. Evolutions séquentielle, diagénétique, paléogéographique. Université de Provence, France, PhD thesis, 194 p.

Hernandez, J.I., Hernandez, R.M., Farjat, A.D., Cristallini, E.O., Alvarez,L.A., Dellmans, L.M., Costilla, M.R., Alvarez, A.F., Becchio, R., Bordese, S., Arzadun, G., Guibaldo, C.,Glasmacher, U.A., Tomezzoli, R.N., Stockli, D.F., Fuentes, F., Galvarro, J.S., Rosales, A., Dzelalija, F.,Haring, C., 2020. Multiple thermochronometers applied to the quantitative analysis of compressive systems: The southern sub-Andean fold and thrust belt of Bolivia. From source rock to trap, Journal of South American Earth Sciences, doi:10.1016/j.jsames.2020.102949.

Heermance, R.V., Chen, J., Burbank, D.W., Miao, J., 2008. Temporal constraints and pulsed Late Cenozoic deformation during the structural disruption of the active Kashi foreland, northwest China. Tectonics, 27, TC6012, doi:10.1029/2007TC002226.

Hinsch, R., 2013. Laterally varying structure and kinematics of the Molasse fold and thrust belt of the Central Eastern Alps: Implications for exploration. AAPG Bulletin, 97, 1805-1831.

Hippolyte, J.-C., Angelier, J., Bergerat, F., Nury, D., Raynaud, S., 1990. Evolution tectono-sédimentaire d'un bassin faille: le bassin oligocène de Marseille. C. R. Acad. Sci. Paris, 310, 53-58.

Hippolyte, J.-C., Nury, D., Angelier, J., Bergerat, F., 1991. Bull. Soc. Géol. Fr., 162, 1083-1094.

Hippolyte, J.-C., Angelier, J., Roure, F., 1992. Les permutations de contraintes dans un orogène: exemple des terrains quaternaires du sud de l'Apennin. C. R. Acad. Sci. Paris, 315, 89-95.

Hippolyte, J.-C., Angelier, J., Nury, D., Bergerat, F., Guieu, G., 1993. Tectonic-stratigraphic record of paleostress time changes in the Oligocene basins of the Provence, southern France. Tectonophysics, 226, 15–35, doi:10.1016/0040-1951(93)90108-V.

Hippolyte, J.-C., Dumont, T., 2000. Identification of Quaternary thrusts, folds and faults in a low seismicity area: examples in the Southern Alps (France). Terra Nova, 12, 156-162.

Hippolyte, J.-C., Clauzon, G., Suc, J.-P., 2011. Messinian-Zanclean canyons in the Digne nappe (southwestern Alps): tectonic implications. Bull. Soc. géol. Fr., 182, No. 2, 111-132.

Hippolyte, J.-C., Bellier, O., Espurt, N., 2012. Quaternary deformation and stress perturbations along the Digne thrust front, Southwestern Alps. C. R. Geoscience, 344, 205–213, doi:10.1016/j.crte.2012.03.002.

Hossack, J.R., 1979. The use of balanced cross-sections in the calculation of orogenic contraction: A review. J. geol, Soc. London, 136, 705-711.

Jamison, W.R., 1993. Mechanical stability of the triangle zone: the backthrust wedge. Journal of geophysical research. 98, B11, 20,015-20,030.

Jakni, B., 2000. Thermochronologie par traces de fission des marges conjuguées du bassin liguro-provençal : la Corse et le massif des Maures-Tanneron. Université Joseph Fourier, Grenoble I, France, PhD thesis, https://tel.archives-ouvertes.fr/tel-00644736/document.

Jolivet, M., Labaume, P., Monié, P., Brunel, M., Arnaud, N., Campani, M., 2007. Thermochronology constraints for the propagation sequence of the south Pyrenean basement thrust system (France-Spain). Tectonics, 26, TC5007, doi:10.1029/2006TC002080.

Jourdon, A., Rolland, Y., Petit, C., Bellahsen, N., 2014. Style of Alpine tectonic deformation in the Castellane fold-and-thrust belt (SW Alps, France): Insights from balanced cross-sections. Tectonophysics, 633, 143-155, doi:10.1016/j.tecto.2014.06.1022.

Jourdon, A., Pourhiet, L.L., Mouthereau, F., Masini, E., 2019. Role of rift maturity on the architecture and shortening distribution in mountain belts. Earth and Planetary Science Letters 512, 89-99, doi.org/10.1016/j.epsl.2019.01.057.

Jourdon, A., Mouthereau, F., Le Pourhiet, L., Callot, J.-P., 2020. Topographic and tectonic evolution of mountain belts controlled by salt thickness and rift architecture. Tectonics, 39, e2019TC005903, doi.org/10.1029/2019TC005903.

Kerckhove, C., Antoine, P., 1963. Nouvelles données sur le chevauchement de Rougon - Pont de Soleil (zone subalpine, région de Castellane, Basses-Alpes). C. R. Acad. Sci. Paris, 257, 716-718.

Kerckhove, C., Roux, M., Mercier, H., 1978. Carte géol. France (1/50000), feuille MOUSTIER-SAINTE-MARIE (970). Orléans: Bureau de recherches géologiques et minières.

Kergaravat, C., Ribes, C., Legeay, E., Callot, J.P., Kavak, K.S., Ringenbach, J.C., 2016. Minibasins and salt canopy in foreland fold-and-thrust belts: The central Sivas Basin, Turkey. Tectonics, 35, 1342–1366, doi:10.1002/2016TC004186.

Kilian, W., 1892. Sur l'existence de phénomènes de recouvrement aux environs de Gréoux (Basses-Alpes) et sur l'âge de ces dislocations. C. R. Acad. Sci. Paris, 115, 1024-1026.

Kley, J., Monaldi, C.R., 2002. Tectonic inversion in the Santa Barbara System of the central Andean foreland thrust belt, northwestern Argentina. Tectonics, vol. 21, 6, 1061, doi:10.1029/2002TC902003, 2002

Labaume, P., Meresse, F., Kolivet, M., Teixell, A., Lahfid, A., 2016. Tectonothermal history of an exhumed thrust-sheet-top basin: An example from the south Pyrenean thrust belt. Tectonics, 35, 1280-1313, doi:10.1002/2016TC004192.

Labaume, P., Teixell, A., 2020. Evolution of salt structures of the Pyrenean rift (Chaînons Béarnais, France): From hyper-extension to tectonic inversion. Tectonophysics, doi:10.1016/j.tecto.2020.228451.

Laborde, A., Barrier, L., Simoes, M., Li, H., Coudroy, T., Van der Woerd, J., Tapponnier, P., 2019. Cenozoic deformation of the Tarim Basin and surrounding ranges (Xinjiang, China): A regional overview. Earth-Science Reviews, 197, 102891, doi.org/10.1016/j.earscirev.2019.102891.

Lacombe, O., 2012. Do fault slip data inversions actually yield "paleostresses" that can be compared with contemporary stresses? A critical discussion. C. R. Geoscience, 344, 159‑173, doi:10.1016/j.crte.2012.01.006.

Lacombe, O., Angelier, J., Laurent, P., 1992. Determining paleostress orientations from faults and calcite twins: a case study near the Sainte-Victoire Range (southern France). Tectonophysics, 201, 141-156.

Lacombe, O., Mouthereau, F., 2002. Basement-involved shortening and deep detachment tectonics in forelands of orogens: Insights from recent collision belts (Taiwan, Western Alps, Pyrenees), Tectonics, 21(4), 1030, doi:10.1029/2001TC901018.

Lacombe, O., Jolivet, L., 2005. Structural and kinematic relationships between Corsica and the Pyrenees-Provence domain at the time of the Pyrenean orogeny. Tectonics, vol. 24, TC1003, doi:10.1029/2004TC001673.

Lacombe, O., Bellahsen, N., 2016. Thick-skinned tectonics and basement-involved fold–thrust belts: insights from selected Cenozoic orogens. Geol. Mag. 153 (5/6), 763–810, doi:10.1017/S0016756816000078.

Lapparent, A.F. de, 1935. Le bassin tertiaire d'Eoulx, près Castellane (Haute-Provence). C. R. Acad. Sci. Paris, 200, 334-336.

Lapparent, A.F. de, 1938. Etudes géologiques dans les régions provençales et alpines entre le Var et la Durance. Bull. Serv. Carte géol. Fr., 40, No. 198, 302 p.

Larroque, C., Baize, S., Albaric, J., Jomard, H., Trévisan, J., Godano, M., Cushing, M., Deschamps, A., Sue, C., Delouis, B., Potin, B., Courboulex, F., Régnier, M., Rivet, D., 2021. Seismotectonics of southeast France: from the Jura mountains to Corsica. Comptes Rendus. Géoscience, 1-47, doi:10.5802/crgeos.69.

Laurent, O., Stephan, J.-F., Popoff, M., 2000. Modalités de la structuration miocène de la branche sud de l'arc de Castellane (chaînes subalpines méridionales). Géologie de la France, 3, 33-65.

Laville, P., 1981. La formation bauxitique provençale (France). Séquence des faciès chimiques et paléomorphologie crétacée, Chron. Rech. Min., 461, 51-68.

Laville, P., Monteau, R., Villeneuve, M., et al., 2018. Carte géologique Aubagne-Marseille à 1/50.000 (1044), 3e éd. BRGM, Orléans. Notice explicative par Villeneuve, M., Floquet, M., Philip, J. et al. (2019).

Leleu, S., Ghienne, J.-F., Manatschal, G., 2009. Alluvial fan development and morpho-tectonic evolution in response to contractional fault reactivation (Late Cretaceous-Palaeocene), Provence, France. Basin Research, 21, 157–187.

Lemoine, M., 1972. Rythme et modalités des plissements superposés dans les chaînes subalpines méridionales des Alpes occidentales françaises. Geologische Rundschau, 61(3), 975–1010.

Lemoine, M., de Graciansky, P.-C., 1988. Histoire d'une marge continentale passive: les Alpes occidentales au Mésozoïque. Introduction. Bull. Soc. géol. Fr., 8, 597–600.

Lemoine, M., Graciansky, P.-C. de, Tricart, P., 2000. De l'océan à la chaîne de montagnes : tectonique des plaques dans les Alpes. Editions scientifiques GB, Paris.

Léonide, P., Floquet, M., Villier, L., 2007. Interaction of tectonics, eustasy, climate and carbonate production on the sedimentary evolution of an early/middle Jurassic extensional basin (Southern Provence Sub-basin,SE France). Basin Research, 19, 125–152, doi:10.1111/j.1365-2117.2007.00316.x.

Le Pichon, X., Rangin, C., Hamon, Y., Loget, N., Lin, J.Y., Andreani, L., Flotte, N., 2010. Geodynamics of the France Southeast Basin. Bull. Soc. géol. Fr., 181, 6, 477-501.

Li, S., Kusky, T.M., Zhao, G., Liu, X., Zhang, G., Kopp, H., Wang, L., 2010. Two-stage Triassic exhumation of HP–UHP terranes in the western Dabie orogen of China: Constraints from structural geology. Tectonophysics, 490, 267-293, doi:10.1016/j.tecto.2010.05.010.

Lickorish, W.H., Ford, M., 1998. Sequential restoration of the external Alpine Digne thrust system, SE France, constrained by kinematic data and synorogenic sediments. *In:* Mascle, A., Puigdefabregas, C., Luterbacher, H.P., Fernandez, M. (Eds), Cenozoic Foreland Basins of Western Europe. Geological Society Special Publications, 134, 189-211.

Lucazeau, F., Mailhe, D., 1986. Heat flow, heat production and fission track data frome the Hercynian basement around the Provençal basin (western Mediterranean). Tectonophysics, 128, 335-356.

Lutaud, L., 1924. Étude tectonique et morphologique de la Provence cristalline. Université de Paris, France, PhD thesis.

Lutaud, L., 1957. La tectogenèse et l'évolution structurale de la Provence. Revue de Géographie physique et de Géologie dynamique, (2), I, (2), 103-112.

Macedo, J., Marshak, S., 1999. Controls on the geometry of fold-thrust belt salient. GSA Bulletin, 111, 1808-1822.

Machhour, L., Philip, J., Oudin, J.-L., 1994. Formation of laminite deposits in anaerobic-dysaerobic marine environments. Marine Geology, 117, 287-302.

Maillart, J., Beaudoin, B., Cojan, I., Joseph, P., Pinoteau, B., 1987. Rôle de la compaction dans la déformation synsédimentaire : exemples dans le Sud-Est de la France. Ier Congr. Français de Sédimentologie, A.S.F., Paris, Livre des Résumés, p. 253-254.

Malavieille, J., Ritz, J.F., 1989. Mylonitic deformation of evaporites in decollements: examples from the southern Alps, France. Journal of Structural Geology, 11, 583-590, doi.org/10.1016/0191-8141(89)90089-8.

Malavieille, J., Konstantinovskaya, E., 2010. Impact of surface processes on the growth of orogenic wedges: Insights from analog models and case studies. Geotectonics, 44, 6, 541-558.

Martín-González, F., Fernández-Lozano, J., De Vicente, G., Crespo-Martín, C., Heredia, N., 2021. Role of multiple inherited basement structures on orogen geometry and evolution: Insights from analogue modelling. Journal of Structural Geology, 144, doi.org/10.1016/j.jsg.2020.104267.

Mascle, G., Arnaud, H., Dardeau, G., Debelmas, J., Delpech, P.-Y., Dubois, P., Gidon, M., Graciansky, P.-C. de, Kerckhove, C., Lemoine, M., 1988,). Salt tectonics, Tethyan rifting and Alpine folding in the French Alps. Bull. Soc. géol. Fr., 5, 747-758.

Masse, J.-P., Philip, J., 1976. Paléogéographie et tectonique du Crétacé moyen en Provence : révision du concept d'isthme Durancien. Revue de géographie physique et de géologie dynamique, XVIII, 1, 49-66.

Masse, J.-P., Villeneuve, M., Leonforte, E., Nizou, J., 2009. Block tilting of the North Provence early Cretaceous carbonate margin: stratigraphic, sedimentologic and tectonic data. Bull. Soc. géol. Fr., 180, No. 2, 105-115, doi:10.2113/gssgfbull.180.2.105.

Matte, P., 2001. The Variscan collage and orogeny (480 ± 290 Ma) and the tectonic definition of the Armorica microplate: A review. Terra Nova, 13, 122–128.

Mazzotti, S., Jomard, H., Masson, F., 2020. Processes and deformation rates generating seismicity in metropolitan France and conterminous Western Europe, BSGF - Earth Sciences Bulletin 2020, 191, 19.

McMechan, M.E., 1985. Low-taper triangle zone geometry: An interpretation for the Rocky Mountains foothills, Pine Pass–Peace River, British Columbia. Bulletin of Canadian Petroleum Geology, 33, 3-38.

Meigs, A.J., Burbank, D.W., 1997. Growth of the South Pyrenean orogenic wedge. Tectonics, 16, No. 2, 239-258.

Ménard, G., 1979. Relations entre structures profondes et structures superficielles dans le sud-est de la France. Essai d'utilisation de donnés géophysiques. Université de Grenoble, France, PhD thesis.

Mennessier, G., 1959. Etude tectonique des confins alpino-provençaux entre le Verdon et l'Argens. Mêm. Soc. géol. Fr., t. XXXVIII, n° 87.

Mennessier, G., 1963. Carte géol. France (1/50000), feuille SALERNES (997). Orléans: Bureau de recherches géologiques et minières.

Mennessier, G., Modret, D., 1966. Carte géol. France (1/50000), feuille TAVERNES (996). Orléans: Bureau de recherches géologiques et minières.

Mennessier, G., Bordet, P., 1969. Carte éeol. France (1/50000), feuille COLLOBRIERES (1046). Orléans: Bureau de recherches géologiques et minières.

Mennessier, G., 1970. Étude tectonique des chaînons situés au Sud-Est du confluent du Verdon et de la Durance (Basse-Provence orientale) Bulletin du BRGM, 1970, I, n°1, 35-72.

Mennessier, G., Modret, D., Aussedat, J.-L., Thiers, R., Caron, J.-P., Durand, J.-P., Ferrandini, J., Guieu, G., Rousset, C., 1979. Carte géol. France (1/50000), feuille BRIGNOLES (1022). Orléans: Bureau de recherches géologiques et minières.

Mercier, H., 1978. Le Néogène et le Pléistocène inférieur duranciens. Université de Grenoble, France, PhD thesis.

Mercier, H., 1979. Le Néogène et le Pléistocène inférieur duranciens. Géologie Alpine, t. 55, 111-132.

Mitra, S., Namson, J., 1989. Equal area balancing. American Journal of Science, 289, 563-599.

Mitra, M., 2002. Fold-accommodation faults. Am. Assoc. Pet. Geol. Bull., 86, 671–693.

Montenat, C., Barrier, P., Hibsch, C., 2005. Enregistrement des événements pyrénéo-provençaux dans les chaînes subalpines méridionales (Baronnies, France). Géologie de la France, 23-73.

Mora, A., Parra, M., Strecker, M.R., Kammer, A., Dimaté, C., Rodriguez, F., 2006. Cenozoic contractional reactivation of Mesozoic extensional structures in the Eastern Cordillera of Colombia. Tectonics, v. 25, TC2010, doi:10.1029/2005TC001854.

Morabito, J., 1967. Evolution tectonique des régions du Bas-Verdon. Bull. Soc. géol. Fr. IX, 4, 585–592.

Morillon, A.-C., 1997. Etude thermo-chronométrique appliquée aux exhumations et contexte orogénique: le Massif des Maures (France) et Les Cordillères Bétiques (Espagne). Université de Nice, France, PhD thesis.

Mouthereau, F., Angrand, P., Jourdon, A., Ternois, S., Fillon, C., Calassou, S., Chevrot, S., Ford, M., Jolivet, L., Manatschal, G., Masini, E., Thinon, I., Vidal, O., Baudin, T., 2021. Cenozoic mountain building and topographic evolution in Western Europe: impact of billions of years of lithosphere evolution and plate kinematics. Bull. Soc. géol. Fr - Earth Sci Bulletin 192, 56. https://doi.org/10.1051/bsgf/2021040.

Mouthereau, F., Filleaudeau, P.-Y., Vacherat, A., Pik, R., Lacombe, O., Fellin, M.G., Castelltort, S., Christophoul, F., and Masini, E., 2014. Placing limits to shortening evolution in the Pyrenees: Role of margin architecture and implications for the Iberia/Europe convergence. Tectonics, 33, 2283–2314, doi:10.1002/2014TC003663.

Mouthereau, F., Watts, A.B., Burov, E., 2013. Structure of orogenic belts controlled by lithosphere age. Nature Geoscience 6, 785-789. https://doi.org/10.1038/ngeo1902.

Nicolas, M., Santoire, J.-P., Delpech, P.-Y., 1990. Intraplate seismicity: new seismotectonic data in Western Europe. Tectonophysics, 179, 27-53.

Nury, D. 1988. L'Oligocène de Provence méridionale. Documents du BRGM, 163, 411 p.

Nury, D., Raynaud, S., 1986. Etude tectono-sédimentaire du fossé oligocène de Marseille, Bouches-du-Rhône. Evolution postérieure. Géologie de la France, 4, 377-397.

Nury, D., Rousset, C., 1985. Extension des dépôts oligocènes de la région de Toulon (Var, Sud-Est France). Cadre structural et implications paléogéographiques. Géologie méditerranéenne, XII-XIII, 3-4, 175-184.

Nury, D., Villeneuve, M., Arlhac, P., Gärtner, A., Linnemann, U., Châteauneuf, J.-J., Riveline, J., Hippolyte, J.-C., 2016. New insights on the Marseille-Aubagne Oligocene basins (France). Boletín Geológico y Minero, 127 (2/3), 483-498.

Onézime, J., Faure, M., Crévola, G., 1999. Etude pétro-struccturale du complexe granitique Rouet – Plan-de-la-Tour (massifs des Maures et du Tanneron occidental, Var). C. R. Acad. Sci. Paris, 328, 773-779.

Oudet, J., Münch, P., Borgomano, J., Quillevere, F., Melinte-Dobrinescu, M.-C., Demory, F., Viseur, S., Cornée, J.-J., 2010. Land and Sea study of the Northeastern Golfe du Lion rifted margin: the Oligocene-Miocene of southern Provence (Nerthe area, SE France). Bull. Soc. géol. Fr., 181, 591-607.

Pairis, J.L., Gidon, M., 1987. Le détritisme néogène et ses relations avec la tectonique, à l'extrémité NE du bassin de Valensole (Alpes externes méridionales). Géologie alpine, Mém. H.S. no. 13, 417-426.

Parra, M., Mora, A., Lopez, C., Rojas, L.E., Horton, B.K., 2012. Detecting earliest shortening and deformation advance in thrust belt hinterlands: Example from the Colombian Andes. Geology, 40, no. 2, pp. 175-178, doi:10.1130/G32519.1.

Philip, J., 1967. Modalités et importance de la transgression du Sénonien inférieur dans la région de Saint-Cyr-sur-Mer (Var). C. R. Acad. Sci. Paris, D, 265, 1883-1886.

Philip**,** J., 1970. Les formations calcaires à rudistes du Crétacé supérieur provençal et rhodanien. Université d'Aix-Marseille, Marseille, France, PhD thesis, 438 p.

Philip, J., 2012. L'exploration géologique de la Provence: deux siècles et demi de débats et de controverses, Paris: Presses des Mines, Collection Histoire Sciences et sociétés. 366 p.

Philip, J., 2018. La bande triasique de l'Huveaune, in Villeneuve, M., et al., Mémoire explicatif, Carte géol. France (1/50.000), feuille Aubagne Marseille, 3ème édition (1044), p. 148-156.

Philip, J. 2019. La bande triasique de l'Huveaune, in Villeneuve, M., Floquet, M., Philip, J.et al., Notice explicative de la carte géologique Aubagne-Marseille à 1/50.000 (1044), 3e éd. BRGM, Orléans, 72-76.

Philip, J., Allemann, J., 1982. Comparaison entre les plates-formes du Crétacé supérieur de Provence et de Sardaigne. Cretaceous Research, 3, 35-45.

Philip, J., Bercovici, C., Machhour, L., Masse, P.J.L. 1985. La tectonique crétacée de la région toulonnaise. Réunion Extraordinaire de la Société Géologique de France du 2 au 7 septembre à Marseille. Première journée. Documents du BRGM, 94, 1-22.

Philip, J., Masse, P.J.-L., Machhour, L., 1987. L'évolution paléogéographique et structurale du front de chevauchement nord-toulonnais (Basse-Provence occidentale, France). Bull. Soc. géol. Fr., 8, III, No. 3, 541-550.

Philip, J., Vianey-Liaud, M., Martin-Closas, C., Tabuce, R., Léonide, P., Margerel, J.-P., Noël, J., 2017. Stratigraphy of the Haut Var Paleogene continental series (Northeastern Provence, France): New insight on the age of the 'Sables bleutés du Haut Var' Formation. Geobios, 50, 319–339, doi:10.1016/j.geobios.2017.06.002.

Philip, J., Argyriadis, I., Bestani, L., 2018. Le massif de la Sainte-Baume, in Villeneuve et al., Mémoire explicatif, Carte géol. France (1/50.000), feuille Aubagne-Marseille, 3e édition (1044), 133-148.

Popoff, M., 1973. La bande triasique de Barjols (Var) : la bordure sud-occidentale. Université Paris VI, Paris, France, PhD thesis, 160 p.

Price, R.A., 1986. The southeastern Canadian Cordillera: thrust faulting, tectonic wedging, and delamination of the lithosphere. J. Struct. Geol., 8, 3/4, 239-254, doi:10.1016/0191-8141(86)90046-5.

Rat, J., Mouthereau, F., Brichau, S., Crémades, A., Balvay, M., Ganne, J., Lahfid, A., Gautheron, C., 2019. Tectonothermal Evolution of the Cameros Basin: Implications for Tectonics of North Iberia. Tectonics, 38, doi:10.1029/2018TC005294.

Répelin, J. (1922). Monographie géologique du massif de la Sainte-Baume.Annales de la Faculté des Sciences de Marseille, XXV (I), 85 p.

Ritz, J.-F., 1992. Recent tectonics and seismotectonics in the southern Alps: stress analysis, Quaternaire, 3, 111–124, doi:10.3406/quate.1992.1980.

Rolland, Y., Corsini, M., Demoux, A., 2009. Metamorphic and structural evolution of the Maures-Tanneron massif (SE Variscan chain): evidence of doming along a transpressional margin. Bull. Soc. géol. Fr., 180, 217-230.

Romagny, A., Jolivet, L., Menant, A., Bessière, E., Maillard, A., Canva, A., Gorini, C., Augier, R., 2020. Detailed tectonic reconstructions of the Western Mediterranean region for the last 35 Ma, insights on driving mechanisms. BSGF-Earth Sciences Bulletin, 191, 37, doi.org/10.1051/bsgf/2020040.

Roure, F., Brun, J.P., Colletta, B., Van Den Driessche, J., 1992. Geometry and kinematics of extensional structures in the Alpine foreland of southeastern France. J. Struct. Geol., 14, 503-519.

Roure, F., Colletta, B., 1996. Cenozoic inversion structures in the foreland of the Pyrenees and Alps, in: Ziegler, P. A., Horvath, F. (Eds), Peri-Tethys Memoir 2: Structure and Prospects of Alpine Basins and Forelands. Mém. Mus. natn. Hist. nat., 170, 173-209.

Rousset, C., Kerckhove, C., Bambier, A., 1983. Notice explicative, Carte géol. Fr. (1/50,000), feuille SEYNE (894). Orléans : Bureau de recherches géologiques et minières.

Roux, M., 1968. Étude géologique du massif des Cadières de Brandis à l'ouest de Castellane. Géologie Alpine, t. 44, 339-352.

Roux, M., 1970. Le synclinal de Taulanne (Basses-Alpes) et les conséquences du chevauchement de Castellane sur sa bordure nord-est. Géologie Alpine, t. 46, 177-188.

Roveri, M., Flecker, R., Krijgsman, W., Lofi, J., Lugli, S., Manzi, V., Sierro, F.J., Bertini, A., Camerlenghi, A., De Lange, G., Govers, R., 2014. The Messinian salinity crisis: past and future of a great challenge for marine sciences. Marine Geology, 352, 25-58, doi:10.1016/j.margeo.2014.02.002.

Rowan, M.G., Urai, J.L., Fiduk, J.C., Kukla, P.A., 2019. Deformation of intrasalt competent layers in different modes of salt tectonics. Solid Earth, 10, 987-1013, doi.org/10.5194/se-10-987-2019.

Saura, E., Ardèvol i Oró, L., Teixell, A., Vergés, J., 2016. Rising and falling diapirs, shifting depocenters, and flap overturning in the Cretaceous Sopeira Brine migration, rifting and thrusting in the Pyrenees and Sant Gervàs subbasins (Ribagorça Basin, southern Pyrenees). Tectonics, 35, 638-662, doi:10.1002/2015TC004001.

Schneider, J., Corsini, M., Reverso-Peila, A., Lardeaux, J.-M., 2014. Thermal and mechanical evolution of an orogenic wedge during Variscan collision: an example in the Maures-Tanneron Massif (SE France). *In*: Schulmann, K., Martínez Catalán, J.R., Lardeaux, J.-M., Janousek, V., Oggiano, G., (Eds), The Variscan Orogeny: Extent, Timescale and the

Formation of the European Crust. Geological Society, London, Special Publications, 405, doi:10.1144/SP405.4.

Schreiber, D., Giannerini, G., Lardeaux, J.-M., 2011. The Southeast France basin during Late Cretaceous times: The spatiotemporal link between Pyrenean collision and Alpine subduction. Geodinamica Acta, 24/1, 23-27, doi:10.3166/ga.24.23-37.

Schwartz, S., Gautheron, C., Audin, L., Dumont, T., Nomade, J., Barbarand, J., Pinna-Jamme, R., van der Beek, P., 2017a. Foreland exhumation controlled by crustal thickening in the Western Alps. Geology, 45, No. 2, 139-142, doi:10.1130/G38561.1.

Schwartz, S. et al., 2017b. Supplemental material: Foreland exhumation controlled by crustal thickening in the Western Alps. Geological Society of America. Journal contribution. https://doi.org/10.1130/2017035

Séranne, M., Couëffé, R., Husson, E., Baral, C., Villard, J., 2021. The transition from Pyrenean shortening to Gulf of Lion rifting in Languedoc (South France)-A tectonic-sedimentation analysis. BSGF-Earth Sciences Bulletin, 192, 27, doi.org/10.1051/bsgf/2021017.

Siddans, A.W.B., 1979. Arcuate fold and thrust patterns in the Subalpine Chains of Southeast France. Journal of Structural Geology, 1, 2, 117-126.

Simonetti, M., Carosi, R., Montomoli, C., Corsini, M., Petroccia, A., Cottle, J.M., Iaccorino, S., 2020. Timing and kinematics of flow in a transpressive dextral shear zone, Maures Massif (Southern France). Int J Earth Sci (Geol Rundsch), 109, 2261-2285, doi.org/10.1007/s00531-020-01898-6.

Souquet, P., Delvolvé, J.-J., Brusset, S., 2003. Identification of an underfilled foreland basin system in the Upper Devonian of the Central Pyrenees: implications for the Hercynian orogeny. Int. J. Earth Sci., 92, 316-337, doi:10.1007/s00531-003-0334-y.

Spitz, R., Bauville, A., Epard, J.-L., Kaus, B.J.P., Popov, A.A., Schmalholz, S.M., 2020. Control of 3-D tectonic inheritance on fold-and-thrust belts: insights from 3-D numerical models and application to the Helvetic nappe system, Solid Earth, 11, 999–1026, doi.org/10.5194/se-11-999-2020.

Suppe, J., 1983. Geometry and kinematics of fault-bend folding. American Journal of Science, 283, 684–721.

Suppe, J., 1985. Principles of structural geology. Prentice-Hall, Inc., Englewood Cliffs, New Jersey.

Suppe, J., Chou, G.T., Hook, S.C., 1992. Rates of folding and faulting determined from growth strata. In McClay, K.R. (Ed), Thrust tectonics. Springer-Science+Business Media, B.V.

Suppe, J., Medwedeff, D.A., 1990. Geometry and kinematics of fault-propagation folding. Eclogae geol. Helv. 83/3, 409-454.

Tămaș, D.M., Tămaș, A., Barabasch, J., Rowan, M.G., Schleder, Z., Krézsek, C., Urai, J.L., 2021. Low-angle shear within the exposed Mânzălești diapir, Romania: Salt decapitation in the Eastern Carpathians fold-and-thrust belt. Tectonics, 40, e2021TC006850, doi:10.1029/2021TC006850.

Tavani, S., Storti, F., Lacombe, O., Corradetti, A., Muñoz, J.A., Mazzoli, S., 2015. A review of deformation pattern templates in foreland basin systems and fold-and-thrust belts:

Implications for the state of stress in the frontal regions of thrust wedges., Earth-Science Reviews, 141, 82-104, doi.org/10.1016/j.earscirev.2014.11.013.

Tavani, S., Bertok, C., Granado, P., Piana, F., Salas, R., Vigna, B., Muñoz, J.A., 2018. The Iberia-Eurasia plate boundary east of the Pyrenees. Earth-Science Reviews, 187, 314-337, doi:10.1016/j.earscirev.2018.10.008.

Tempier, C., 1963. Étude tectonique du double pli des Pallières à l'Est de Rians (Var). Travaux du Laboratoire de Géologie de la Faculté des Sciences de l'Université d'Aix-Marseille, VII, p. 159-173.

Tempier, C., 1987. Modèle nouveau de mise en place des structures provençales, Bull. Soc. géol. Fr., 8, 533-540.

Thomas, W.A., Bayona, G., 2002. Palinspastic restoration of the Anniston transverse zone in the Appalachian thrust belt, Alabama. J. Struct. Geol., 24, 797-826.

Torres Carbonell, P.J., Cao, S.J., Dimieri, L.V., 2017. Spatial and temporal characterization of progressive deformation during orogenic growth: Example from the Fuegian Andes, southern Argentina. J. Struct. Geol., 99, 1-19, doi:10.1016/j.jsg.2017.04.003.

Touraine, F., 1967. Les rapports de l'Oligocène avec les structures N-S du Nord-Varois. Bull. Soc. géol. Fr., 7, IX, 530-536.

Toutin-Morin, N., Bonijoly, D., Brocard, C., Dardeau, G., Dubar, M., 1993. Enregistrement sédimentaire de l'évolution post-hercynienne, en bordure des Maures et du Tanneron, du Carbonifère supérieur à l'Actuel. Géologie de la France, No. 2, 3-22.

Toutin-Morin, N., Bonijoly, D., Brocard, C., Broutin, J., Crévola, G., Dardeau, G., Dubar, M., Féraud, J., Giraud, J.D., Godefroy, P., Laville, P., Meinesz, A., 1994. Carte géologique de la France à 1/50.000. Fréjus- Cannes 2e édition. Notice explicative. vol. 187.

Uba, C.E., Kley, J., Strecker, M.R., and Schmitt, A.K., 2009. Unsteady evolution of the Bolivian Subandean thrust belt: The role of enhanced erosion and clastic wedge progradation: Earth and Planetary Science Letters. 281, 134–146, doi:10.1016/j.epsl.2009.02.010.

Unalan. G., 1970. Etude géologique de la bordure ouest de l'arc de Castellane (Alpes de Haute Provence-Var). Minéralogie. Université de Grenoble, France, PhD thesis.

van Hinsbergen, D.J.J., Vissers, R.L., Spakman, W., 2014. Origin and consequences of western Mediterranean subduction, rollback, and slab segmentation. Tectonics, 33(4), 393-419.

van Hinsbergen, D.J.J. van, Torsvik, T.H., Schmid, S.M., Maţenco, L.C., Maffione, M., Vissers, R.L.M., Gürer, D., Spakman, W., 2020. Orogenic architecture of the Mediterranean region and kinematic reconstruction of its tectonic evolution since the Triassic. Gondwana Res 81, 79-229, https://doi.org/10.1016/j.gr.2019.07.009.

Vann, I.R., Graham, R.H., Hayward, A.B., 1986. The structure of mountain fronts. J. Struct. Geol., 8, 215-227, doi:10.1016/0191-8141(86)90044-1.

Vergés, J., Munoz, J.A., 1990. Thrust sequences in the Southern Central Pyrenees. Bull. Soc. Géol. Fr., 8, VI, No. 2, 265-271, doi:10.2113/gssgfbull.VI.2.265.

Vergés, J., Ramos, V.A., Meigs, A., Cristallini, E., Bettini, F.H., Cortés, J.M.,2007. Crustal wedging triggering recent deformation in the Andean thrust front between 31°S and 33°S: Sierras Pampeanas-Precordillera interaction. J. Geophys. Res., 112, B03S15, doi:10.1029/2006JB004287.

Villeger, M., Andrieux, J., 1987. Phases tectoniques post-éocènes et structuration polyphasée du panneau de couverture nord provençal (Alpes externes méridionales). Bull. Soc. géol. Fr., 8, t. III, no. 1, 147-156.

Villeneuve, M., Nury, D., Arlhac, P., Gärtner, A., Linnemann, U., 2018. Les bassins oligocènes, in Villeneuve et al., Mémoire explicatif, Carte géol. France (1/50.000), feuille Aubagne-Marseille, 3e édition (1044), 179-199.

Walpersdorf, A., Pinget, L., Vernant, P., Sue, C., Deprez, A., the RENAG team, 2018. Does long-term GPS in the Western Alps finally confirm earthquake mechanisms? Tectonics, 37, doi:10.1029/2018TC005054.

Westphal, M., Durand, J.-P., 1990. Magnétostratigraphie des séries continentales fluvio-lacustres du Crétacé supérieur dans le synclinal de l'Arc (région d'Aix-en-Provence, France). Bull. Soc. géol. Fr., 8, VI, No. 4, 609-620.

Weydert, P., Nury, F., 1978. Données nouvelles sur la stratigraphie et la tectonique de la zone méridionale du bassin de Marseille. C. R. Acad. Sci. Paris, 287, 591-594.

Wicker, V., Ford, M., 2021. Assessment of the tectonic role of the Triassic evaporites in 1 the north Toulon fold-thrust belt. BSGF-Earth Sci. Bull., 192, 51.

Wu, Z., Yin, H., Li, C., Yang, X., Wang, L., Wang, F., Dong, S., Jia, D., 2021. Influence of regional erosion and sedimentary loading on fault activities in active fold-thrust belts: Insights from discrete element simulation and the southern and central Longmen Shan fold-thrust belt. Front. Earth Sci. 9:659682, 10.3389/feart.2021.659682.

Zapata, T.R., Allmendinger, R.W., 1996. Growth stratal records of instantaneous and progressive limb rotation in the Precordillera thrust belt and Bernejo basin. Argentina.Tectonics, 15, No. 5, 1065-1083.

Zubieta-Rossetti, D., Huyghe, P., Mascle, G., Mugnier, J.L., Baby, P., 1993. The influence of the pre-Devonian on the front of the Andean Belt, central Bolivia. C.R.Acad.Sc.Paris, Série II, 316, 951-957.

Zürcher, P., 1891. Les zones de plissements de Salernes et d'Aups. Bull. Soc. géol. Fr., 3, XIX, 1178-1201.

Zürcher, P., 1893. Note sur les phénomènes de recouvrement des environs de Toulon. Bull. Soc. géol. Fr., 3, XXI, 65-77.

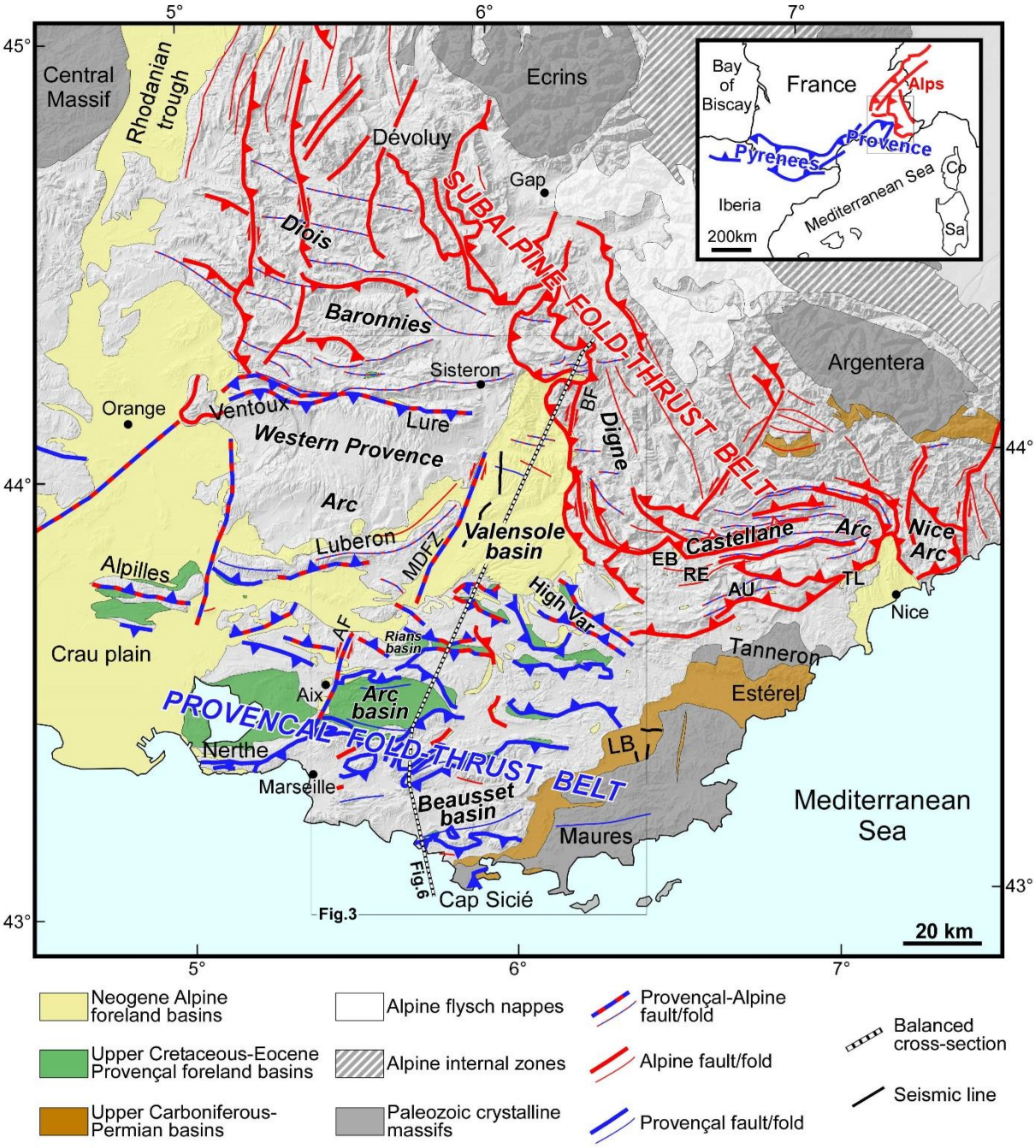

Fig. 1. Synthetic structural map of the junction of the Provençal and Subalpine fold-thrust belts in southeastern France. The map shows the traces of the main structures and main polyphase structures compiled from Guieu (1968), Gidon et al. (1970), Lemoine (1972), Gidon and Pairis (1976), Angelier and Aubouin (1976), Dubois and Curneille (1978), Dupire (1985), Haccard et al. (1989a), Hippolyte et al. (1993), Lemoine et al. (2000), Champion et al. (2000), Montenat et al. (2005), Chardon et al. (2005), Cushing et al. (2008), Espurt et al.

(2012), Bestani et al. (2016), Villeneuve et al. (2018) and Espurt et al. (2019b), and from this study. Thin black square indicates location of the geological map of Fig. 3. Dashed thick black and white line shows the trace of the balanced and restored cross-section of Fig. 6 across the upper Cretaceous Beausset and upper Cretaceous-Eocene Arc and Rians foreland basins and Neogene Valensole foreland basin. MDFZ: Middle Durance fault zone. AF: Aix fault. BF: Bès fault. LB: Luc basin. Locations of Miocene-Pliocene syn-orogenic basins of Eoulx-Brenon (EB), Roque-Esclapon (RE), Aubarède (AU) and Tourette-sur-Loup (TL) in the Castellane Arc are also shown.

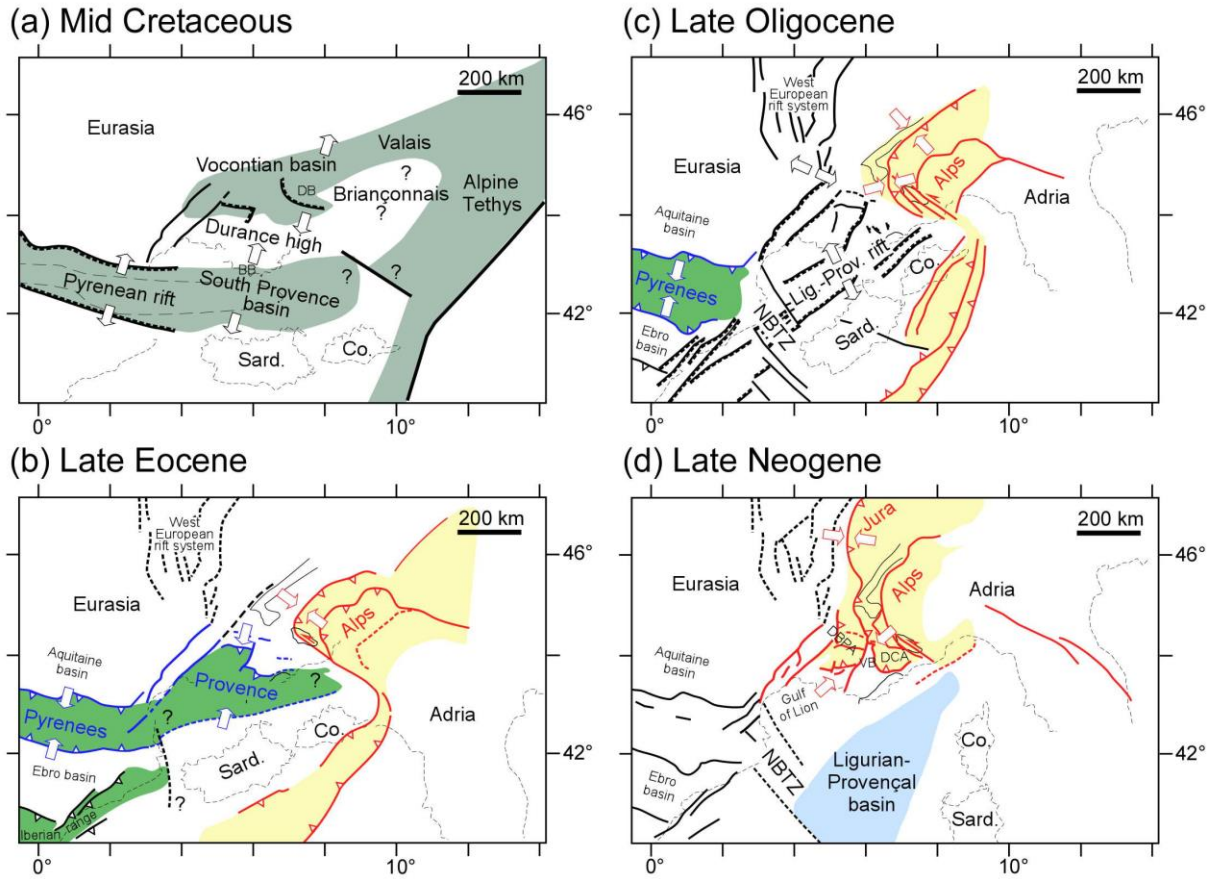

Fig. 2. Geological map of the central Provençal and southwestern Subalpine zones. This is a compilation of existing geological maps of BRGM (1/50000) of Mennessier (1963), Goguel (1964), Flandrin et al. (1964), Dorkel et al. (1966), Mennessier and Modret (1966), Catzigras et al. (1969), Mennessier and Bordet (1969), Gouvernet et al. (1969), Arlhac et al. (1970),

Blanc et al. (1973), Blanc et al. (1974), Bordet et al. (1976), Blanc et al. (1977), Mennessier et al. (1979), Gigot et al. (1981b), Rousset et al. (1983), Haccard et al. (1989a), Gigot et al. (2013) and Laville et al. (2018), our field observations and subsurface data. Thick dashed black and white line shows the trace of the balanced and restored cross-section of Fig. 6.

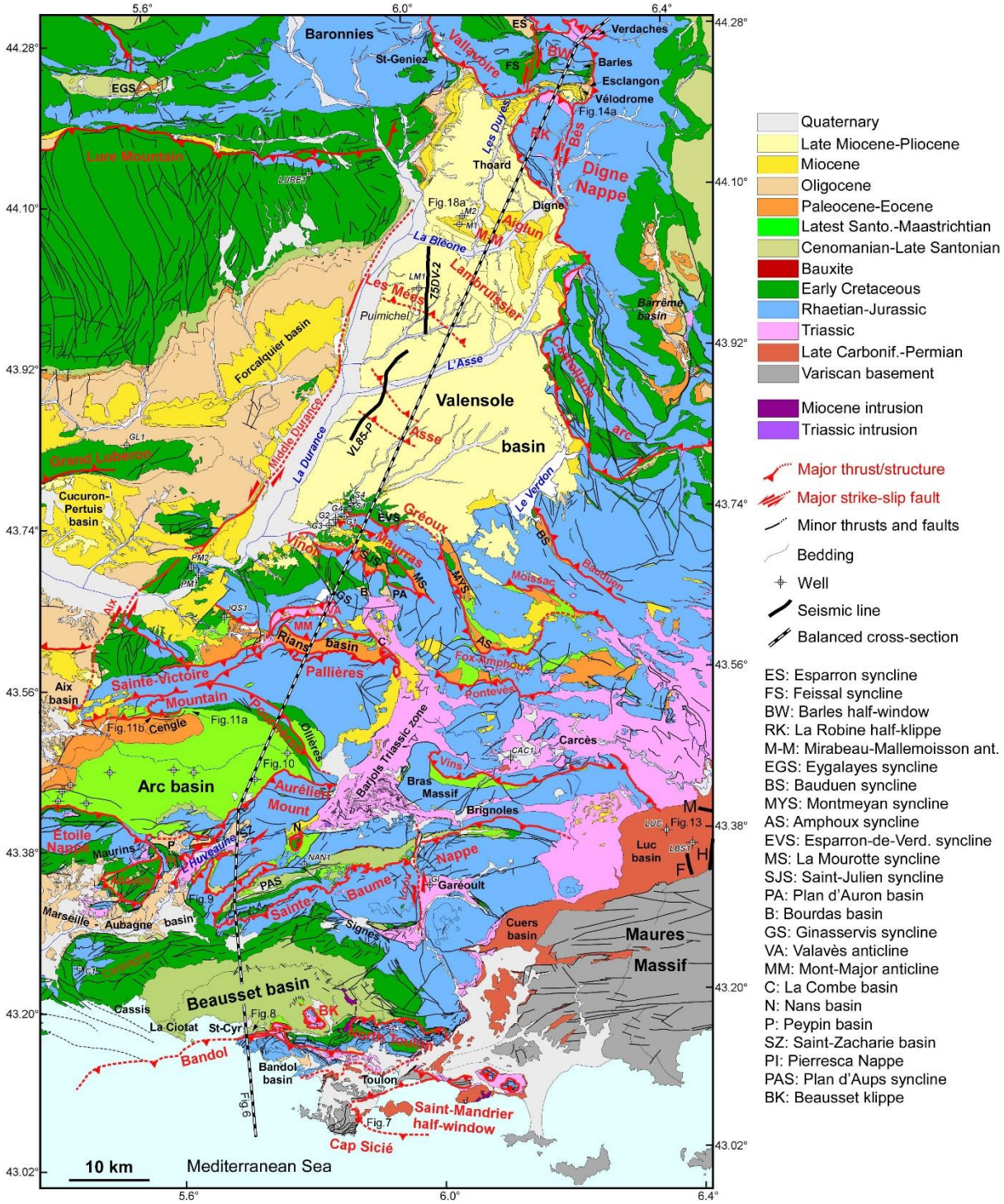

Fig. 3. Geological map of the central Provençal and Subalpine zones. This is a compilation of existing geological maps of BRGM (1:50,000) of Goguel (1966), Rouire et al. (1969a,b), Rouire et al. (1970), Rouire et al. (1974), Rouire et al. (1977), Rouire et al. (1979), Rouire et al. (1981), De Graciansky et al. (1981), Gigot et al. (1981b), Haccard et al. (1989a), Rousset et al. (1983), Gigot et al. (2013) and Laville et al. (2018), our field observations and subsurface data. Thick dashed black and white line shows the trace of the balanced and restored cross-section of Fig. 6.

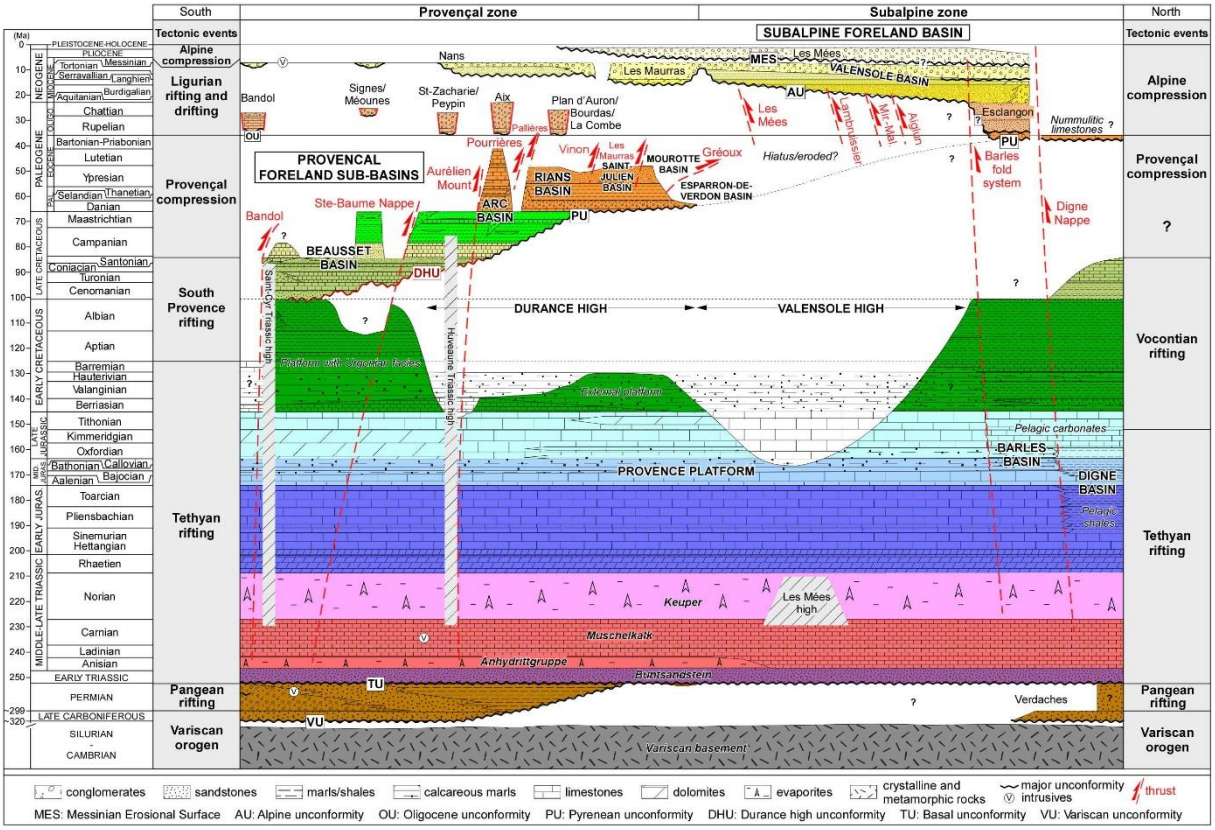

Fig. 4. Synthetic stratigraphic chart along the studied cross-section across the Provençal zone and southwestern Subalpine zone. Locations of the Oligocene-Miocene Bandol, Signes/Méounes, Saint-Zacharie/Peypin, Nans, Aix, Plan d'Auron/Bourdas/La Combe basins are shown in Fig. 3. See details in text for references.

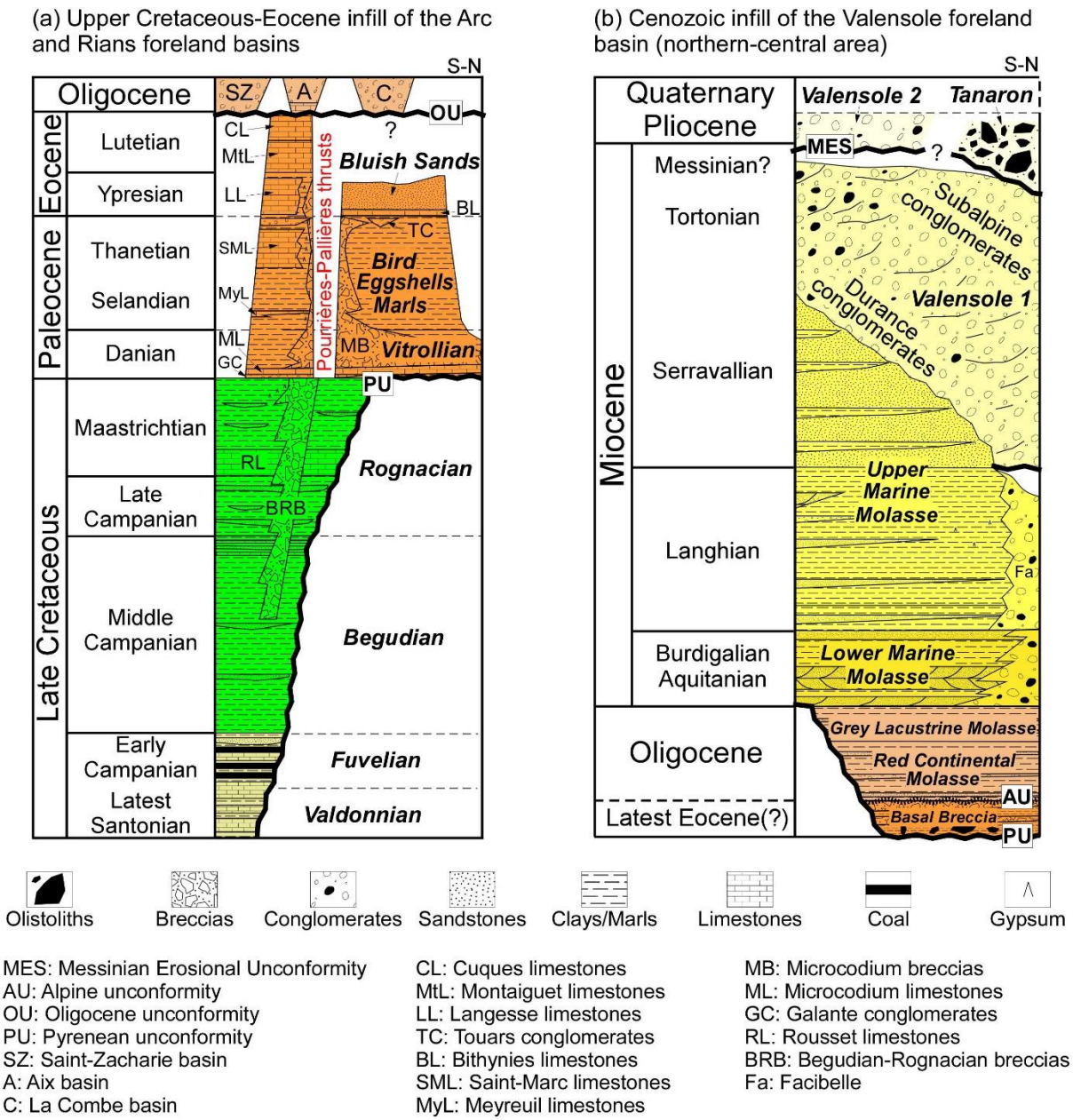

Fig. 5. Details of the syn-orogenic sedimentary successions of the (a) upper Cretaceous-Eocene infill of the Arc and Rians foreland basins and (b) Cenozoic infill of the Valensole foreland basin. Locations of the Oligocene Saint-Zacharie, Aix and La Combe basins are shown in Fig. 3. See details in text for references.

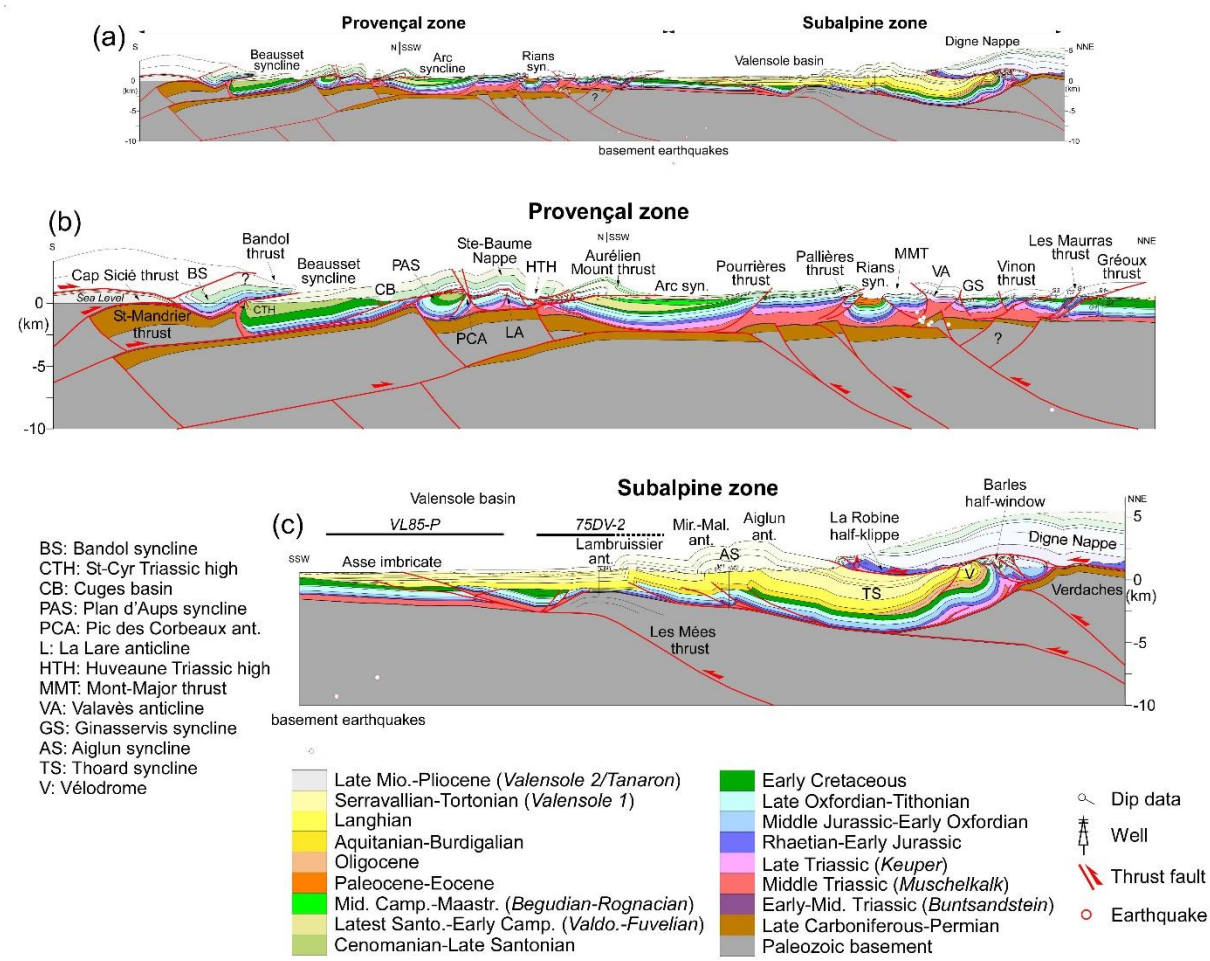

Fig. 6. (a) Cross-sectional geometry of the Provençal and southwestern Subalpine foreland thrust wedges. Details of the (b) Provençal zone and (c) Subalpine zone. For location of section trace, see Fig. 3. Location of seismic profiles VL85-P and 75DV-2 (Fig. 19) are shown. Note that transparency has been applied to the eroded structures.

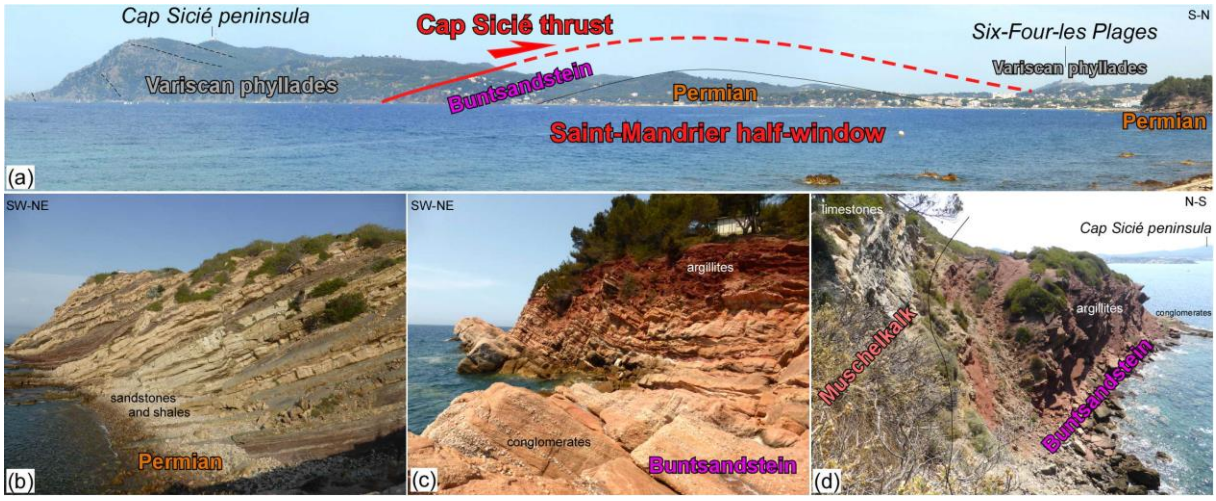

Fig. 7. (a) Panoramic view of the Saint-Mandrier half-window and folded N-verging Cap Sicié basement thrust (view looking westward; 43.070431°, 5.907101°). For location, see also Fig. 3. (b) Permian strata in the southern limb of the Saint-Mandrier anticline (43.067175°, 5.913673°). (c) North-dipping lower-middle Triassic (Buntsandstein) conglomerates and sandstones at the front of the Cap Sicié thrust (43.112546°, 5.792338°). (d) Stratigraphic contact between lower-middle Triassic sandstones (Buntsandstein) and middle Triassic carbonates (Muschelkalk) at the northern front of the Cap Sicié thrust (43.113050°, 5.791026°).

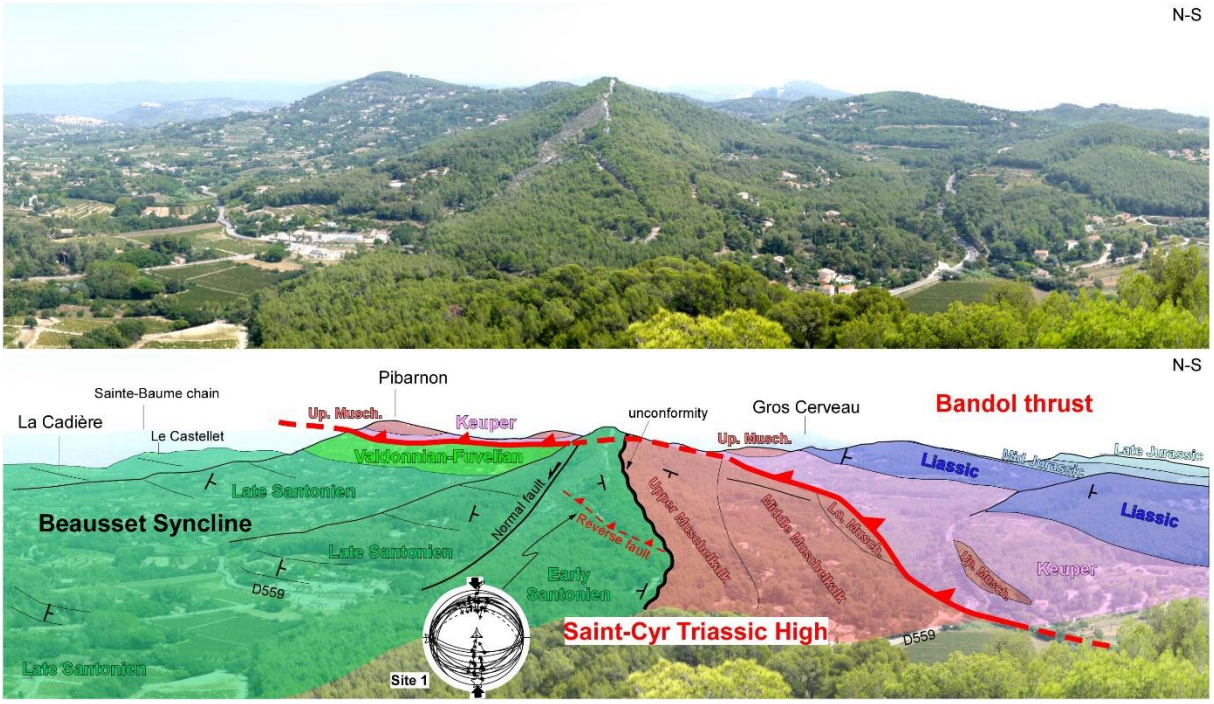

Fig. 8. Panoramic view of the Bandol thrust and southern limb of the Beausset syncline (modified from Philip et al., 1985 and Espurt et al., 2019b) (view looking eastward; 43.165794°, 5.709031°). For location, see also Fig. 3. The N-verging Bandol thrust is detached above upper Triassic evaporites (Keuper) embedding upper Muschelkalk carbonate slices (e.g., Pibarnon) and overthrusts Valdonnian-Fuvelian facies strata of the Beausset syncline. In the southern limb of the Beausset syncline, the Saint-Cyr Triassic high is formed by middle Triassic (Muschelkalk) limestones, cargneules and volcano-detritic basaltic facies.

The upper Muschelkalk fossiliferous limestones are unconformably overlain by lower Santonian conglomerates and rudist bearing limestones. Striated faults measured in N-dipping lower Santonian limestones are consistent with a N-trending compression. Fault data and bedding (dashed line) have been projected in an equal area stereogram, lower hemisphere.

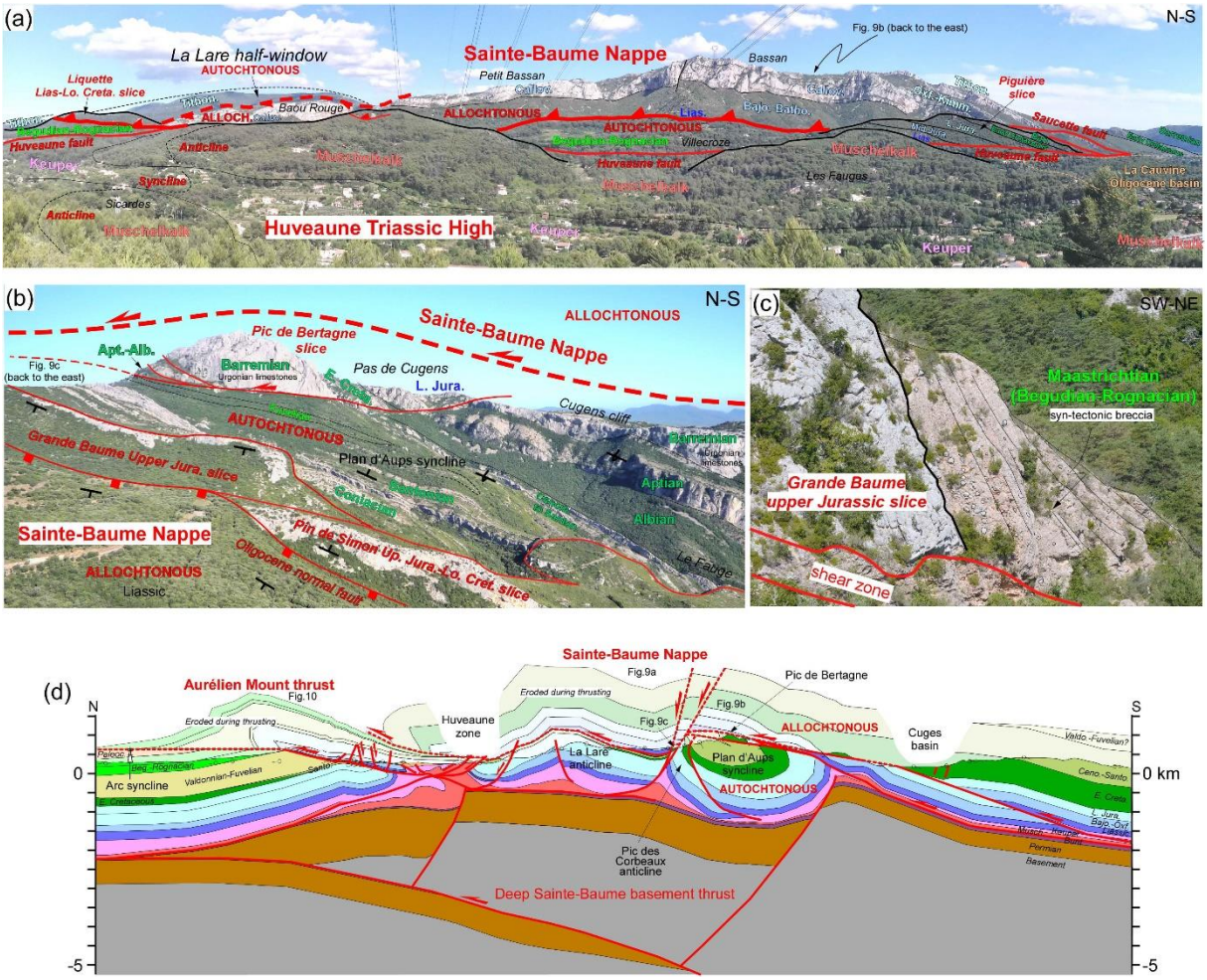

Fig. 9. (a) Panoramic view looking eastward of the Sainte-Baume Nappe and its analogous units formed by the Piguière and Liquette slices (view looking eastward; 43.352896°, 5.615643°). For location, see also Fig. 3. The nappe overthrusts northward Begudian-Rognacian facies strata of the Villecroze zone tectonically separated from the Huveaune Triassic anticlinorium high by the Huveaune fault. Oligocene conglomeratic strata of the La Cauvine basin unconformably rest on the Triassic of the Huveaune high. Under the Sainte-Baume Nappe, the La Lare half-window corresponds to a large autochtonous anticline armed

of upper Jurassic and Cretaceous limestones. Geological data and structural features are from Aubagne-Marseille 1:50,000 geological map, 3rd edition, 2018. (b) Panoramic view of the southern Plan d'Aups half-window (view looking eastward; 43.312377°, 5.660989°). The tight Plan d'Aups syncline located under the Pic de Bertagne slice and the Sainte-Baume Nappe is cored by Fuvelian facies strata. The northern flank of the Plan d'Aups syncline is truncated by the Grande Baume and Pin de Simon slices. Northward, an Oligocene normal fault separates the collapsed Sainte-Baume Nappe from these slices. (c) Syn-tectonic breccias (Begudian-Rognacian facies) embedding the Grande Baume upper Jurassic unit at the Source de Cros (NW Plan d'Aups; view looking westward; 43.317931°, 5.689054°). The syn-tectonic breccias occur on the northern flank of the Pic des Corbeaux anticline (location on Fig. 9d). Photograph from Jean-Claude Tempier. (d) Zoom of the structural cross-section for more clarity of the Sainte-Baume Nappe and Aurélien Mount thrust.

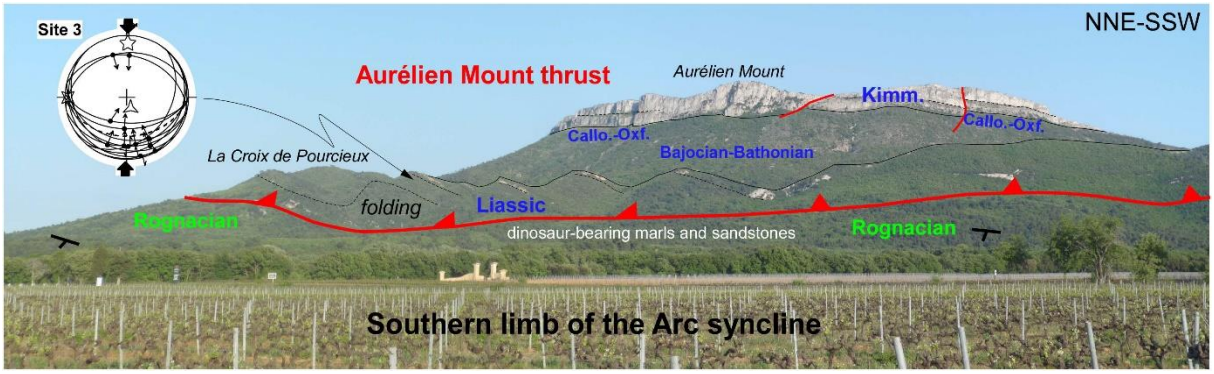

Fig. 10. Panoramic view of the Aurélien Mount thrust overthrusting Rognacian facies strata of the southern limb of Arc syncline (view looking eastward; 43.479551°, 5.73129°). For location, see also Fig. 3. Striated faults measured in lower Jurassic strata are consistent with a ~N-trending compression. Fault data and bedding (dashed line) have been projected in an equal area stereogram, lower hemisphere. Geological data and structural features are from Aix-en-Provence and Brignoles 1:50,000 geological maps.

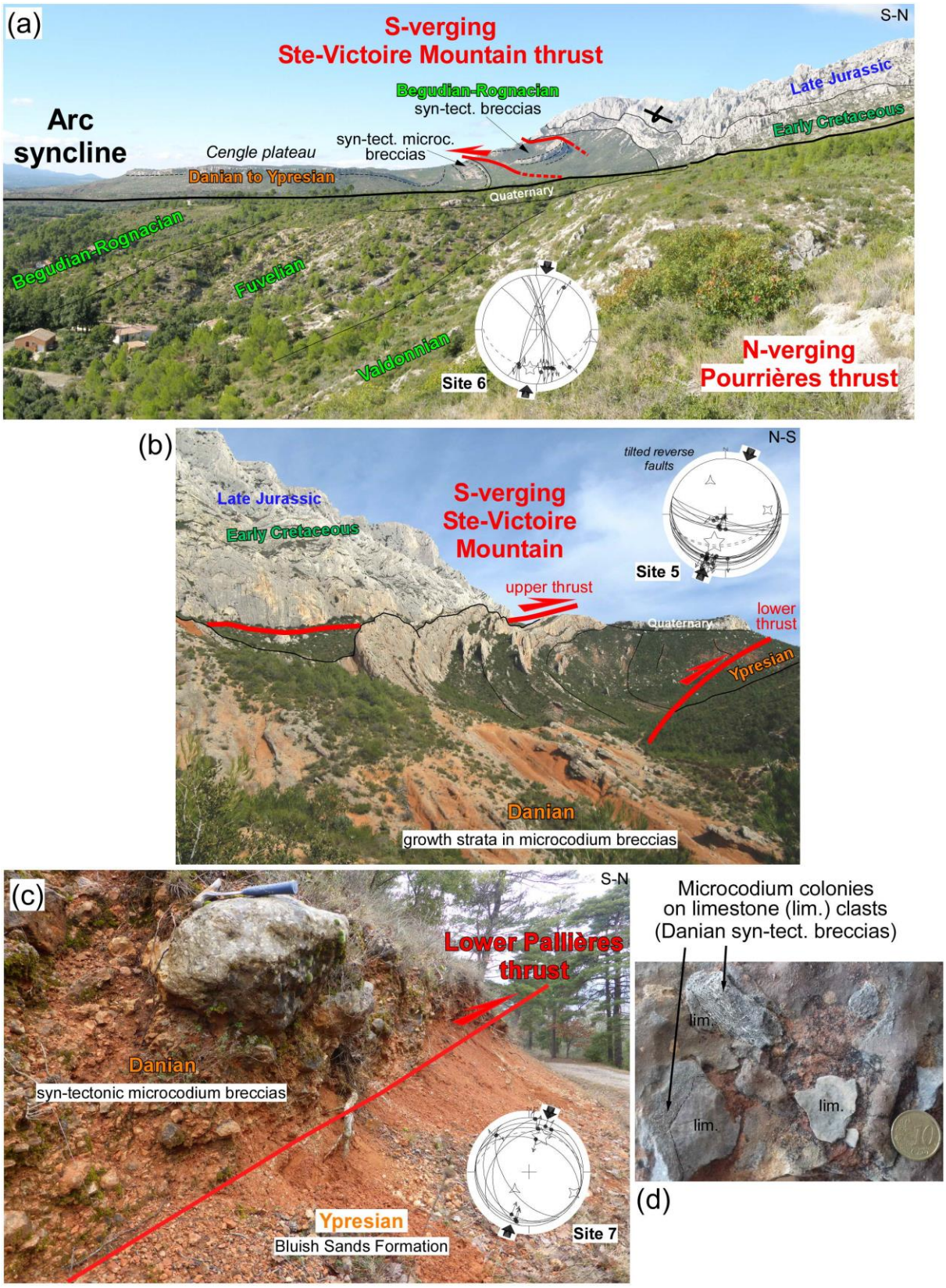

Fig. 11. (a) Panoramic view of the northern edge of the Arc syncline (view looking westward; 43.529058°, 5.676583°). For location, see also Fig. 3. Westward, the syncline is thrusted by

the S-verging Sainte-Victoire Mountain thrust system, including Begudian-Rognacian and Danian microcodium syn-tectonic breccias. Eastward, the upper Cretaceous foreland rocks of the Arc syncline pinch-out on lower Cretaceous limestones. The syncline is transported northward onto the Pourrières thrust. (b) Panoramic view of the S-verging Sainte-Victoire Mountain thrust system with growth strata in Danian microcodium breccias (modified from Espurt et al. (2012); view looking eastward; 43.524806°, 5.569858°). For location, see also Fig. 3. (c) Danian microcodium breccias on the Pallières unit thrusting Ypresian Bluish Sands Formation (43.590979°, 5.837873°). (d) Details of the microcodium breccias including Mesozoic limestone clasts corroded by microcodium. Striated faults measured in Valdonnian limestones and Danian microcodium breccias are consistent with a NNE-trending compression. Fault data and bedding (dashed line) have been projected in an equal area stereogram, lower hemisphere.

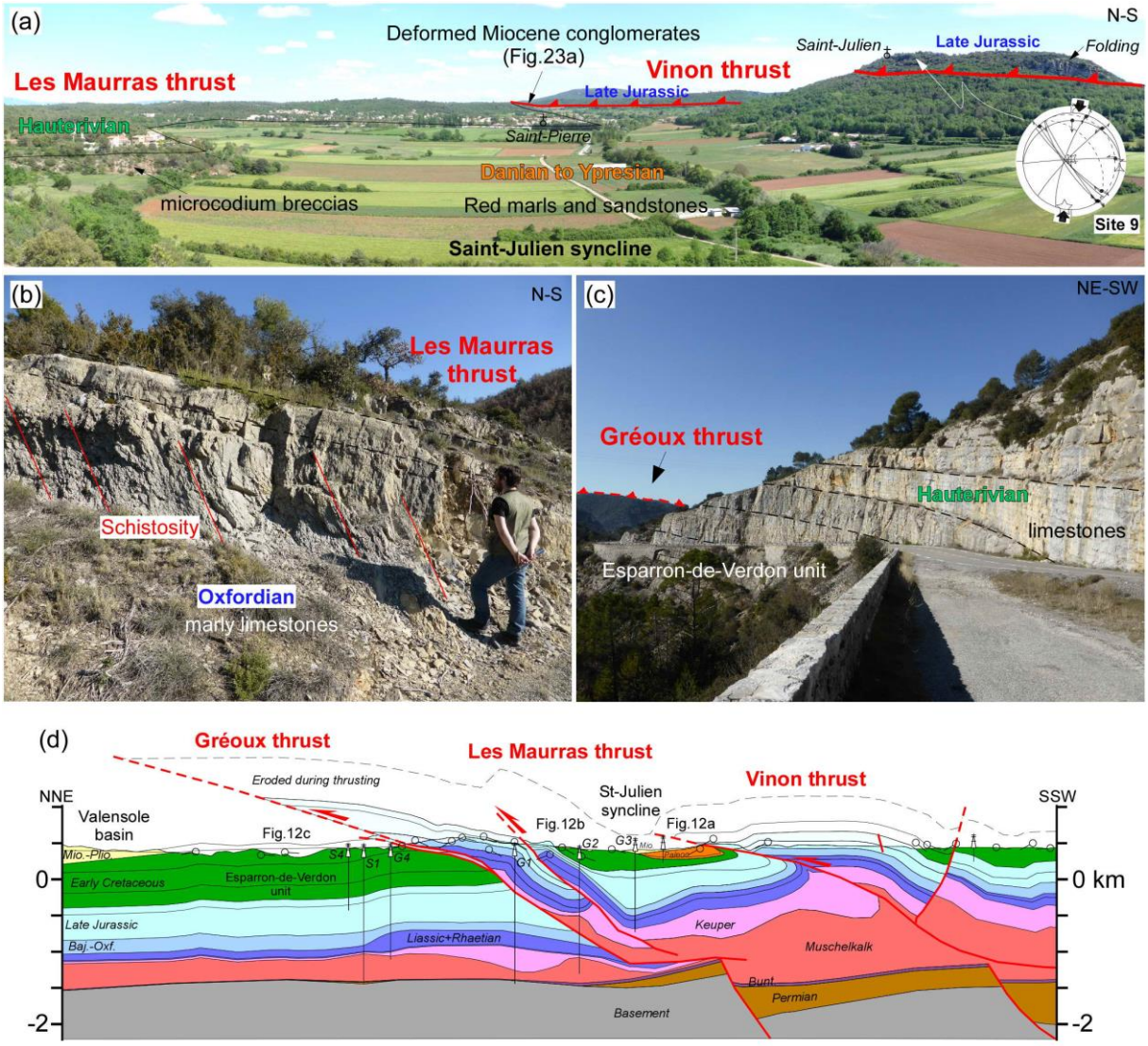

Fig. 12. Field observations along the Vinon, Les Maurras and Gréoux thrusts. (a) Panoramic view of the Vinon thrust overlying Paleocene strata in the Saint-Julien syncline (view looking eastward; 43.702067°, 5.899911°). For location of the Saint-Julien syncline, see also Fig. 3. The activity of this thrust was recorded at least by Danian microcodium breccias outcropping in the norther limb of the Saint-Julien syncline. Striated faults measured in upper Jurassic limestones of the Vinon thrust are consistent with a NNE-trending compression. Fault data and bedding (dashed line) have been projected in an equal area stereogram, lower hemisphere. Eastward, the Vinon thrust is covered by Miocene conglomerates with sheared and striated pebbles (see Fig. 23a). Geological data and structural features are from Tavernes 1.50 000

geological map. (b) Sheared middle Jurassic marly limestones in the hanging wall of the Les Maurras thrust (43.737375°, 5.874535°). (c) N-dipping Hauterivian limestones in the footwall of the Gréoux thrust (43.764164°, 5.928908°). (d) Zoom of the structural cross-section for more clarity of the Vinon, Les Maurras and Gréoux thrusts.

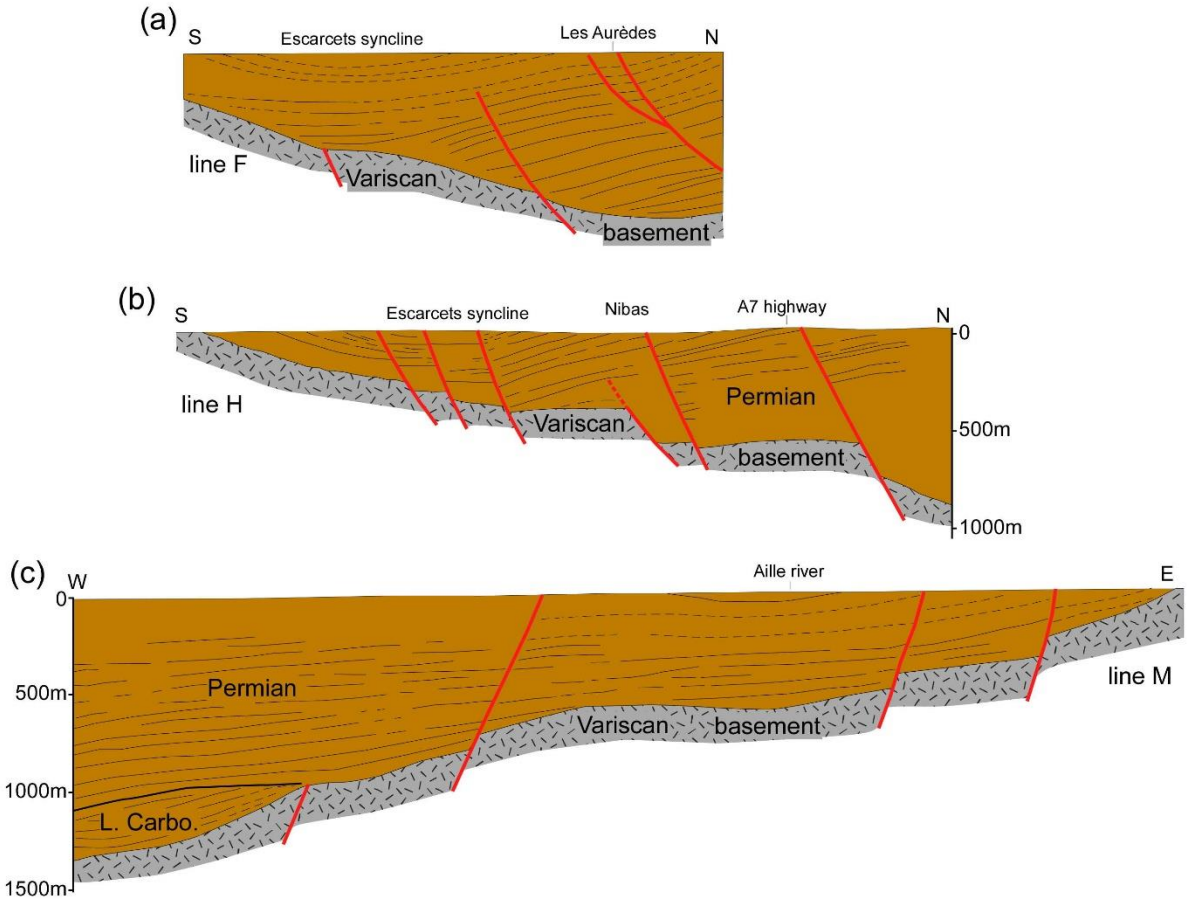

Fig. 13. Interpreted cross-sections documenting the structure of the Permian extensional basin of Luc along the seismic lines F (a), H (b) and M (c). Modified from Baudemont (1985). For locations, see Fig. 3.

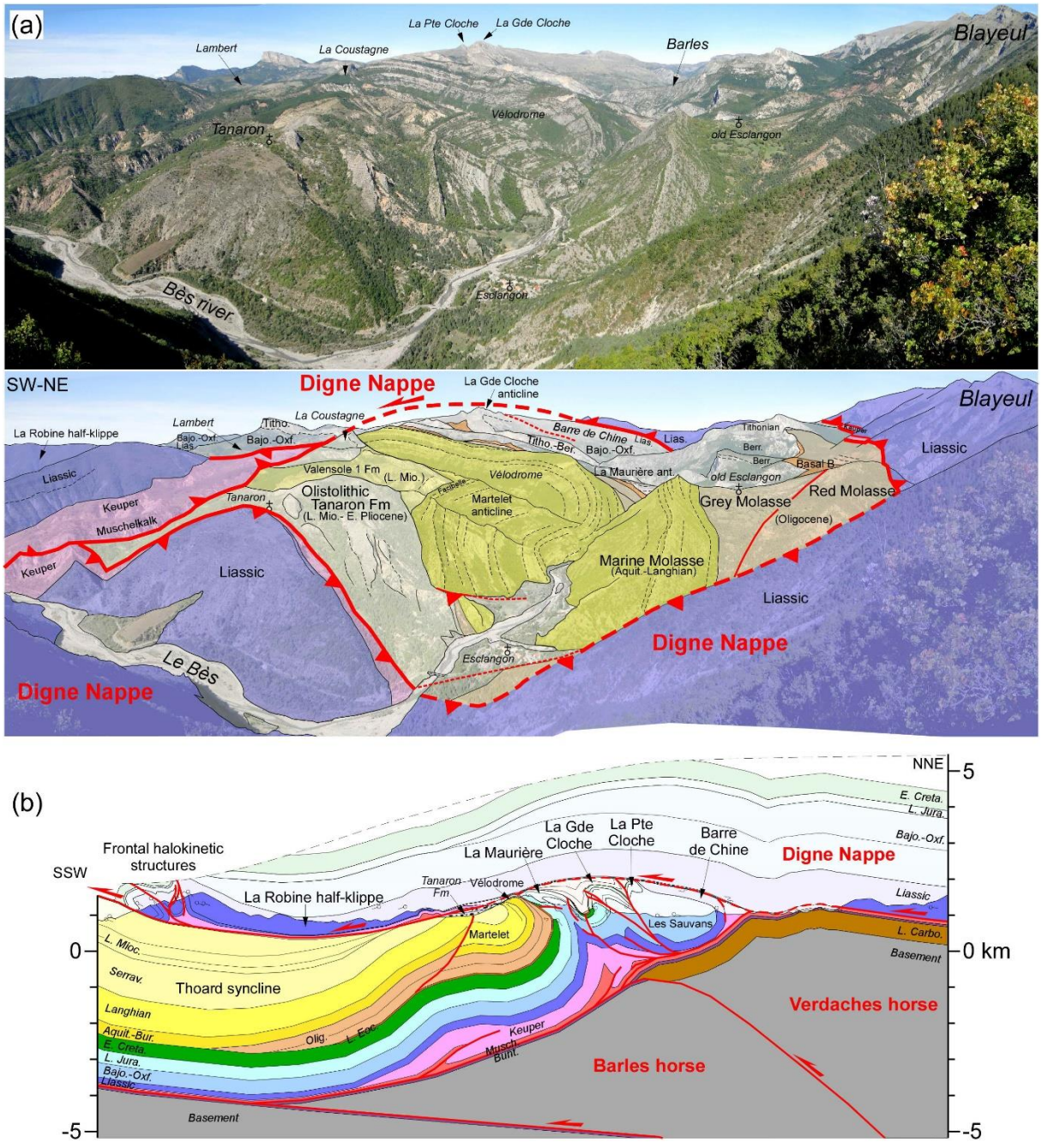

Fig. 14. Structures of Barles half-window and Digne Nappe. (a) Panoramic view of the Barles half-window and folded Digne Nappe from l'Escuichière (view looking NW-ward; 44.190201°, 6.288481°). For location, see also Fig. 3. The cross-section trace is in the second plan of this panoramic view. Along the Bès valley, the Digne Nappe overthrusts SW-ward the Barles fold system (La Maurière, La Grande Cloche, La Petite Cloche and Barre de Chine flap) and the Vélodrome structure and Martelet anticline, corresponding to the northern limb

of the Thoard syncline. The Miocene strata of the Vélodrome structure (Marine Molasse and conglomerates of the Valensole 1 Formation) show sedimentary wedging. These strata are unconformably covered by the upper Miocene-lower Pliocene olistolithic Tanaron Formation, a chaotic melange of large middle Jurassic olistoliths with evaporites (Lambert locality), upper Jurassic-Berriasian limestone (e.g., La Coustagne) and Eocene-Miocene olistoliths included in red marls, sandstones and conglomerates beds. Geological data and structural features are from La Javie 1:50,000 geological map. (b) Zoom of the structural cross-section for more clarity of the more clarity of the Barles half-window and Digne Nappe.

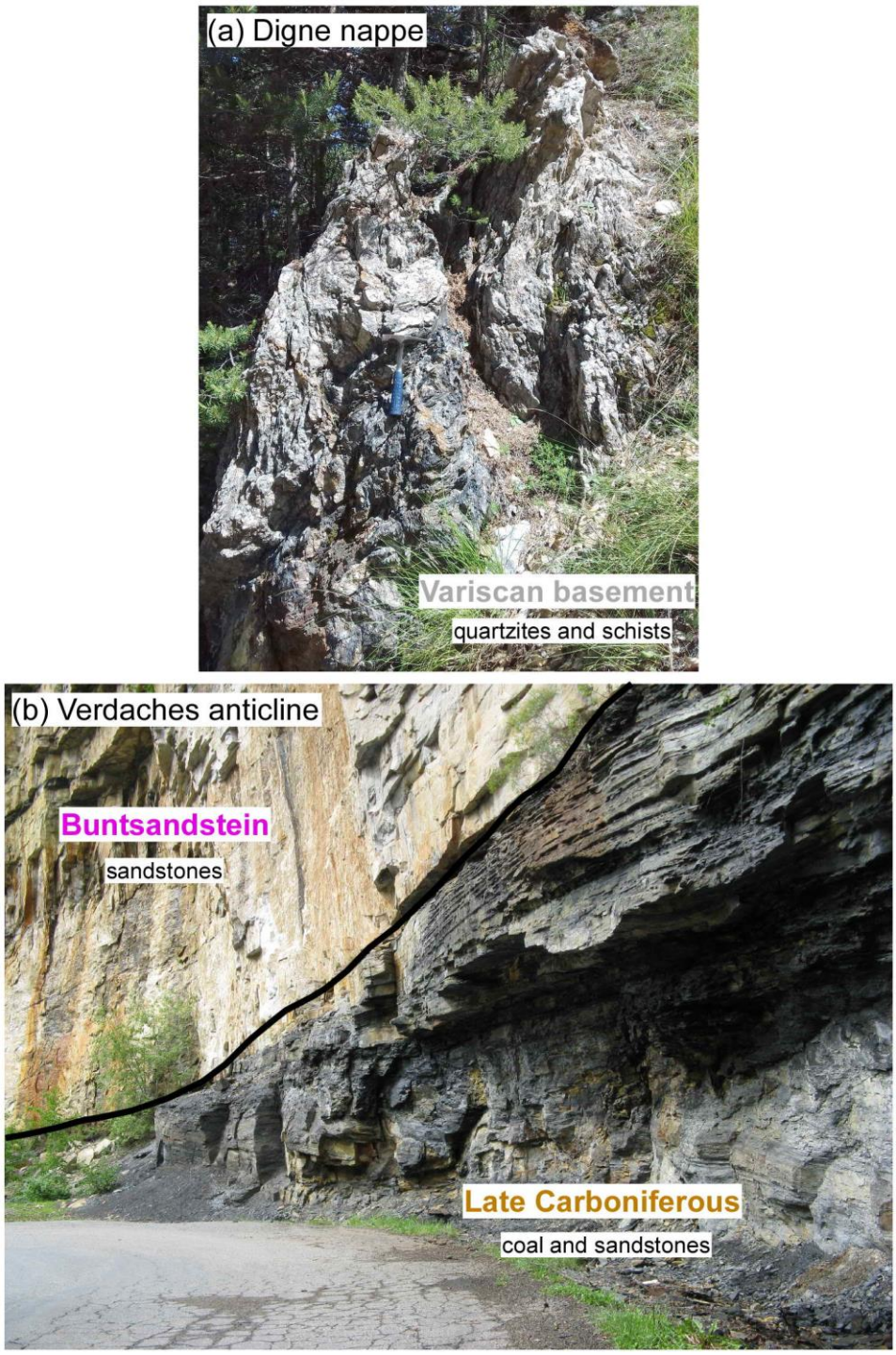

Fig. 15. (a) Tectonic slice of Variscan basement at the base of the Digne Nappe (Guiomar, 1990) (44.263578°, 6.293548°). (b) Upper Carboniferous coal and sandstones unconformably covered by lower Triassic sandstones in the Verdaches basement anticline (44.273110°, 6.299909°).

Fig. 16. Outcrops of upper Eocene-lower Oligocene Basal Breccia Formation in the erosional Barles half-window. (a) Hauterivian strata unconformably covered by the Basal Breccia Formation on the southern limb of the La Grande Cloche anticline (44.228736°, 6.287899°). (b) Fan-shaped geometry in the Basal Breccia Formation in the northern limb of the Feissal syncline (44.246639°, 6.201392°). Striated faults are consistent with a syn-sedimentary NNE-trending compression. Fault data and bedding (dashed line) have been projected in an equal area stereogram, lower hemisphere. (c) Details of the breccias including Mesozoic limestone clasts (Le Pas de Terre Rouge, southern lim of the La Grande Cloche anticline; 44.232062°, 6.229132°).

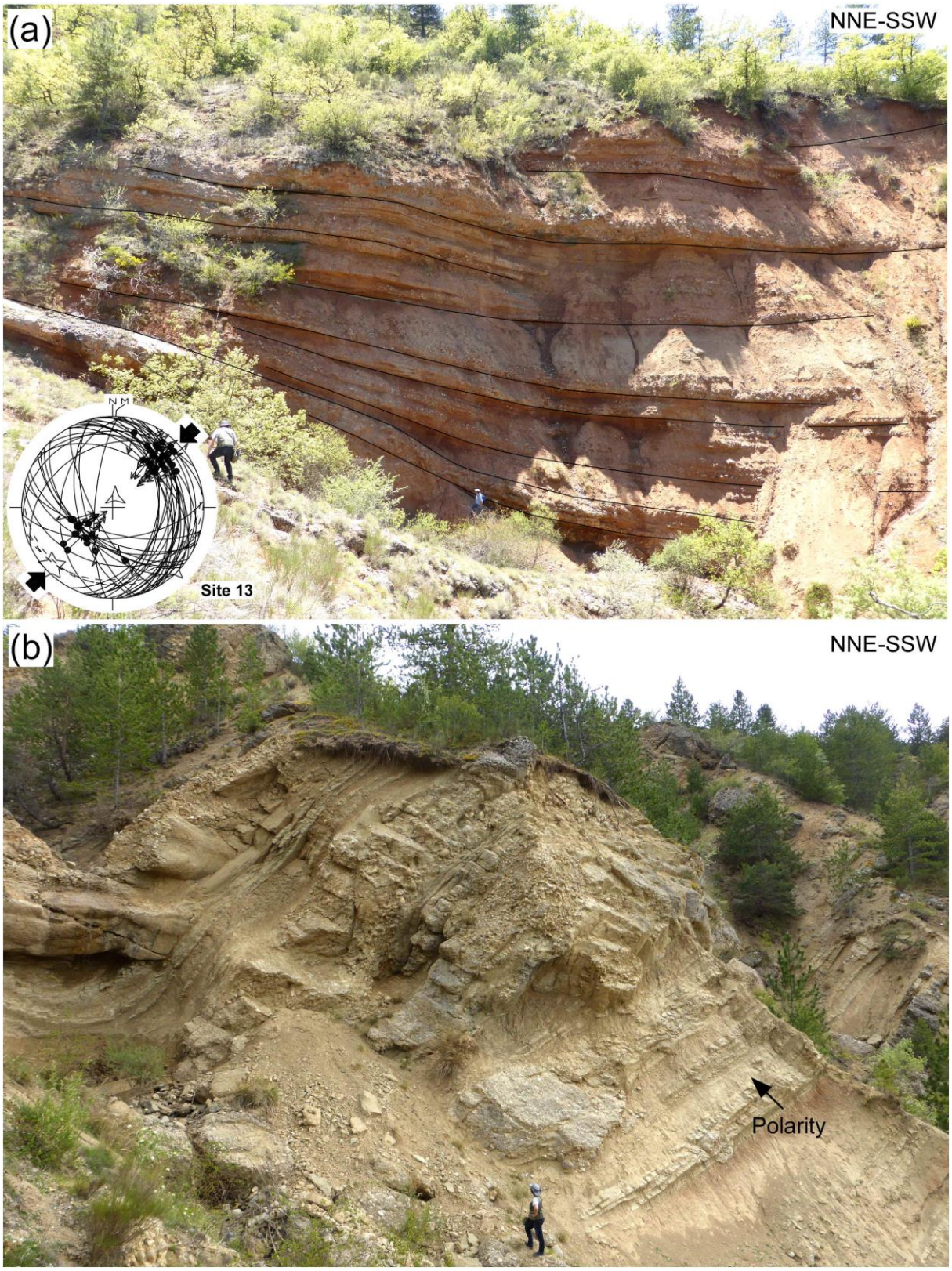

Fig. 17. Upper Miocene (Serravallian-Tortonian) Subalpine conglomerate accumulations in the Thoard unit along the Duyes valley west of the La Robine half-klippe (Fig. 3). (a) Growth strata near Thoard town (44.164978°, 6.151822°). Striated faults in these Subalpine

conglomerates are consistent with a NE-trending Alpine compression. The conjugated and tilted reverse faults of the stereogram confirm the tectonic origin of the sedimentary fan. Fault data and bedding (dashed line) have been projected in an equal area stereogram, lower hemisphere. (b) Base of the syn-tectonic Subalpine conglomerates in the Bramefan-Mauduech ravine, high Duyes valley (44.181431°, 6.174494°).

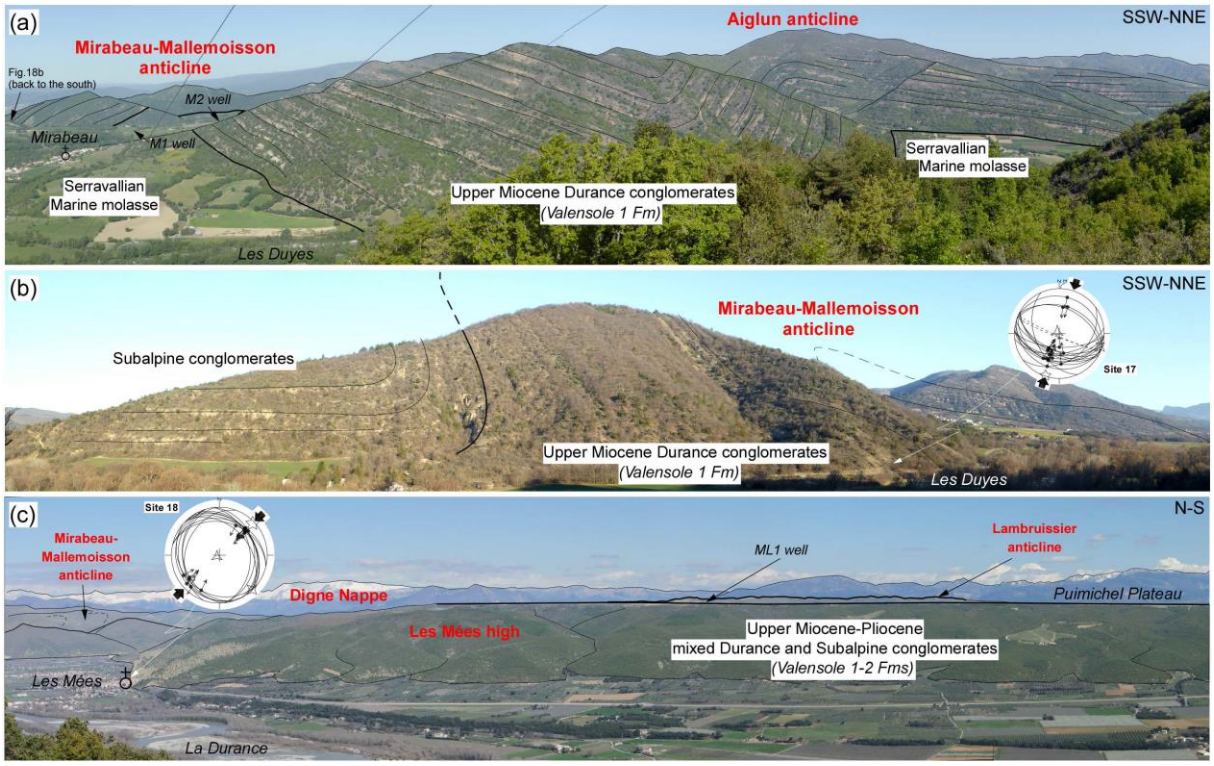

Fig. 18. (a-b) Panoramic views of the Aiglun and Mirabeau-Mallemoisson fault-propagation folds armed by upper Miocene conglomerates (Valensole 1 Formation) along the Duyes valley (views looking westward; 44.066856°, 6.121088°; 44.039937°, 6.103457°). For location, see also Fig. 3. (c) Panoramic view of the southern Valensole foreland basin (view looking NE-ward; 43.994556°, 5.906601°). Here, the basin is filled by upper Miocene-Pliocene conglomerates (Valensole 1-2 Formations), topped by slightly S-dipping surface of the Puimichel plateau. Northward, the sedimentary pile is deformed by the Lambruissier and Mirabeau-Mallemoisson anticlines. Striated faults measured in conglomerate beds of the southern limb of the Mirabeau-Mallemoisson anticline and close to the Les Mées town are

consistent with a NE-trending compression. Fault data and bedding (dashed line) have been projected in an equal area stereogram, lower hemisphere.

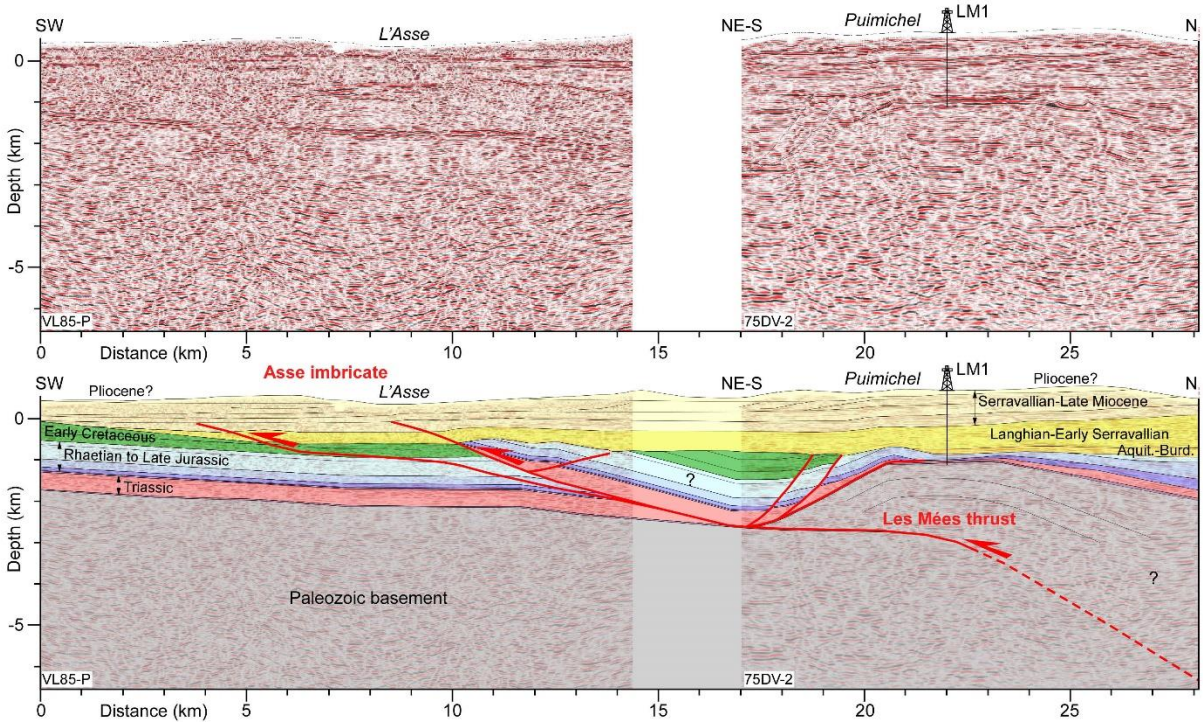

Fig. 19. Structural interpretation of southern and central part of the Valensole foreland basin using reprocessed seismic profiles VL85-P and 75DV-2 calibrated using the Les Mées-1 well. For locations, see Fig. 3. The interpretation of the seismic profiles shows Provençal compressional structures (Les Mées basement thrust and upper Asse thrusts) eroded and sealed by Miocene strata. These thrusts have been slightly reactivation by the Alpine compression.

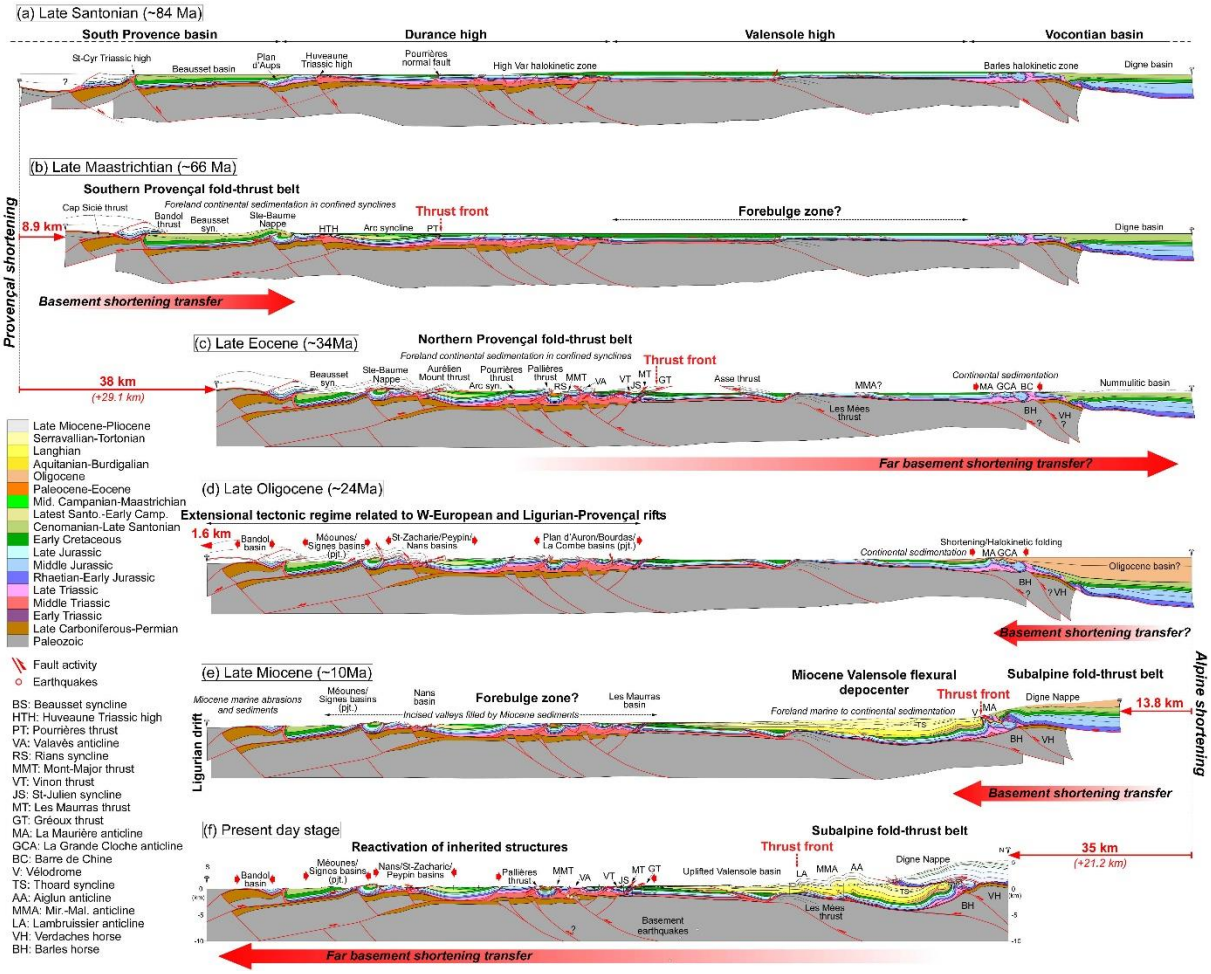

Fig. 20. Tectonic evolution of the superimposed Provençal and southwestern Subalpine thrust wedges. (a) Late Santonian restoration showing the structural architecture of the South Provence basin (Beausset basin) and Vocontian basin (Digne basin) separated by the Durance-Valensole high system. (b) Restoration of Provençal belt in Late Maastrichtian with activation of the Bandol thrust and Sainte-Baume Nappe, and sedimentary infill of the Arc depocenter. (c) Restoration of the Provençal belt in Late Eocene with northward transmission of the shortening through the northern part of the Provençal zone, Valensole high, and up to the Barles area. (d) Late Oligocene stage illustrating the deformation of the southern Provençal wedges by extensional faulting and initiation of the Alpine shortening in the Barles area to the north. (e) Growth of the Barles triangle zone during Miocene and concomitant sedimentary infill of the Valensole foreland basin. (f) Late Miocene-Pliocene emplacement of

the Digne Nappe and southward propagation of the Subalpine thrust front into the Valensole foreland basin in cover and up to Mediterranean coast (Bandol basin) through the basement.

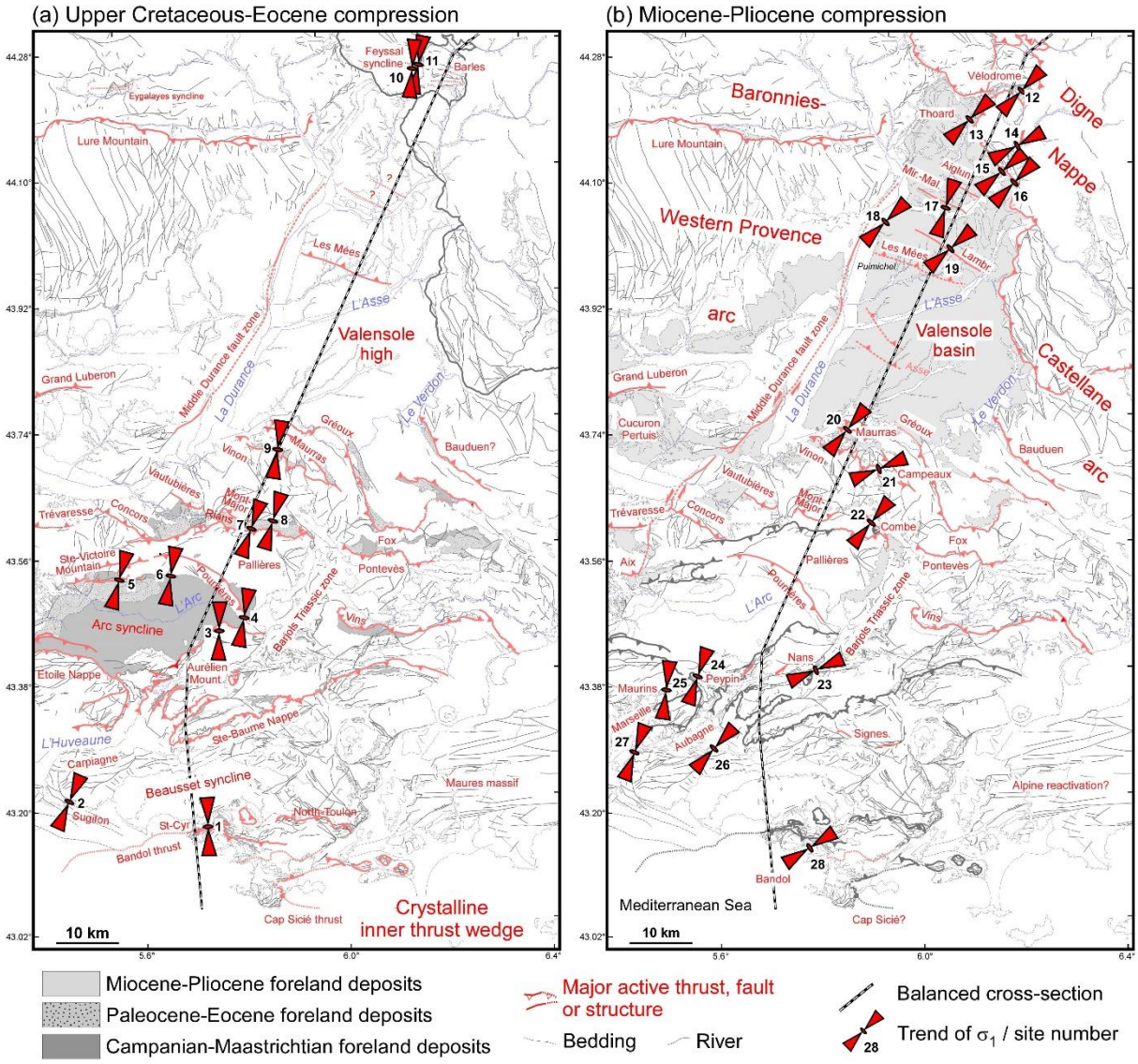

Fig. 21. Reconstruction of compression directions (trend of σ_1 is shown by red double arrow). (a) Provençal compressional stress field. (b) Alpine compressional stress field. Site numbers, fault slip data and computed principal stress axes are shown in Fig. 22 and Table 1. The names of the major active structures are indicated in red. Thick dashed black and white line shows the trace of the balanced and restored cross-section of Fig. 6.

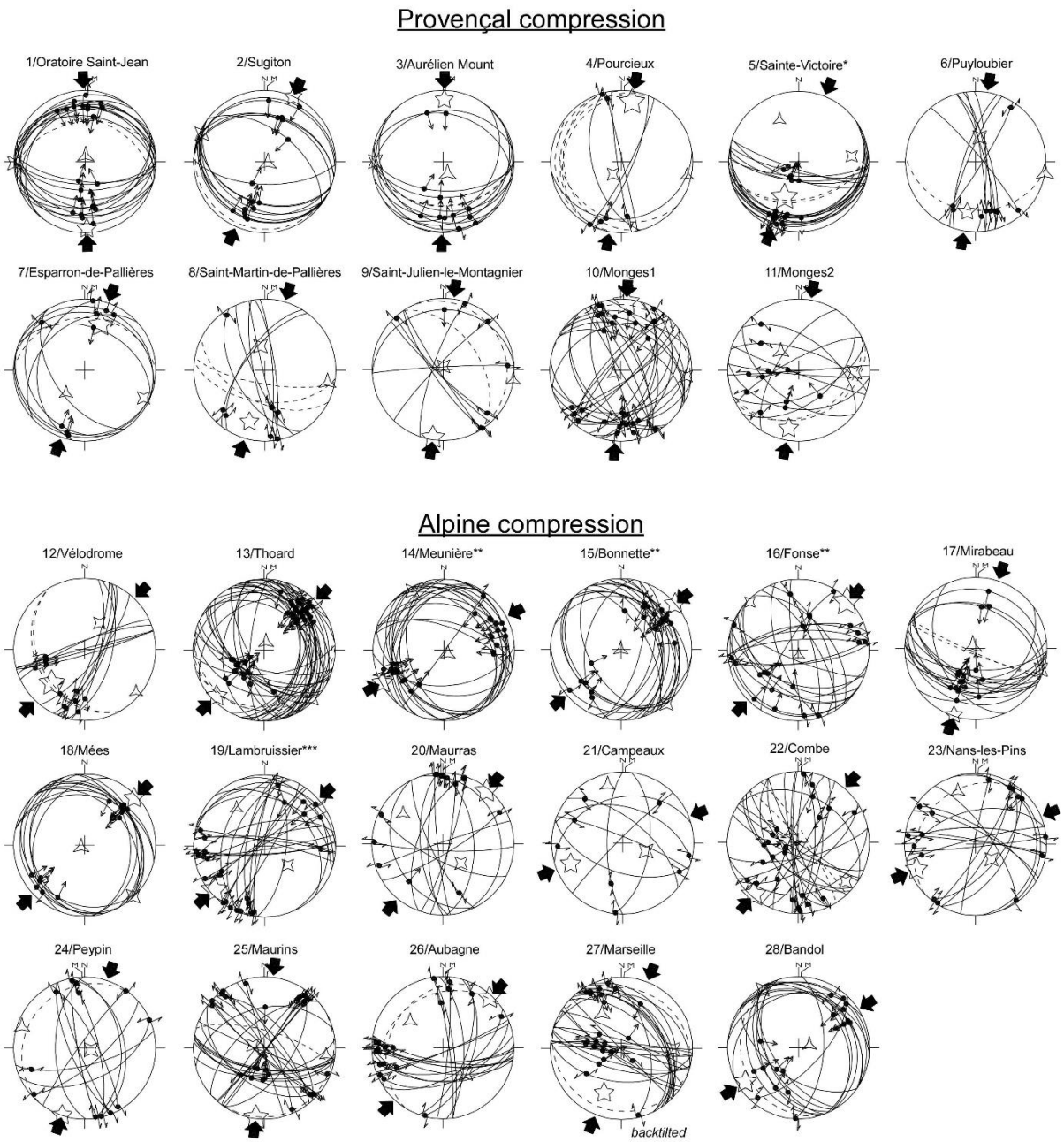

Fig. 22. Fault data and principal computed stress axes (see Angelier (1990) for more details). Principal stress axes (σ_1, σ_2, and σ_3) are symbolized by five-branch, four-branch, and three-branch stars, respectively. Trend of σ_1 is shown by arrows. For locations, see Fig. 21. Data are projected in an equal area stereogram, lower hemisphere (see Table 1). Dashed line corresponds to the projection of bedding dip in the stereogram. *Espurt et al. (2012). **Hippolyte et al. (2012). ***Hippolyte and Dumont (2000).

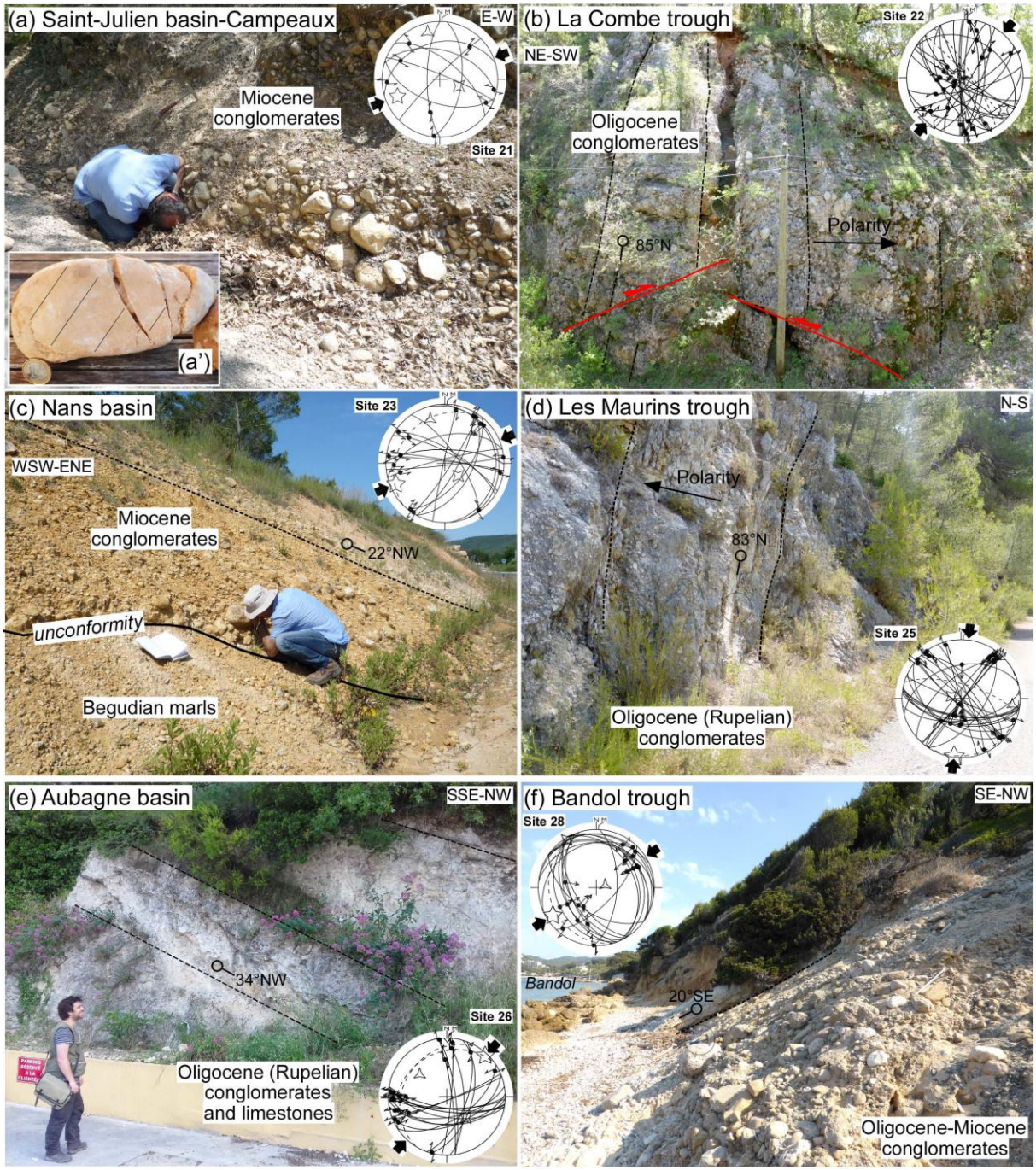

Fig. 23. Field evidence for Alpine contractional deformations in the Provençal zone. For location, see Fig. 2. (a) Striated and sheared Miocene conglomerates above the Vinon thrust, eastern edge of the Saint-Julien basin-Campeaux (43.677722°, 5.946401°; Figs. 3 and 12a). (a') Zoom on a sheared and striated (thin black lines) limestone pebble. (b) Overturned Oligocene strata in the La Combe trough, eastern edge of the Rians basin (43.600228°, 5.927771°; modified from Espurt et al., 2019b). (c) Tilted Miocene strata in the Nans basin,

southern edge of the Barjols Triassic zone (43.392411°, 5.798388°). (d) Tilted Oligocene (Rupelian) conglomerate beds in the Les Maurins trough (43.363886°, 5.512575°). (e) NW-dipping Oligocene (Rupelian) conglomerate and limestone beds in the southern edge of the Aubagne basin (43.282596°, 5.597940°). (f) SE-dipping Oligocene-Miocene conglomerate beds in the Bandol trough (43.133639°, 5.779645°). Striated faults in these Oligocene and Miocene strata are consistent with a ~NE-trending Alpine compression. Fault data and bedding (dashed line) have been projected in an equal area stereogram, lower hemisphere.

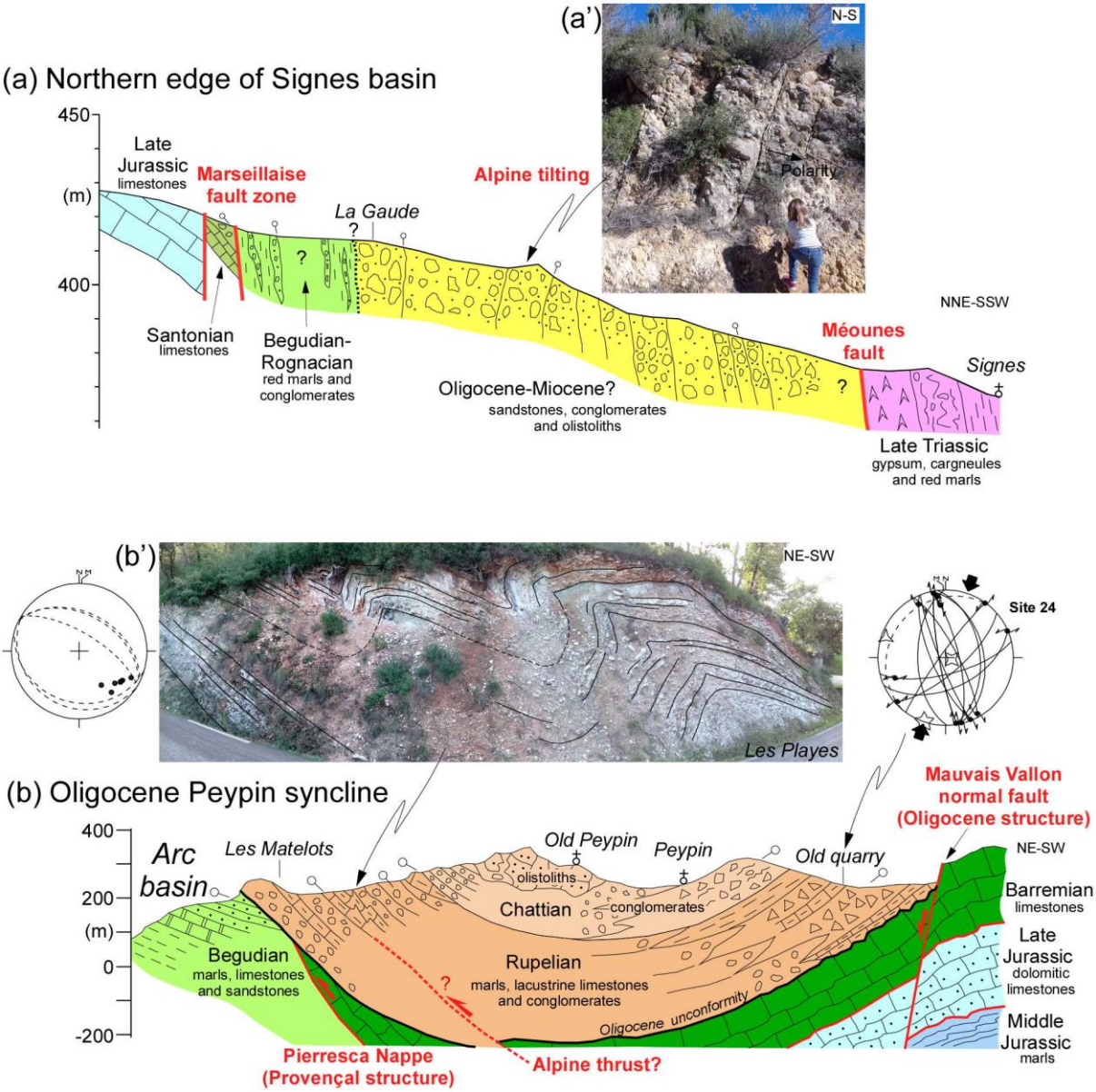

Fig. 24. Surficial cross-sections and field evidence showing Alpine contractional deformations in the southern part of the Provençal domain. For location, see Fig. 3. (a) Surface cross-section across the northern part of the Signes basin (43.295733°, 5.867607°). (a') Photograph of overturned beds of Oligocene-Miocene conglomerates is shown. (b) Surface cross-section of the Peypin syncline (43.381589°, 5.575817°). Photograph of SE-trending folds in Oligocene limestone and conglomerate beds on the northern limb of the Peypin syncline is shown (43.386835°, 5.603627°). Striated faults and fold axis in these Oligocene strata are consistent with a NE-trending Alpine compression. Fault data, fold axis (point) and bedding (dashed line) have been projected in equal area stereograms, lower hemisphere.

Site number/name	Latitude (m)	Longitude (m)	Elevation (masl)	Age/Lithology	Number of faults	σ_1		σ_2		σ_3		Φ	ANG	RUP	Stress regime
						Trend	Plunge	Trend	Plunge	Trend	Plunge				
1/Oratoire Saint-Jean	43.166772	5.719908	139	Santonian/Limestones	22	179	6	269	1	5	84	0.448	10	30	reverse
2/Sugiton	43.217049	5.450640	208	Berriasian/Limestones	15	24	0	294	4	115	86	0.559	6	27	reverse
3/Aurélien Mount	43.455585	5.775748	631	Early Jurassic/Limestones	12	1	14	270	5	160	75	0.524	14	34	reverse
4/Pourcieux	43.475319	5.796727	351	Late Jurassic/Limestones	12	1	14	270	5	160	75	0.524	14	33	strike-slip
5/Sainte-Victoire*	43.524806	5.569858	334	Danian/Conglomerates	17	202	45	284	25	335	35	0.08	8	31	reverse
6/Puyloubier	43.528522	5.675310	396	Early Campanian/Limestones	9	190	28	10	62	100	0	0.569	8	36	reverse
7/Esparron-de-Pallières	43.590707	5.838716	495	Danian/Conglomerates	9	19	33	115	9	219	55	0.207	9	39	strike-slip reverse
8/Saint-Martin-de-Pallières	43.601974	5.887519	400	Danian/Conglomerates	8	197	25	350	62	101	11	0.489	14	36	strike-slip
9/Saint-Julien-le-Montagnier	43.692550	5.905738	565	Late Jurassic/Limestones	8	189	3	6	87	99	0	0.238	10	32	strike-slip reverse
10/Monges1	44.242379	6.192825	1450	Late Eocene-Oligocene/Conglomerates	29	5	5	95	8	243	80	0.106	10	38	strike-slip reverse
11/Monges2	44.246639	6.201392	1535	Late Eocene-Oligocene/Conglomerates	11	190	18	92	22	316	60	0.418	17	44	strike-slip reverse
12/Vélodrome	44.203386	6.256325	1191	Late Miocene/Conglomerates	12	224	34	29	55	130	7	0.113	9	33	strike-slip
13/Thoard	44.171178	6.151978	785	Late Miocene/Conglomerates	38	226	8	135	5	14	81	0.356	8	24	reverse
14/Meunières**	44.123561	6.245412	866	Late Pliocene/Conglomerates	25	242	2	332	6	134	83	0.34	10	38	strike-slip reverse
15/Bonnette**	44.093349	6.221008	767	Late Pliocene/Conglomerates	21	50	0	140	0	249	90	0.29	10	32	strike-slip reverse
16/Fonse**	44.072696	6.249599	1050	Late Pliocene/Conglomerates	21	45	4	315	4	177	85	0.01	11	34	strike-slip reverse
17/Mirabeau	44.043538	6.105934	536	Late Miocene/Conglomerates	17	192	2	108	4	309	85	0.605	7	18	reverse
18/Mées	44.030339	5.980524	424	Late Miocene/Conglomerates	15	46	5	137	1	238	85	0.407	8	36	reverse
19/Lambruissier***	43.981107	6.105508	845	Late Miocene/Conglomerates	26	229	6	130	55	323	34	0.083	10	39	strike-slip reverse
20/Maurras	43.733025	5.891955	458	Miocene/Conglomerates	14	40	4	137	59	307	90	0.223	11	35	strike-slip reverse
21/Campeaux	43.677643	5.946504	522	Miocene/Conglomerates	8	248	22	109	62	345	17	0.393	15	37	strike-slip
22/Combe	43.600039	5.927321	337	Oligocene/Conglomerates	23	221	4	129	15	327	75	0.162	17	45	strike-slip reverse
23/Nans-les-Pins	43.392464	5.798273	369	Miocene/Conglomerates	8	251	18	54	71	159	5	0.434	11	36	strike-slip
23/Peypin	43.381959	5.573757	303	Oligocene/Conglomerates	12	199	1	105	82	289	8	0.389	11	29	strike-slip
25/Maurins	43.366172	5.506941	300	Oligocene/Conglomerates	27	187	2	283	76	97	14	0.17	11	30	strike-slip reverse
26/Aubagne	43.282650	5.597922	114	Oligocene/Conglomerates	19	43	4	138	49	309	40	0.288	13	30	strike-slip
27/Marseille	43.279588	5.444457	97	Oligocene/Conglomerates	23	201	26	82	44	311	35	0.324	13	32	strike-slip reverse

28/Bandol	43.133639	5.779645	1	Oligocene-Miocene/Conglomerates	18	237	12	328	4	76	77	0.454	13	33	reverse

Table 1. Paleo-stress tensors computed from fault slip data. See location of sites in Fig. 21. Fault data and principal computed stress axes are shown in Fig. 22. σ_1, σ_2, σ_3: maximum, intermediary, and minimum principal stress axis, respectively. $\Phi=(\sigma_2-\sigma_3)/(\sigma_1-\sigma_3)$. ANG=average angle between computed shear stress and observed slickenside lineation (in degrees). RUP=quality estimator ($0\leq RUP\leq 200$) taking into account the relative magnitude of the shear stress on fault planes (see Angelier (1990) for more details). *Espurt et al. (2012). **Hippolyte et al. (2012). ***Hippolyte and Dumont (2000).